ABSTRACT

NIGHOT, PRASHANT KESHAV. Role of ClC-2 and NHE transport proteins in Intestinal Mucosal Barrier. (Under the direction of Anthony Blikslager.)

The intestinal mucosal barrier is critical to prevent the invasion of the host by pathogens and toxic products that are present in the intestinal lumen. We studied the role of membrane ion transporters in the recovery of intestinal barrier function after ischemic injury and found that mice lacking chloride channel ClC-2 or the sodium hydrogen exchanger NHE2 have impaired barrier recovery as determined by epithelial restitution-independent increases in *in vivo* blood-to-lumen clearance of a labeled probe. Further ultrastructural, biochemical, and histochemical analyses revealed that impaired barrier recovery is associated with an inadequate assembly of the intracellular tight junctions. The studies indicated an increased association between ClC-2 and the tight junction membrane protein occludin in the form of co-immunoprecipitation and co-localization during barrier recovery. We speculate that ClC-2 might act as scaffold protein and be a specific target in the process of the reassembly of tight junctions. The mechanism of NHE2 mediated tight junction recovery could involve the NHE regulatory protein EBP50 which is an important NHE-associated protein linking the actin cytoskeleton and tight junctions with the plasma membrane proteins.

In alternate studies, we investigated role of ion transport in infectious diarrhea by using an experimental *in vivo* Turkey Astrovirus (TAstV-2) model. The study aimed at elucidating mechanisms of astrovirus-induced diarrhea and revealed that the astrovirus infection leads to sodium malabsorptive diarrhea. This is accompanied by redistribution

of plasma membrane sodium hydrogen exchanger NHE3, possibly associated with apical F-actin rearrangement.

We conclude that NHE and ClC-2 transport proteins are critical for recovery from acute injury, via an interaction with tight junction-associated proteins. Furthermore, NHE3 is intimately involved in diarrheal disease in an infectious disease model. This was also associated with changes in the link between the transport protein and tight junction elements.

Role of ClC-2 and NHE transport proteins in Intestinal Mucosal Barrier

by
Prashant Keshav Nighot

A dissertation submitted to the Graduate Faculty of
North Carolina State University
in partial fulfillment of the
requirements for the Degree of
Doctor of Philosophy

Comparative Biomedical Sciences

Raleigh, North Carolina

2008

APPROVED BY:

_____	_____
Dr. Anthony T. Blikslager Chair of Advisory Committee	Dr. Sam L. Jones
_____	_____
Dr. Jody L. Gookin	Dr. Matthew D Koci

BIOGRAPHY

Prashant Nighot was born and brought up in Nagpur, a city in the central part of India. He completed his Bachelor's degree in Veterinary Sciences from Nagpur Veterinary College. He attended Indian Veterinary Research Institute, Izatnagar for his Master's in Veterinary Pathology. He worked in Industry for few years before joining North Carolina State University for PhD study in August 2005.

Prashant would like to continue work in the area of gastro-intestinal research.

ACKNOWLEDGEMENTS

I would like to acknowledge and appreciate the enormous support that I received throughout my PhD degree at North Carolina State University. I sincerely thank Dr. Anthony Blikslager for providing me this wonderful opportunity of graduate research in his laboratory. I have always found an accomplished mentor and an amazing person in him. I would also like to thank Drs. Sam Jones, Jody Gookin, and Matthew Koci for agreeing to be member of my Graduate committee and their valuable advice throughout my degree.

I would like to express my deepest gratitude to my fellow laboratory colleagues Adam Moeser, Kathleen Ryan, Vanessa Cook, Jenna Wooten, Lauraine Rivier, and John Marshall for their support and help with my research studies. I thank the staff at Central Procedures Laboratory (Donna Hardin, Teri Lucas, and others) and Laboratory Animal Resources for their excellent technical advice and support. The services of Laboratory for Advanced Electron and Light Optical Methods, CVM are greatly appreciated. Dr. Troy Ghashghaei helped us with confocal microscopy.

This is also a time to say thanks to colleagues and friends including Raja, Siddharth, Shweta, Vikrant, Ravi, Anirudh, and others for their help throughout this period.

I am grateful to my family, and parents Mr. Keshav and Mrs. Maya Nighot for their support. Lastly, I am indebted to my wife Meghali, and son Rudraksh for their support that always exceeded my expectations.

TABLE OF CONTENTS

LIST OF TABLES

Chapter III

Chapter V.

LIST OF FIGURES

Chapter I.

Chapter II.

Chapter III.

Chapter IV.

Chapter V.

CHAPTER I. LITERATURE REVIEW

ClC-2 CHLORIDE CHANNEL: CHLORIDE TRANSPORT AND BEYOND

Introduction

The ClC-2 chloride channel is a member of a large ClC super family of voltage-gated Cl^- channels and is expressed almost ubiquitously in the different tissues and organs. Although the function and regulation of ClC-2 channels is yet to be explored completely, the conservation of ClC genes in widely divergent organisms such as plants, yeast, bacteria, vertebrate and invertebrate animals indicate that they have important and fundamental physiological roles. Indeed, perception of ClC in housekeeping physiological roles of Chloride membrane transport is fast changing due to the work done in the last two decades.[1] This review pertains to the ClC-2 member of the ClC family, and will deal with current knowledge about structure, gating, distribution, regulation, and functions of ClC-2.

ClC Family

CLC-0 was the first member of the voltage gated Cl^- channel ClC family identified by expression cloning of the electric organ of the ray *Torpedo marmorata*.[2] The nine ClC genes identified so far in mammals are categorized into 3 groups: channels that are present in plasma membranes and responsible for transepithelial transport and dampening muscle excitability (ClC-1, -2, -Ka/K1, and -Kb/K2); and channels that are present mainly in the endosomal-lysosomal system (ClC-3, -4, and -5) or other intracellular membranes (ClC-6 and -7) where they may participate in regulation of luminal chloride concentration.[3] The salient characteristic of ClC channels is the voltage dependent gating with either inward or outward rectification. Besides chloride channel activity, ClCs

residing in vesicles e.g. ClC-4 and ClC-5 are Cl^-/H^+-exchangers.[4] All ClC members have a unique pH dependent permeability sequence for monovalent anions- $P_{Cl^-} > P_{Br^-} > P_{I^-}$.[3] The importance of ClC members in organ homeostasis has been confirmed by the identification of human diseases associated with the mutations or functional defects in ClC family members. Prominent among them are myotonia (ClC-1),[5] epilepsy (ClC-2),[4] Bartter III- renal salt loss (ClC-Kb),[6] Dent's disease- proteinuria (ClC-5),[7] and osteopetrosis (ClC-7).[8] Besides these human diseases, a number of mouse models and expression systems are characterized for study of ClC function.

ClC-2 structure and gating

The crystal structure of the ClC in *Salmonella enterica* and *Escherichia coli* described by Dutzler *et al*. [9] not only confirmed earlier electrophysiological and biochemical findings, but also provided impetus for further clarifications of ClC function and regulation. The channel has 18 helices that partially span the membrane. The two halves of the double barreled structure form two identical pores that have a binding site for chloride. A glutamate residue that protrudes into the pore is proposed to participate in gating.[10] Though the exact gating mechanism is not known for ClC-2, is has been shown that the voltage dependent gating is influenced by intracellular Cl^- concentration. In this scheme, E217, the conserved glutamate residue, acts as a hyper polarization-dependent protopore gate in ClC-2 and that access of intracellular Cl^- to this site stabilizes the open state of ClC-2 channel.[11] Unlike ClC-0 that has been used as a prototype for ClC gating studies and in which slow gating relates to simultaneous gating of two identical homodimeric

pores and fast gating control each protopore individually, the slow and fast gating in ClC-2 is thought to be coupled. A conformational change that leads to the opening of a slow gate is also capable of facilitating the fast opening mechanism.[12] The large C terminus which is present in mammalian but not bacterial ClC-2 has been of interest to researchers because it contains two large highly conserved CBS (cystathionine beta synthase) domains encoding sorting information.[10,13] The CBS domains from several proteins, including ClC-2, bind nucleotides like ATP *in vitro* suggesting that they may act as energy sensors.[14] Mutagenesis studies have also revealed that residues 16-61 within the N-terminus compose the inhibitory region which if deleted lead to a constitutively open channel without the need of hyperpolarizing voltage steps.[15] Further studies will likely reveal how these structural motifs are related to the regulation of ClC-2.

ClC-2 distribution

ClC-2 is ubiquitously expressed and its presence has been described in many epithelia, cell lines and organs including brain, pancreas, lung, liver, and intestine.[16] A combination of electrophysiology, PCR, Western blotting, and immunolocalization has been used to study the distribution of ClC-2 in different organs and systems. In the hippocampus region of the brain, besides a dense network in the end feet of astrocytes, ClC-2 was localized in the membrane of dendrites, dendritic spines, cell bodies and axon initial segments of neurons. The distribution of ClC-2 in membranes with intense γ-aminobutyric acid (GABA) responsive synaptic transmission activity correlates with chloride transport, increasing the efficacy of GABA (A) receptor-mediated inhibition

attributed to ClC-2.[17, 18] The mRNA of ClC-2 along with ClC-3 was detected in corneal endothelium, stroma, and epithelium and these channels are assumed to be responsible for stromal hydration that maintains corneal transparency.[19] Northern blot analysis studies in cultured human aortic and coronary vascular smooth muscle cells, aortic endothelial cells,[20] human leukemic cell lines (T, B, and myeloid type), T cells, B cells and neutrophils[21] have revealed expression of CLCN2, though to a lesser extent as compared to CLCN3. In cardiac tissue, ClC-2 has been co- localized in sarcolemmal membranes of atrial and ventricular wall consistent with cardiac cell volume and electric activity regulatory roles.

The presence of ClC-2 in two major systems, the airway and intestine, was pursued mostly to find a rescue channel for another chloride channel Cystic Fibrosis Transmembrane Receptor (CFTR). It was thought that the Chloride channel activity of ClC-2 could ameliorate cystic fibrosis, a condition caused by defective function of CFTR. In rat, the transcript of ClC-2 was identified in the lung among multiple organs,[16] and ClC-2 was localized in the apical membrane of airway epithelia in a developmentally regulated fashion. The ClC-2 expression was high during the perinatal period indicating a role of ClC-2 in lung development.[22] Though expression of ClC-2 is unquestionable in intestine, there are some differences in its localization in different species and sections of intestine as reported by various research groups. ClC-2 was detected in a supranuclear compartment or the basolateral membrane of human, and murine and guinea pig colon cells.[13,23-24] In murine small intestine, ClC-2 is reported to be localized to the apical

membrane adjacent to the apical tight junction complex,[25] but it is also reportedly localized on the basolateral side in murine duodenum.[13] In the Caco-2 cell line that models the human small intestinal epithelium, ClC-2 expression was limited to the apical membrane at the level of the tight junction.[26] In another study of the same cell line, ClC-2 expression was shown to be limited to basolateral membranes, with no evidence of apical expression.[13] Interestingly, the latter study also indicated absence of ClC-2 expression in murine jejunum, ileum, and stomach. Although the above studies have justifications for the functioning of ClC-2 at its respective localization, considering the complexity of intestinal epithelial function along the crypt-villus axis, the larger picture of the role of ClC-2 in intestine remains elusive. Expression of ClC-2 in the stomach is also not clear. In one study, the presence of ClC-2 mRNA and protein was described in parietal cells of the rabbit gastric mucosa.[27] In one other study no expression of ClC-2 protein was observed in isolated rat and human gastric mucosa and although mRNA of ClC-2 was detected in isolated rabbit gastric glands, the presence of ClC-2 protein was not confirmed.[28]

ClC-2 functions

ClC-2 is a ubiquitous, inwardly rectifying plasma membrane Cl^- channel and is activated by membrane hyperpolarization, cell swelling, and mildly acidic extracellular pH.[4,15] Although no human disease associated with ClC-2 mutation has been clearly identified, it is fascinating to discover how important this channel is in the physiological functions of different organ systems. Many of the functional attributes of ClC-2 are derived from

knock out (KO) studies or studies in heterogeneous expression systems, although there is a consistent lack of a match between the physiological role of ClC-2 and expected knock out results. For instance, consistent with the regulatory role of ClC-2 in excitatory responses to GABA,[29] ClC-2 knockout mice were expected to display epilepsy, but they did not.[30] Jenstch (2008)[4] has reviewed the justification for this observation, and the current findings on the role of ClC-2 in epilepsy. Recently, ClC-2 KO mice were reported to have leucoencephalopathy in the form of progressive vaccuolation in the central nervous system without abnormal neuronal morphology and unchanged epilepsy threshold as compared to WT mice.[31] In another case of epithelial Cl^- secretion, although ClC-2 has been shown to contribute to native chloride secretion and antisense treatment reduced Cl^- secretion in the human intestinal Caco-2 cells, [26] additional disruption of ClC-2 in CFTR KO mice did not exacerbate the phenotype.[32] In this respect, as described earlier, the current literature has different opinions for ClC-2 function depending upon the localization. Studies showing basolateral localization propose an absorptive role for ClC-2 while the apical localization suggests Cl^- secretory function. Despite the proposed role of ClC-2 in airways, and gastric secretion, the ClC-2 KO mice did not have abnormalities in lung development and gastric function.[30,33] However, these knock out mice demonstrated an important role of ClC-2 in tissue homeostasis in that they displayed degenerative changes in retina and testis. Both these tissues depend heavily on the supporting tissue for nutrition (retinal pigment epithelial cells and Sertoli cells, respectively) [4, 30, 34] CLH-3, a ClC-2 ortholog, produced hyperpolarization- and swelling-activated inwardly rectifying Cl^- currents in *Caenorhabditis elegans* oocytes. Although

CLH-3 played no apparent role in oocyte volume homeostasis, it was found to be activated during oocyte meiotic maturation and modulate ovulatory contractions of gonadal sheath cells that closely surround and couple the oocytes via gap junctions.[35] In salivary acinar cells, although ClC-2 has been shown to be the hyperpolarization-activated Cl^- channel, ClC-2 deficient mice had similar volume and composition of saliva as in wild type mice.[33] Overall, most of the examples from KO studies suggest an important role of ClC-2 in cell-to-cell contact, communication, and homeostasis aside from chloride transport.

ClC-2 currents are described to have a volume regulatory role when exogenously expressed in Xenopus oocytes [36] or with endogenous expression in rat HTC hepatoma cells.[37] In cardiac tissues, Cl^- conductance due to ClC-2 has been suggested to contribute to the depolarization of cardiac membrane seen in conditions like ischemia and acidosis and thus drugs inhibiting ClC-2 could prove to be anti-arrhythmatic.[38] In experimental infection of *Plasmodium berghei* in mice, ClC-2 was involved in the increase of cell volume and altered permeability of Plasmodium-infected erythrocytes but was not required for intraerythrocytic parasite survival.[39] There is little evidence of ClC-2 involvement in chronic processes. Expression of ClC-2 and CLC-3 was found to be increased in glandular epithelium of the ethmoid sinus in cases of chronic rhino sinusitis as well as nasal polyps.[40] ClC-2 was believed to contribute to the regulatory volume decrease in human glioma cells and inhibition of ClC-2 with siRNA was shown to inhibit cell proliferation of a human glioma cell line U-87.[41, 42]

ClC-2 regulation

As is true in the case of several other intestinal membrane transport proteins, [43] evidence is being gathered regarding regulation of ClC-2 by transcriptional regulation or by modification by phosphorylation, and by modulation of abundance in the plasma membrane. As a part of transcriptional regulation, transcriptional factors SP1and SP3 were shown to interact with the ClC-2 promoter region and associated with modulation of ClC-2 expression in airway during perinatal period.[44, 45] Further studies revealed that in fetal (preII-19) and adult (L2) rat lung Type 2 cell lines, phosphorylation and glycosylation of SP1 correlated with ClC-2 expression. *In vivo*, too, young murine lung with high ClC-2 expression had hyperphosphorylation and hyperglycosylation of SP1 as compared to an adult murine lung with low ClC-2 expression.[46] IFN-gamma was found to stabilize ClC-2 transcripts when exogenously expressed in the Calu-3 lung adenocarcinoma cell line.[45] Single amino acid polymorphs of the ClC-2 gene (CLCN2), when exogenously expressed in *Xenopus laevis* oocytes, have revealed effects on surface expression and voltage- or cell- swelling-stimulated channel gating. All of these alterations were in the cytoplasmic domain of ClC-2, including both N and C-terminus and the pore, thus underscoring the importance of ClC-2 cytoplasmic domains in channel regulation.[47]

In stably transfected HEK293 cells, cholesterol depletion and oxidative stress not only moved membrane ClC-2 from the detergent insoluble fraction to the detergent soluble membrane fraction but also increased its activation kinetics. The abundance of

ClC-2 in the plasma membrane was also reduced after cholesterol repletion.[48] Although the exact mechanism of this modulation of gating and abundance of ClC-2 in the membrane is not yet known, this study has proven the regulatory role of cholesterol, and thus the composition of plasma membrane lipid rafts on ClC-2 function. Interestingly, the modulation of ClC-2 gating was less cholesterol dependent in the tissues that express ClC-2 endogenously.[48] Thus, in native tissues the localization of and polarity of for instance epithelial lining cells would certainly have an effect on ClC-2 function.

There is now evidence that other mechanisms e.g. endocytic trafficking or intracellular signaling could play a role in ClC-2 function at the plasma membrane. Disruption of actin in the Xenopus oocyte expression system resulted into increased chloride-channel activity of exogenously expressed ClC-2, suggesting an inhibitory role of the actin cytoskeleton on ClC-2 activity. The fusion protein expressing inhibitory domain in the N-terminus of ClC-2 was shown to be capable of binding with actin.[49] Furthermore, ATP depletion, which could disrupt the actin cytoskeleton, was recently shown to reduce ClC-2 endocytosis and this was at least partially dynamin-dependent.[50, 51] The GTPases rab-5 and rab-11 played roles in the dynamin-dependent early endosomal sorting and recycling back to the cell surface, respectively. Of relevance to stressful conditions, association between ClC-2 and heat shock protein Hsp90 resulted in increased abundance of ClC-2 on the cell surface and increased sensitivity of ClC-2 gating towards intracellular chloride concentration.[52] Hsp90 is a chaperone protein involved in processes like correct protein folding and its membrane translocation; this association would

provide the basis for fine regulation of ClC-2 in response to intracellular signaling targeted at the cytoplasmic domain of ClC-2. The partnership of Hsp90 with ClC-2 would also explain varying expression and activity of ClC-2 in the different expression systems and tissues.[53]

Different protein kinases have been shown to regulate ClC-2 under specific situations. The role of ClC-2 in the cell cycle was evident when expression of ClC-2 was shown to be regulated during M phase by M phase specific p34(cdc2)/cyclin B phosphorylation dependent ubiquitination targeted at the S632 residue.[54-55] Among the major protein kinases, protein kinase A phosphorylated rat ClC-2 that was exogenously expressed in the TSA-210 cell line; but this phosphorylation did not affect channel activity.[56] However, more recently, differential regulation of ClC-2 at two sites was demonstrated: at pH 7.4, RRAT655 or RGET691 activation was independent of each other; at a mild acidic pH of 6 alone RGET691 activation was independent while RRAT655 activation was dependent on RGET691 activation.[57] Though Protein kinase C activation with phorbol 12-myristate 13-acetate and Ca^{++}/calmodulin-dependent protein kinase II did not phosphorylate exogenously expressed ClC-2 in the TSA-210 cell line,[56] natively expressed ClC-2 in colonic T84 cells was a target of Protein Kinase C dependent tyrosine phosphorylation initiated by EGFR signaling.[58] TGF-alpha, at low concentrations, irreversibly inhibited ClC-2 current by EGFR tyrosine kinase activity dependent on activated phosphoinositide 3-kinase, and protein kinase C. At higher concentrations TGF-alpha lead to reversible activation of the ClC-2 current, possibly

related to intracellular alkalinization. Though serine/threonine dephosphorylation was shown to activate CLH-3, the *Caenorhabditis elegans* ClC-2 ortholog,[35] serine/threonine phosphorylation by serum and glucocorticoid inducible kinase isoforms SGK1-3 lead to ClC-2 activation via inhibiting the ubiquitin ligase Nedd4-2 in Xenopus oocytes.[59] The functional consequences of ClC-2 phosphorylation/ dephosphorylation are not yet known; however it is clear that this type of regulation is highly sensitive to pH and volume changes and varies between species and expression systems.

Among other regulatory components, hormonal regulation of ClC-2 was identified by studies demonstrating modulation of ClC-2 mRNA in the kidney of adrenalectomized rats. Oestrogen was shown to increase ClC-2 mRNA and protein expression in the rat kidney.[60, 61] Renal ClC-2 expression was decreased in hypothyroid rats and increased in hyperthyroid rats. In addition, renal proximal tubule primary culture cells treated with thyroxine showed dose dependent increases in ClC-2 mRNA, indicating a role of thyroid hormone in ClC-2 regulation.[62] As a response to infectious processes, expression of ClC-2 was up regulated in rat small intestine after exposure to cholera toxin.[63]

Beyond Chloride transport:

Overall, the knockout models, exogenous expression studies, mutagenesis studies, and distribution pattern and localization data related to ClC-2 suggest multiple roles of this protein in cell-to-cell communication, tissue homeostasis, as well as innate chloride

transport activity. In our laboratory, we have accumulated evidence about the role of ClC-2 in intestinal barrier recovery after ischemic injury. In a chloride secretion mediated post-ischemic barrier recovery model initiated by prostaglandins, it was discovered that inhibition of ClC-2 and not CFTR impaired recovery of barrier function in porcine intestine.[64, 65] Furthermore, this recovery process was independent of the magnitude of chloride secretion and also involved signaling molecules such as PI3K. The recovery response was mimicked by increasing mucosal osmotic load.[66] Similar to localization of ClC-2 on the apical membrane adjacent to the tight junction in murine small intestine, porcine small intestine also revealed the same localization for ClC-2.[65] Recently we confirmed these previous findings in the porcine model by using ClC-2 knockout mice. Our results indicate that ClC-2 knockout mice have impaired post-ischemic barrier recovery that is attributable to failure of tight junction recovery. Specifically, we obtained evidence about a close association between ClC-2 and the tight junction protein occludin during barrier recovery (unpublished data). Although the ClC-2 channels concentrated around apical tight junctions could have an advantage in influencing paracellular permeability via chloride transport through paracellular spaces, [67] its localization at the tight junction suggests the possibility of its interaction with signaling molecules densely present in this region as well as the tight junction proteins. Thus, evidence from our experiments suggest the possibility of ClC-2 being specifically targeted as a signaling molecule in barrier function recovery rather than just acting as a chloride channel. Another interesting finding was that lubiprostone, a ClC-2 agonist, improved the barrier function recovery by a mechanism that was not fully dependent on Cl^- secretion but

associated with tight junction assembly.[68] Lubiprostone, which is considered a potent treatment for relieving chronic constipation, has been shown to stimulate chloride transport in T84 cells, activate currents of exogenously expressed ClC-2 in HEK-293 cell lines,[69] and accelerate small intestinal and colonic transit in humans.[70] In our post-ischemic barrier recovery model, Cl^- secretion was indispensable for barrier recovery; blockade of chloride entry into the epithelial cells, by inhibiting the basolateral NKCC1 cotransporter with bumetanide abolished barrier recovery.[64] Thus, in reference to ClC-2 mediated barrier recovery, the role of chloride secretion is not clear. It is quite possible that increased intracellular chloride concentrations are required for ClC-2 activation. A separate signaling pathway involving a cytoplasmic domain of ClC-2 may lead to tight junction recovery (Figure 1). It is also not unreasonable to think that we are still missing specific functions of ClC-2 in native tissues out of studies in exogenous expression systems and cell cultures. The presence of the CBS domains in the C-terminus of multicellular mammalians and not in the unicellular bacteria is probably a big clue towards the role of ClC-2 in cell-to-cell homeostasis.

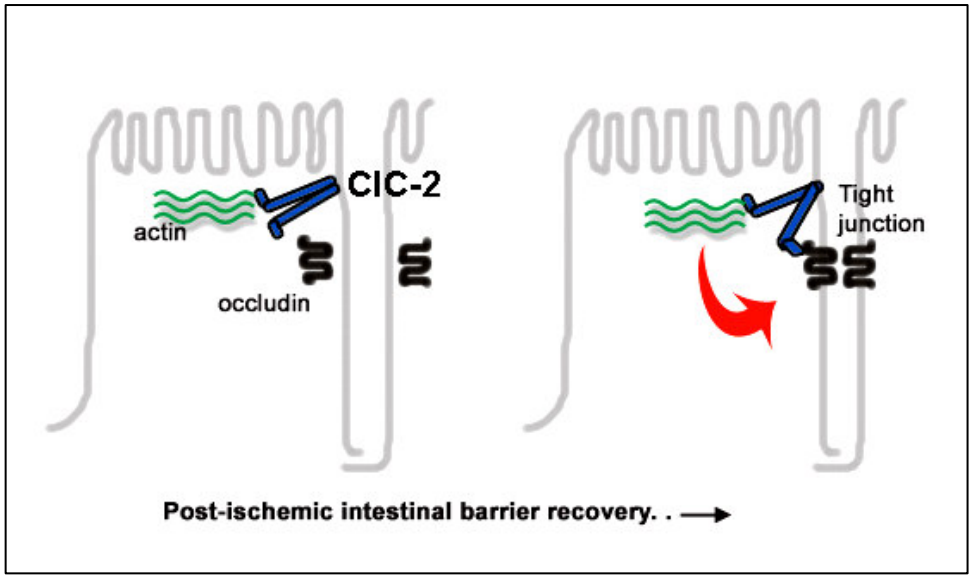

Figure 1. Proposed role of ClC-2 in the post-ischemic barrier recovery. Based on results of experiments in ClC-2 knockout mice, we speculate that ClC-2 might act as a scaffold protein facilitating reassembly of tight junction.

REFERENCES

1. Miller C. ClC chloride channels viewed through a transporter lens. Nature 2006;440:484-489.
2. Jentsch TJ, Steinmeyer K, Schwarz G. Primary structure of Torpedo marmorata chloride channel isolated by expression cloning in Xenopus oocytes. Nature 1990;348:510-514.
3. Nilius B, Droogmans G. Amazing chloride channels: an overview. Acta Physiol.Scand. 2003;177:119-147.
4. Jentsch TJ. CLC chloride channels and transporters: from genes to protein structure, pathology and physiology. Crit.Rev.Biochem.Mol.Biol. 2008;43:3-36.
5. Koch MC, Steinmeyer K, Lorenz C, Ricker K, Wolf F, Otto M, Zoll B, Lehmann-Horn F, Grzeschik KH, Jentsch TJ. The skeletal muscle chloride channel in dominant and recessive human myotonia. Science 1992;257:797-800.
6. Estevez R, Jentsch TJ. CLC chloride channels: correlating structure with function. Curr.Opin.Struct.Biol. 2002;12:531-539.
7. Piwon N, Gunther W, Schwake M, Bosl MR, Jentsch TJ. ClC-5 Cl^- -channel disruption impairs endocytosis in a mouse model for Dent's disease. Nature 2000;408:369-373.
8. Kornak U, Kasper D, Bosl MR, Kaiser E, Schweizer M, Schulz A, Friedrich W, Delling G, Jentsch TJ. Loss of the ClC-7 chloride channel leads to osteopetrosis in mice and man. Cell 2001;104:205-215.

9. Dutzler R, Campbell EB, Cadene M, Chait BT, MacKinnon R. X-ray structure of a ClC chloride channel at 3.0 A reveals the molecular basis of anion selectivity. Nature 2002;415:287-294.
10. Jentsch TJ. Chloride channels are different. Nature 2002;415:276-277.
11. Niemeyer MI, Cid LP, Zuniga L, Catalan M, Sepulveda FV. A conserved pore-lining glutamate as a voltage- and chloride-dependent gate in the ClC-2 chloride channel. J.Physiol. 2003;553:873-879.
12. Zuniga L, Niemeyer MI, Varela D, Catalan M, Cid LP, Sepulveda FV. The voltage-dependent ClC-2 chloride channel has a dual gating mechanism. J.Physiol. 2004;555:671-682.
13. Pena-Munzenmayer G, Catalan M, Cornejo I, Figueroa CD, Melvin JE, Niemeyer MI, Cid LP, Sepulveda FV. Basolateral localization of native ClC-2 chloride channels in absorptive intestinal epithelial cells and basolateral sorting encoded by a CBS-2 domain di-leucine motif. J.Cell.Sci. 2005;118:4243-4252.
14. Scott JW, Hawley SA, Green KA, Anis M, Stewart G, Scullion GA, Norman DG, Hardie DG. CBS domains form energy-sensing modules whose binding of adenosine ligands is disrupted by disease mutations. J.Clin.Invest. 2004;113:274-284.
15. Grunder S, Thiemann A, Pusch M, Jentsch TJ. Regions involved in the opening of CIC-2 chloride channel by voltage and cell volume. Nature 1992;360:759-762.
16. Thiemann A, Grunder S, Pusch M, Jentsch TJ. A chloride channel widely expressed in epithelial and non-epithelial cells. Nature 1992;356:57-60.

17. Sik A, Smith RL, Freund TF. Distribution of chloride channel-2-immunoreactive neuronal and astrocytic processes in the hippocampus. Neuroscience 2000;101:51-65.

18. Walz W. Chloride/anion channels in glial cell membranes. Glia 2002;40:1-10.

19. Davies N, Akhtar S, Turner HC, Candia OA, To CH, Guggenheim JA. Chloride channel gene expression in the rabbit cornea. Mol.Vis. 2004;10:1028-1037.

20. Lamb FS, Clayton GH, Liu BX, Smith RL, Barna TJ, Schutte BC. Expression of CLCN voltage-gated chloride channel genes in human blood vessels. J.Mol.Cell.Cardiol. 1999;31:657-666.

21. Jiang B, Hattori N, Liu B, Kitagawa K, Inagaki C. Expression of swelling- and/or pH-regulated chloride channels (ClC-2, 3, 4 and 5) in human leukemic and normal immune cells. Life Sci. 2002;70:1383-1394.

22. Murray CB, Chu S, Zeitlin PL. Gestational and tissue-specific regulation of C1C-2 chloride channel expression. Am.J.Physiol. 1996;271:L829-37.

23. Lipecka J, Bali M, Thomas A, Fanen P, Edelman A, Fritsch J. Distribution of ClC-2 chloride channel in rat and human epithelial tissues. Am.J.Physiol.Cell.Physiol. 2002;282:C805-16.

24. Catalan M, Niemeyer MI, Cid LP, Sepulveda FV. Basolateral ClC-2 chloride channels in surface colon epithelium: regulation by a direct effect of intracellular chloride. Gastroenterology 2004;126:1104-1114.

25. Gyomorey K, Yeger H, Ackerley C, Garami E, Bear CE. Expression of the chloride channel ClC-2 in the murine small intestine epithelium. Am.J.Physiol.Cell.Physiol. 2000;279:C1787-94.
26. Mohammad-Panah R, Gyomorey K, Rommens J, Choudhury M, Li C, Wang Y, Bear CE. ClC-2 contributes to native chloride secretion by a human intestinal cell line, Caco-2. J.Biol.Chem. 2001;276:8306-8313.
27. Sherry AM, Malinowska DH, Morris RE, Ciraolo GM, Cuppoletti J. Localization of ClC-2 Cl- channels in rabbit gastric mucosa. Am.J.Physiol.Cell.Physiol. 2001;280:C1599-606.
28. Hori K, Takahashi Y, Horikawa N, Furukawa T, Tsukada K, Takeguchi N, Sakai H. Is the ClC-2 chloride channel involved in the Cl- secretory mechanism of gastric parietal cells? FEBS Lett. 2004;575:105-108.
29. Staley K, Smith R, Schaack J, Wilcox C, Jentsch TJ. Alteration of GABAA receptor function following gene transfer of the CLC-2 chloride channel. Neuron 1996;17:543-551.
30. Bosl MR, Stein V, Hubner C, Zdebik AA, Jordt SE, Mukhopadhyay AK, Davidoff MS, Holstein AF, Jentsch TJ. Male germ cells and photoreceptors, both dependent on close cell-cell interactions, degenerate upon ClC-2 Cl(-) channel disruption. EMBO J. 2001;20:1289-1299.
31. Blanz J, Schweizer M, Auberson M, Maier H, Muenscher A, Hubner CA, Jentsch TJ. Leukoencephalopathy upon disruption of the chloride channel ClC-2. J.Neurosci. 2007;27:6581-6589.

32. Zdebik AA, Cuffe JE, Bertog M, Korbmacher C, Jentsch TJ. Additional disruption of the ClC-2 Cl(-) channel does not exacerbate the cystic fibrosis phenotype of cystic fibrosis transmembrane conductance regulator mouse models. J.Biol.Chem. 2004;279:22276-22283.
33. Nehrke K, Arreola J, Nguyen HV, Pilato J, Richardson L, Okunade G, Baggs R, Shull GE, Melvin JE. Loss of hyperpolarization-activated Cl(-) current in salivary acinar cells from Clcn2 knockout mice. J.Biol.Chem. 2002;277:23604-23611.
34. Strange K. Of mice and worms: novel insights into ClC-2 anion channel physiology. News Physiol.Sci. 2002;17:11-16.
35. Rutledge E, Bianchi L, Christensen M, Boehmer C, Morrison R, Broslat A, Beld AM, George AL, Greenstein D, Strange K. CLH-3, a ClC-2 anion channel ortholog activated during meiotic maturation in C. elegans oocytes. Curr.Biol. 2001;11:161-170.
36. Furukawa T, Ogura T, Katayama Y, Hiraoka M. Characteristics of rabbit ClC-2 current expressed in Xenopus oocytes and its contribution to volume regulation. Am.J.Physiol. 1998;274:C500-12.
37. Roman RM, Smith RL, Feranchak AP, Clayton GH, Doctor RB, Fitz JG. ClC-2 chloride channels contribute to HTC cell volume homeostasis. Am.J.Physiol.Gastrointest.Liver Physiol. 2001;280:G344-53.
38. Duan DY, Liu LL, Bozeat N, Huang ZM, Xiang SY, Wang GL, Ye L, Hume JR. Functional role of anion channels in cardiac diseases. Acta Pharmacol.Sin. 2005;26:265-278.

39. Huber SM, Duranton C, Henke G, Van De Sand C, Heussler V, Shumilina E, Sandu CD, Tanneur V, Brand V, Kasinathan RS, Lang KS, Kremsner PG, Hubner CA, Rust MB, Dedek K, Jentsch TJ, Lang F. Plasmodium induces swelling-activated ClC-2 anion channels in the host erythrocyte. J.Biol.Chem. 2004;279:41444-41452.
40. Li H, Han D, Zhou B, Fan E, Liu Z. Expressions of chloride channel ClC-2 and ClC-3 in human nasal polyps. Lin Chuang Er Bi Yan Hou Ke Za Zhi 2003;17:266-267.
41. Yang XY, Lai XG, Zhang Y, Pei JM, Yang AG, Zhou SS. siRNA-mediated silencing of ClC-2 gene inhibits proliferation of human U-87 glioma cells. Ai Zheng 2006;25:805-810.
42. Ernest NJ, Weaver AK, Van Duyn LB, Sontheimer HW. Relative contribution of chloride channels and transporters to regulatory volume decrease in human glioma cells. Am.J.Physiol.Cell.Physiol. 2005;288:C1451-60.
43. Barrett KE. New ways of thinking about (and teaching about) intestinal epithelial function. Adv.Physiol.Educ. 2008;32:25-34.
44. Holmes KW, Hales R, Chu S, Maxwell MJ, Mogayzel PJ,Jr, Zeitlin PL. Modulation of Sp1 and Sp3 in lung epithelial cells regulates ClC-2 chloride channel expression. Am.J.Respir.Cell Mol.Biol. 2003;29:499-505.
45. Chu S, Blaisdell CJ, Bamford P, Ferro TJ. Interferon-gamma regulates ClC-2 chloride channel in lung epithelial cells. Biochem.Biophys.Res.Commun. 2004;324:31-39.

46. Vij N, Zeitlin PL. Regulation of the ClC-2 lung epithelial chloride channel by glycosylation of SP1. Am.J.Respir.Cell Mol.Biol. 2006;34:754-759.

47. Paul J, Jeyaraj S, Huber SM, Seebohm G, Bohmer C, Lang F, Kremsner PG, Kun JF. Alterations in the cytoplasmic domain of CLCN2 result in altered gating kinetics. Cell.Physiol.Biochem. 2007;20:441-454.

48. Hinzpeter A, Fritsch J, Borot F, Trudel S, Vieu DL, Brouillard F, Baudouin-Legros M, Clain J, Edelman A, Ollero M. Membrane cholesterol content modulates ClC-2 gating and sensitivity to oxidative stress. J.Biol.Chem. 2007;282:2423-2432.

49. Ahmed N, Ramjeesingh M, Wong S, Varga A, Garami E, Bear CE. Chloride channel activity of ClC-2 is modified by the actin cytoskeleton. Biochem.J. 2000;352 Pt 3:789-794.

50. Dhani SU, Mohammad-Panah R, Ahmed N, Ackerley C, Ramjeesingh M, Bear CE. Evidence for a functional interaction between the ClC-2 chloride channel and the retrograde motor dynein complex. J.Biol.Chem. 2003;278:16262-16270.

51. Dhani SU, Kim Chiaw P, Huan LJ, Bear CE. ATP depletion inhibits the endocytosis of ClC-2. J.Cell.Physiol. 2008;214:273-280.

52. Hinzpeter A, Lipecka J, Brouillard F, Baudoin-Legros M, Dadlez M, Edelman A, Fritsch J. Association between Hsp90 and the ClC-2 chloride channel upregulates channel function. Am.J.Physiol.Cell.Physiol. 2006;290:C45-56.

53. Cid LP, Niemeyer MI, Sepulveda FV. ClC-2 channels get new partners. Focus on "association between Hsp90 and the ClC-2 chloride channel upregulates channel function". Am.J.Physiol.Cell.Physiol. 2006;290:C42-4.

54. Furukawa T, Ogura T, Zheng YJ, Tsuchiya H, Nakaya H, Katayama Y, Inagaki N. Phosphorylation and functional regulation of ClC-2 chloride channels expressed in Xenopus oocytes by M cyclin-dependent protein kinase. J.Physiol. 2002;540:883-893.

55. Zheng YJ, Furukawa T, Ogura T, Tajimi K, Inagaki N. M phase-specific expression and phosphorylation-dependent ubiquitination of the ClC-2 channel. J.Biol.Chem. 2002;277:32268-32273.

56. Park K, Begenisich T, Melvin JE. Protein kinase A activation phosphorylates the rat ClC-2 Cl- channel but does not change activity. J.Membr.Biol. 2001;182:31-37.

57. Cuppoletti J, Tewari KP, Sherry AM, Ferrante CJ, Malinowska DH. Sites of protein kinase A activation of the human ClC-2 Cl(-) channel. J.Biol.Chem. 2004;279:21849-21856.

58. Bali M, Lipecka J, Edelman A, Fritsch J. Regulation of ClC-2 chloride channels in T84 cells by TGF-alpha. Am.J.Physiol.Cell.Physiol. 2001;280:C1588-98.

59. Palmada M, Dieter M, Boehmer C, Waldegger S, Lang F. Serum and glucocorticoid inducible kinases functionally regulate ClC-2 channels. Biochem.Biophys.Res.Commun. 2004;321:1001-1006.

60. Ornellas DS, Nascimento DS, Christoph DH, Guggino WB, Morales MM. Aldosterone and high-NaCl diet modulate ClC-2 chloride channel gene expression in rat kidney. Pflugers Arch. 2002;444:193-201.
61. Nascimento DS, Reis CU, Goldenberg RC, Ortiga-Carvalho TM, Pazos-Moura CC, Guggino SE, Guggino WB, Morales MM. Estrogen modulates ClC-2 chloride channel gene expression in rat kidney. Pflugers Arch. 2003;446:593-599.
62. Santos Ornellas D, Grozovsky R, Goldenberg RC, Carvalho DP, Fong P, Guggino WB, Morales M. Thyroid hormone modulates ClC-2 chloride channel gene expression in rat renal proximal tubules. J.Endocrinol. 2003;178:503-511.
63. Flach CF, Lange S, Jennische E, Lonnroth I. Cholera toxin induces expression of ion channels and carriers in rat small intestinal mucosa. FEBS Lett. 2004;561:122-126.
64. Blikslager AT, Roberts MC, Argenzio RA. Prostaglandin-induced recovery of barrier function in porcine ileum is triggered by chloride secretion. Am.J.Physiol. 1999;276:G28-36.
65. Moeser AJ, Haskell MM, Shifflett DE, Little D, Schultz BD, Blikslager AT. ClC-2 chloride secretion mediates prostaglandin-induced recovery of barrier function in ischemia-injured porcine ileum. Gastroenterology 2004;127:802-815.
66. Little D, Dean RA, Young KM, McKane SA, Martin LD, Jones SL, Blikslager AT. PI3K signaling is required for prostaglandin-induced mucosal recovery in ischemia-injured porcine ileum. Am.J.Physiol.Gastrointest.Liver Physiol. 2003;284:G46-56.

67. Kirk KL. Chloride channels and tight junctions. Focus on "Expression of the chloride channel ClC-2 in the murine small intestine epithelium". Am.J.Physiol.Cell.Physiol. 2000;279:C1675-6.

68. Moeser AJ, Nighot PK, Engelke KJ, Ueno R, Blikslager AT. Recovery of mucosal barrier function in ischemic porcine ileum and colon is stimulated by a novel agonist of the ClC-2 chloride channel, lubiprostone. Am.J.Physiol.Gastrointest.Liver Physiol. 2007;292:G647-56.

69. Cuppoletti J, Malinowska DH, Tewari KP, Li QJ, Sherry AM, Patchen ML, Ueno R. SPI-0211 activates T84 cell chloride transport and recombinant human ClC-2 chloride currents. Am.J.Physiol.Cell.Physiol. 2004;287:C1173-83.

70. Camilleri M, Bharucha AE, Ueno R, Burton D, Thomforde GM, Baxter K, McKinzie S, Zinsmeister AR. Effect of a selective chloride channel activator, lubiprostone, on gastrointestinal transit, gastric sensory, and motor functions in healthy volunteers. Am.J.Physiol.Gastrointest.Liver Physiol. 2006;290:G942-7.

CHAPTER 2: LITERATURE REVIEW

SODIUM HYDROGEN EXCHANGERS NHE2 AND NHE3 IN THE INTESTINE

Organization of Sodium hydrogen exchangers NHE2 and NHE3 in the intestine

Movement of sodium, chloride, and other ions across the intestinal, renal and other epithelia is crucial for tissue homeostasis. Ion transport is a highly dynamic process in the intestine considering the polarity of intestinal epithelium, the crypt-villous axis, compartmentalization of absorptive and secretory processes in different segments of the intestine, anatomical variations along the length of the intestine, and the influence of the luminal contents. Several mechanisms are responsible for absorption of sodium in the intestine such as nutrient coupled absorption (e.g. Sodium Glucose co-transport SGLT), electrogenic absorption (ENac), and electroneutral absorption (Sodium Hydrogen Exchange).

The sodium hydrogen exchangers (NHEs) are antiporters that are widely expressed on the epithelial membrane and play an important role in salt and water absorption and cell volume regulation by virtue of Na^+/H^+ exchange. Particularly in distal small intestine and proximal large intestine the Na^+/H^+ exchange is coupled with Cl^-/HCO_3^- and short-chain fatty acid/OH exchange and is the major mechanism for NaCl absorption. NHEs belong to the gene family called SLC9A comprising nine isoforms NHE1-9.[1] The NHEs1-5 are grouped as plasma membrane NHEs while NHEs6-9 are grouped as intracytoplasmic organellar isoforms.[1]NHE1 is prominently localized to the basolateral membrane of enterocytes and is involved in intracellular pH and cell volume regulation. [2] NHE2 and 3 are present in the apical brush border of intestinal

epithelium and are the major isoforms contributing to sodium absorption. The localization of NHE2 and NHE3 in the intestine varies between different species and also along the crypt-villous axis. For example, in humans NHE3 is more abundant in ileum and proximal colon while NHE2 is heavily expressed in distal colon and small intestine.[3,4] In rabbit small intestine, NHE3 is present on the apical membrane of the entire villus whereas in rat small intestine it is present only in the upper half of the villous.[3,5] In mouse colon NHE3 is expressed predominantly in villi and NHE2 in crypts.[1] NHE2 and NHE3 also differ with regard to their abundance in the plasma membrane based on studies in different tissues and cell types. Out of total exogenous expression in PS120 and AP1 cells, only 15% of NHE3 but 90% of NHE2 was basally present on the plasma membrane.[6,7] In contrast, Caco-2 cells have approximately 80% of total NHE3 in the brush border and 20% in a diffuse supranuclear location.[8] The mechanism of NHE3 trafficking from plasma membrane via intervillous clefts to the endosomes and back to the plasma membrane has been recently investigated, while no such mechanism is known for NHE2. With few exceptions NHE3 contributes relatively more than NHE2 towards basal sodium absorption. In dog ileum only NHE3 is involved in sodium absorption while in avian ileum both NHE2 and NHE3 have equal contribution towards Na^+/H^+ exchange.[9-11] NHE3 plays a major role in rabbit, rat, and mouse while NHE2 in avian large intestinal sodium absorption.[11-13] The mechanism of cooperation between Na^+/H^+ exchange with Cl^-/HCO_3^- exchange for electroneutral NaCl absorption is not well understood but at least partially explained by direct physical linkage between NHE3 and Cl^-/HCO_3^- exchangers DRA (down-regulated in adenoma; SLC26A3) and PAT1

(putative anion transporter; SLC26A6) through brush border PDZ domain-containing proteins (members of the NHERF and PDZK1 families).[114]

Structure and Functions of NHE2 and NHE3

Structurally, human NHEs have between 645 and 898 amino acids[15] with 12 putative encoded membrane-spanning domains (MSD) (the first being a cleaved signal peptide as demonstrated for NHE3 and the yeast NHE homologue, Nhx1).[16,17] The transmembrane N-terminus of about 500 aa is the transport domain that carries out electroneutral exchange of 1 Na^+ for 1 H^+.[18-21] The hydrophilic C-terminus domain is a regulatory domain and is involved in regulation of the NHE by growth factors and protein kinases.[22] Although NHE3 and NHE2 COOH termini have been shown to interact with the same regulatory proteins and contain both inhibitory and stimulatory domains,[23] there is considerable variation in their activity depending on the cell model or epithelium being studied.[24] The transport characteristics of NHEs include substrate specificity (Na^+ concentration), ATP dependence, Cl^- dependence, and their sensitivity to a diuretic, amiloride.[25] NHE2 is more sensitive to amiloride (IC_{50} ~ 1μM) as compared to NHE3 (IC_{50} > 100μM).[25] Several potent amiloride derivatives e.g. HOE-694 or specific inhibitors are now being used in experimental studies. Although NHE2 null mice developed chronic gastritis and achlorhydria, they do not have an abnormal intestinal phenotype.[26] Alternatively NHE3 null mice developed moderate diarrhea, abnormal intestinal phenotype and metabolic acidosis.[27] The phenotype of NHE2/NHE3 double knockout mice was similar to NHE3 null mice, consistent with the major role of NHE3 in

intestinal sodium absorption.[28] Interestingly neither NHE2 nor NHE3 was found to compensate for each other in knockout models while other sodium absorptive mechanisms such as ENaC, K^+ channel, and H^+, K^+-ATPase were up regulated.[29] However, one study has shown up-regulation of NHE3 in NHE2 null murine colon.[13] In NHE2 null mice, a Na^+-dependent, 5-(*N*ethyl-*N*-isopropyl) amiloride (EIPA)-sensitive acid extruder mechanism that was distinct from NHE1/3 was found to be up regulated in mouse colonic crypts.[30] In porcine intestine, following small intestinal ischemia, expression of both NHE2 and NHE3 was increased and only selective inhibition of NHE2 was found to improve prostaglandin-mediated intestinal barrier function recovery.[24] We recently studied recovery of intestinal barrier function in mice and found that NHE2 deficient mice had impaired barrier recovery following intestinal ischemia. This phenomenon was found to be associated with re-assembly of intercellular tight junctions in the restituted epithelium following ischemic injury (unpublished data).

In a human congenital disorder called microvillus inclusion disease NHE2 expression was found to be reduced while NHE3 expression was completely absent in duodenal biopsies.[31] However, in another case of congenital diarrhea, Congenital Sodium Diarrhea (CSD) was found to be an autosomal recessive disorder unrelated to mutations in either NHE2 or NHE3.[32]

Acute regulation of NHE2 and NHE3 by Protein Kinases and second messengers

Various signal transduction pathways and second messengers regulate NHE2 and NHE3 differentially. Exogenous expression in human intestinal C2/bbe cells revealed inhibition of NHE2 and NHE3 by 8-(4-chlorophenylthio)adenosine 3',5'-cyclic monophosphate, Ca^{++} , and thapsigargin. While serum supplementation stimulated NHE2, cGMP- and protein kinase C had no effect on NHE2; NHE3 was inhibited by Protein Kinase C when activated by phorbol ester.[33,34] NHE3 is inhibited by PKA and PKC, whereas NHE2 appears to be activated by these kinases in transfected PS120 fibroblasts. Protein kinase C (PKC) mediated elevated $[Ca^{2+}]_i$ inhibits NHE3 by increased binding of PKCα and α-actinin-4 to NHERF2 (Sodium hydrogen exchanger regulatory factor 2).[35,36] Sodium-hydrogen exchange regulatory factors are PDZ (post synaptic density protein (PSD95), Drosophila disc large tumor suppressor (DlgA), and zonula occludens-1 protein (ZO-1) domain containing scaffold proteins that connect plasma membrane proteins with members of the ezrin/moesin/radixin family and thereby helps to link them to the actin cytoskeleton. NHE3 inhibition by cAMP in PS120 fibroblasts requires presence of sodium hydrogen exchanger regulatory factor NHERF1 that links NHE3 to the actin cytoskeleton via binding to ezrin. In this case ezrin also acts as a low-affinity protein kinase A anchoring protein (AKAP).[37,38] In the case of cGMP mediated inhibition of NHE3, NHE regulatory factor-2 (NHERF2) acts as a G kinase-anchoring protein (GKAP) forming a complex between NHE3, NHERF2, and cGMP-activated protein kinase II (cGKII). This complex is also anchored to the cellular cytoskeleton via the ezrin-binding domain of NHERF2.[39,40] Different GTPase proteins known to play

integral roles in organization of actin cytoskeleton e.g. Rac1, Cdc42, and RhoA, effect NHE3 regulation.[41] Thus proteins like NHERFs are critical for regulation of NHE3, and this has emerged as a paradigm for multi-protein complexes required for regulation of cellular processes (figure 1). NHE3 also binds to ezrin and in turn the actin cytoskeleton, independent of the PDZ domain containing proteins NHERF1 and NHERF2 at a site in its C terminus between aa 475-589. This direct association of NHE3 with ezrin is important for basal trafficking, including basal exocytosis, delivery from the synthetic pathway and movement of NHE3 in the brush border.[42,43] The association of NHE2 with the cytoskeleton was shown by the interaction of C-terminus proline-rich region with the SH3 domain of a cytoskeletal protein α-spectrin.[44] Another sodium channel ENaC was shown to be targeted to the apical membrane by α-spectrin, and in LLC-PK_1 cells transfected with NHE2, the proline-rich NHE2 C terminal area was found to be necessary for apical localization. Mutation of this region led to targeting of NHE2 to the basolateral membrane.[45] Thus the association with the cytoskeleton seems to be intimately involved in regulation of both NHE2 and 3 isoforms.

In the cytoplasm as well as the plasma membrane NHE3 is present in large protein complexes ranging from 400-1000 Kda. These complexes include various proteins, including NHERF1, NHERF2, PDZK1, Hsc70, DPPIV, PP2A, megalin, and CaM kinase II.[1]. Such large complexes and particularly the association with PDZ domain adaptor proteins are not known to occur in the case of NHE2. Only recently, NHE2 was shown to be immunoprecipitated with EBP50 (ezrin/moesin/radixin binding

protein/NHERF1) and this association was found to be increased during post-ischemic intestinal barrier recovery, indicating possible regulation of NHE2 via EBP50.[24] In contrast to short term regulation of NHE3 by change in protein turnover or by trafficking between cytoplasmic locations and plasma membrane[1], NHE2 is largely known to be regulated specifically by change in turnover. However a recent study has demonstrated translocation of NHE2 from the intracellular pool to the plasma membrane. In transfected PS-120 cells recruitment of NHE2-CFP fusion protein to the plasma membrane was specifically triggered by a decrease in pHi while the recruitment of NHE3-CFP to the plasma membrane was specifically stimulated by removal of external sodium alone.[46] In the case of NHE3, stimulation of trafficking is initiated by increasing exocytosis in the synthesis pathway while inhibitory agents would increase endocytosis. These processes are independent of change in turnover. The mechanisms of NHE3 internalization involve clathrin-coated vesicles and lipid rafts.[47-49] Regulation of NHE3 trafficking and turnover number and the role of NHE3 phosphorylation have been defined. For instance in OK cells the inhibition of NHE3 by PKA-mediated phosphorylation at Ser552 and Ser605 was found to be initiate transient stimulation of turnover number, reduced surface expression, increased endocytosis and decreased exocytosis.[50] Alternatively, either phosphorylation of NHE3 is not involved in the regulation e.g. in case of PKC inhibition[51] or FGF stimulation,[52] or the phosphorylation of Ser residues vary among different cell types in conjunction with other signal transduction pathways.[1]

Genomic regulation of NHE2 and NHE3

The genomic organization of NHE2 and NHE3 has been recently studied. Human NHE2 consists of 12 exons separated by 11 introns.[53] The rat and human NHE2 and NHE3 promoters have GC rich regions; NHE2 but not the NHE3 promoter lack canonical TATA and CCAAT boxes.[53,54] Transcription factor-binding sites in the NHE2 promoter include Sp1, AP-2, CACCC, NF-κB, and Oct-1 while human NHE3 promoter has binding sites for Sp1, AP-2, and glucocoticoid and thyroid response elements.[55,56] There are a few studies focused on transcriptional regulation of NHE2 and NHE3. For example, glucocorticoid treatment significantly increased the luciferase activity of the chimeric NHE3 gene in renal epithelial OK cells and LLC-PK1 cells, thereby indicating that glucocorticoid regulation of NHE3 is mediated primarily by a transcriptional mechanism.[55] *In vivo*, methylprednisolone stimulated ileal brush border Na^+/H^+ exchange in a dose-dependent manner, associated with an increase in NHE3 transcripts.[57] EGF treatment increased NHE2-mediated intestinal brush-border membrane Na^+ absorption and NHE2 mRNA abundance by nearly two-fold in juvenile rats.[58] A study of loop ileostomies created in Sprague-Dawley rats revealed that as early as 8 days after intestinal diversion, NHE-3 gene expression is selectively attenuated in ileal mucosa distal to the ileostomy.[59] Interactions of multiple transcription factors and/or response elements are supposed to either up- or down-regulate NHE mRNA expression and regulate NHE2 and NHE3 genes.[1]

The influence of ion and nutrient transport on NHE2 and NHE3 regulation

The importance of intestinal nutrient absorption via ion transport while maintaining pH and ion gradients was demonstrated when H(+)/solute-induced acidification of Caco-2 cells using glycylsarcosine or beta-alanine selectively activated apical but not basolateral Na^+/H^+ exchange.[60] The overall absorptive response of enterocytes to the luminal nutrients was evident when cytoplasmic alkalinization due to NHE3 activation occurred after initiation of SGLT1-mediated Na^+-glucose cotransport.[61] NHE2 and NHE3 activities, protein expression, and mRNA levels were found to be increased in rats fed with ammonium chloride that produces metabolic acidosis.[62] The Na^+/H^+ exchange is also coupled with bicarbonate transport and probably plays a role in epithelial protection as demonstrated by increased bicarbonate secretion in human duodenum in response to inhibition of NHE isoforms 2 and 3.[63] CFTR, a major channel for bicarbonate secretion in intestine, is believed to regulate NHE3-mediated Na^+ absorption by alteration of epithelial cell volume in the villus.[64] In the distal colon of guinea pig and the HT29-19a cell line, apical Na^+/H^+ exchange had no impact on pH regulation after feeding and treatment with short chain fatty acids (SCFA).[65] However, in human colonic C2/bbe (C2) monolayers and in rats SCFA increased sodium absorption by induction of NHE3.[66] In rat distal colon, the mechanism of HCO_3-stimulated and butyrate-stimulated Na^+ absorption was found to be different. NHE3 mediated HCO_3-stimulated Na^+ absorption, whereas NHE2 or NHE3 mediated butyrate-stimulated Na absorption. Furthermore, dibutyryl cAMP selectively inhibited NHE3 but stimulated NHE2.[67] In rat proximal colon, dietary sodium depletion increased NHE2 and NHE3

isoform-specific Na^+/H^+ exchange activities, protein expression, and mRNA abundance while exactly the opposite effect was seen in distal colon.[12] Among other nutritional influences, acute as well as chronic vitamin D_3 deficiency resulted into the up regulation of NHE3 in rat ileum with no effect on NHE2.[68] Enteral feeding of lectin-phytohemagglutinin to suckling rats induced increased apical Na^+/H^+ exchange and expression of NHE3.[69] Following small bowel resection (SBR) and EGF treatment in mice, NHE3 expression was found to be increased in the remaining ileal segment and this gain in NHE3 expression was lost following salivarectomy implying complimentary mechanisms of enterocyte proliferation and sodium absorption.[70] In another report on small bowel resection in the rat, both NHE2 and NHE3 isoforms were up regulated in the ileum and colon distal to the anastomosis.[5] In PS120 fibroblasts, hyperosmolarity inhibited NHE2 and NHE3, in contrast to the stimulatory effect on the housekeeping isoform NHE1.[23]

Neuro-hormonal regulation of NHE2 and NHE3

Glucocorticoid treatment stimulated rat ileal Na^+ absorptive cell brush border Na^+/H^+ exchange due to increased expression of NHE3, specifically in the villous compartment of epithelial lining.[57,71] Furthermore, the effect of glucocorticoids on NHE3, which was dependent on expression of glucocorticoid receptors, was maximal in the proximal small intestine of suckling rats and distal small intestine of adult rats.[72] NHE3 activity as well as surface expression was increased in PS120 cells and OK cells incubated with basic fibroblast growth factor[73] or epidermal growth factor;[74] dependent at

least partially in both cases on active phosphatidylinositol 3-kinase (PI3-K). Epidermal growth factor (EGF) was also involved in acute regulation of NHE by phosphorylation and long term effects on up regulation of NHE2 via gene transcription.[58] Aldostorone up regulated apical ileal and colonic NHE2 activity in birds[75] while serotonin inhibited activity of both NHE2 and NHE3 isoforms in human intestinal Caco cells.[76] In human colonic adenocarcinoma T84 cells 5-HT enhances intestinal NHE activity, likely mediated by NHE2 and NHE1 isoforms, through stimulation of G(ialpha1,2)-coupled 5-HT(1A) and G(q/11)-coupled 5-HT(2) receptors.[77] The dipeptide transport through H (+)/dipeptide transporter hPepT1 in conjunction with Na^+/H^+ exchanger NHE3 was modulated by Vasoactive Intestinal Peptide (VIP) indirectly through the inhibition of NHE3.[78] In T84 cells the modulation of intracellular pH by angiotensin II (ANG II) was mediated in part via the NHE1 and NHE2 isoforms. ANG II stimulated Na^+/H^+ exchange at lower $[Ca^{++}]i$ levels and inhibited Na^+/H^+ exchange at higher $[Ca^{++}]i$ levels.[79]

NHE2 and NHE3 in intestinal pathophysiology

Following advances in the understanding of NHE physiology, investigation of the role of NHEs under pathophysiological conditions has recently received attention. Studies on NHEs have taken into consideration the aberrant cytokine/chemokine milieu of the intestine in inflammatory conditions. In acute T cell-mediated diarrhea that is associated with increased mucosal expression of the proinflammatory cytokine TNF (Tumor Necrosis Factor), Na^+ absorption is inhibited due to PKCα-mediated activation of TNF which in turn induced internalization of NHE3 from the apical plasma membrane to

the sub-apical region. Inhibition of PKCα prevented NHE3 internalization, Na^+ malabsorption, and diarrhea.[80] Interferon gamma (INF-γ), which is increased in patients with inflammatory bowel disease (IBD), was shown to down-regulate NHE3 mRNA and protein expression in rat intestine and in Caco-2 cells.[81] In an IL-2-deficient mouse colitis model, reduced electroneutral NaCl absorption in the right colon was associated with reduced mRNA and protein levels of NHE3.[82] In a dextran sulfate-treated colitis mice model, NHE inhibition led to decreases in IL-8 mRNA and suppression of activation of the p42/p44 mitogen-activated protein kinase and nuclear factor-kappaB.[83] In Caco-2 cells infected with enteropathogenic *Escherichia coli* (EPEC), differential regulation of NHE was seen. NHE2 and NHE1 were markedly activated and NHE3 was significantly inhibited; both effects were dependent on type III secretion system (TTSS).[84] In further studies, EPEC led activation of NHE2 was found to be PKC mediated and EPEC effector protein EspF was responsible for decreased NHE3 activity.[85,86] So called 'hijacking of cellular mechanisms' occurs in the case of enterotoxigenic *Escherichia coli* (ETEC or Traveler's diarrhea) when the heat-stable toxin of *Esherichia coli* (ST_a) binds to its brush-border receptor, guanylate cyclase C. The latter is also a receptor for the endogenous ligand guanylin. cGMP is generated in the proximity to the complex consisting of NHE3, NHERF2, and cGMP-activated protein kinase II (cGKII) leading to activation of the latter, which phosphorylates NHE3 (figure 3). NHE3 phosphorylation inhibits its activity and contributes to diarrhea because of Na^+ malabsorption.[39,40] In another animal-associated cause of infectious diarrhea, we recently discovered that Turkey astrovirus (TAstV-2) induced Na^+ malabsorptive diarrhea that is associated with redistribution of

apical NHE3. Although total expression of NHE3 in TAstV-2-infected jejunum was not changed, NHE3 was significantly redistributed from the detergent insoluble membrane fraction associated with the cytoskeleton to the detergent soluble membrane fraction (unpublished data). Microbial toxins are also known to cause NHE translocation. For instance *C. difficile* Toxin B caused translocation of the apical NHE3 to the subapical endomembrane compartment in LLC-PK cells by inactivation of Rho-family GTPases that possibly affect interaction of NHE3 with the cytoskeleton through impaired bridging activity of ezrin.[87] In a model pertaining to necrotizing enterocolitis (NEC), the bacterial endotoxin lipopolysaccharide (LPS) was shown to cause a dose-dependent reduction in basolateral NHE1 activity in IEC-6 cells, leading to failure of maintenance of cytoplasmic pH under conditions of extracellular acidosis.[88] Cholera toxin (CT) has varying effects on NHE2 and NHE3. In rat ileal loops exposed to CT, activity of both isoforms was inhibited but protein expression of only NHE3 and not NHE2 was reduced. Removal of CT and supplementation with butyrate restored activity of both isoforms by mechanisms that are unclear.[89] These examples provide evidence for the important role of NHE isoforms in infectious enteritis. A greater understanding of these pathophysiological processes will help to improve intestinal health.

Overall, the understanding of NHE physiology has been greatly benefited by studies on structure, function, gene targeting and regulation of NHE isoforms. The association of NHE3 with several other accessory proteins in large protein complexes has emerged as an important theme not only for gut physiology but as a general mechanism

of regulation for cellular processes. Although such information on NHE2 is lacking, new findings are emerging about the role of NHE2 in gut physiology. Besides NHE2 and NHE3, the contribution other NHE isoforms to gut physiology continues to be investigated. For instance, NHE8 was recently cloned and shown to be expressed along the gastrointestinal tract. Although its physiological function is not yet clear, NHE8 had different Na^+/H^+ exchange kinetics than apical membrane NHE isoforms NHE2 and NHE3.[90,91] Our understanding of intestinal function under normal physiological circumstances as well as in pathophysiological conditions will continue to benefit from advances in knowledge about sodium hydrogen exchange.

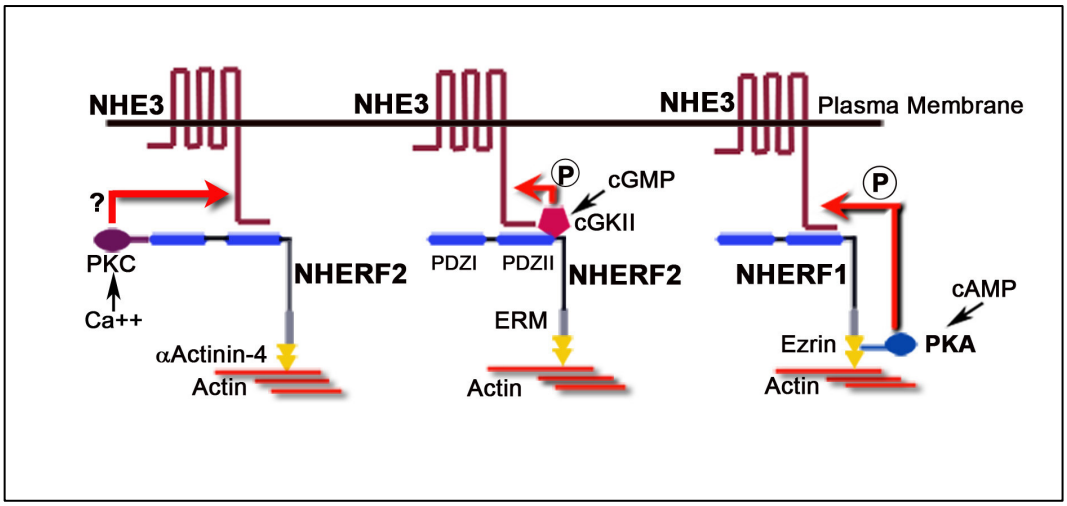

Figure 1. The role of the Na^+/H^+ exchange regulatory factor (NHERF) proteins in NHE3 regulation. NHERFs are the PDZ domain containing scaffold proteins that physically link plasma membrane NHE3 to the cytoskeleton. This link is established through the ezrin-rodexin-myosin (ERM) domain of NHERF binding to ezrin, and ultimately to the actin cytoskeleton. NHERF1 is required for PKA mediated phosphorylation and inhibition of NHE3.[37,38] NHERF2 facilitates cGMP-activated protein kinase II (cGKII)-mediated phosphorylation and inhibition of NHE3.[39,40] The formation of the protein complex consisting of PKCα, NHERF2, and α-Actnin4 is Ca^{++} dependent. Although the downstream target of PKCα is not clear; its activation leads to inhibition of NHE3 by increased endocytosis possibly through involvement of dynamin, AP2, or clathrin coated vescilces.[92]

References

1. Zachos NC, Tse M, Donowitz M. Molecular physiology of intestinal Na+/H+ exchange. Annu.Rev.Physiol. 2005;67:411-443.

2. Fliegel L. The Na+/H+ exchanger isoform 1. Int.J.Biochem.Cell Biol. 2005;37:33-37.

3. Hoogerwerf WA, Tsao SC, Devuyst O, Levine SA, Yun CH, Yip JW, Cohen ME, Wilson PD, Lazenby AJ, Tse CM, Donowitz M. NHE2 and NHE3 are human and rabbit intestinal brush-border proteins. Am.J.Physiol. 1996;270:G29-41.

4. Dudeja PK, Rao DD, Syed I, Joshi V, Dahdal RY, Gardner C, Risk MC, Schmidt L, Bavishi D, Kim KE, Harig JM, Goldstein JL, Layden TJ, Ramaswamy K. Intestinal distribution of human Na+/H+ exchanger isoforms NHE-1, NHE-2, and NHE-3 mRNA. Am.J.Physiol. 1996;271:G483-93.

5. Musch MW, Bookstein C, Rocha F, Lucioni A, Ren H, Daniel J, Xie Y, McSwine RL, Rao MC, Alverdy J, Chang EB. Region-specific adaptation of apical Na/H exchangers after extensive proximal small bowel resection. Am.J.Physiol.Gastrointest.Liver Physiol. 2002;283:G975-85.

6. Akhter S, Kovbasnjuk O, Li X, Cavet M, Noel J, Arpin M, Hubbard AL, Donowitz M. Na(+)/H(+) exchanger 3 is in large complexes in the center of the

apical surface of proximal tubule-derived OK cells. Am.J.Physiol.Cell.Physiol. 2002;283:C927-40.

7. Kurashima K, Szabo EZ, Lukacs G, Orlowski J, Grinstein S. Endosomal recycling of the Na+/H+ exchanger NHE3 isoform is regulated by the phosphatidylinositol 3-kinase pathway. J.Biol.Chem. 1998;273:20828-20836.

8. Janecki AJ, Montrose MH, Tse CM, de Medina FS, Zweibaum A, Donowitz M. Development of an endogenous epithelial Na(+)/H(+) exchanger (NHE3) in three clones of caco-2 cells. Am.J.Physiol. 1999;277:G292-305.

9. Maher MM, Gontarek JD, Jimenez RE, Donowitz M, Yeo CJ. Role of brush border Na+/H+ exchange in canine ileal absorption. Dig.Dis.Sci. 1996;41:651-659.

10. Maher MM, Gontarek JD, Bess RS, Donowitz M, Yeo CJ. The Na+/H+ exchange isoform NHE3 regulates basal canine ileal Na+ absorption in vivo. Gastroenterology 1997;112:174-183.

11. Donowitz M, De La Horra C, Calonge ML, Wood IS, Dyer J, Gribble SM, De Medina FS, Tse CM, Shirazi-Beechey SP, Ilundain AA. In birds, NHE2 is major brush-border Na+/H+ exchanger in colon and is increased by a low-NaCl diet. Am.J.Physiol. 1998;274:R1659-69.

12. Ikuma M, Kashgarian M, Binder HJ, Rajendran VM. Differential regulation of NHE isoforms by sodium depletion in proximal and distal segments of rat colon. Am.J.Physiol. 1999;276:G539-49.

13. Bachmann O, Riederer B, Rossmann H, Groos S, Schultheis PJ, Shull GE, Gregor M, Manns MP, Seidler U. The Na+/H+ exchanger isoform 2 is the predominant NHE isoform in murine colonic crypts and its lack causes NHE3 upregulation. Am.J.Physiol.Gastrointest.Liver Physiol. 2004;287:G125-33.

14. Lamprecht G, Heil A, Baisch S, Lin-Wu E, Yun CC, Kalbacher H, Gregor M, Seidler U. The down regulated in adenoma (dra) gene product binds to the second PDZ domain of the NHE3 kinase A regulatory protein (E3KARP), potentially linking intestinal Cl-/HCO3- exchange to Na+/H+ exchange. Biochemistry 2002;41:12336-12342.

15. Orlowski J, Grinstein S. Diversity of the mammalian sodium/proton exchanger SLC9 gene family. Pflugers Arch. 2004;447:549-565.

16. Zizak M, Cavet ME, Bayle D, Tse CM, Hallen S, Sachs G, Donowitz M. Na(+)/H(+) exchanger NHE3 has 11 membrane spanning domains and a cleaved signal peptide: topology analysis using in vitro transcription/translation. Biochemistry 2000;39:8102-8112.

17. Wells KM, Rao R. The yeast Na+/H+ exchanger Nhx1 is an N-linked glycoprotein. Topological implications. J.Biol.Chem. 2001;276:3401-3407.

18. Sardet C, Franchi A, Pouyssegur J. Molecular cloning, primary structure, and expression of the human growth factor-activatable Na+/H+ antiporter. Cell 1989;56:271-280.

19. Levine SA, Montrose MH, Tse CM, Donowitz M. Kinetics and regulation of three cloned mammalian Na+/H+ exchangers stably expressed in a fibroblast cell line. J.Biol.Chem. 1993;268:25527-25535.

20. Orlowski J. Heterologous expression and functional properties of amiloride high affinity (NHE-1) and low affinity (NHE-3) isoforms of the rat Na/H exchanger. J.Biol.Chem. 1993;268:16369-16377.

21. Yu FH, Shull GE, Orlowski J. Functional properties of the rat Na/H exchanger NHE-2 isoform expressed in Na/H exchanger-deficient Chinese hamster ovary cells. J.Biol.Chem. 1993;268:25536-25541.

22. Knickelbein R, Aronson PS, Atherton W, Dobbins JW. Sodium and chloride transport across rabbit ileal brush border. I. Evidence for Na-H exchange. Am.J.Physiol. 1983;245:G504-10.

23. Nath SK, Hang CY, Levine SA, Yun CH, Montrose MH, Donowitz M, Tse CM. Hyperosmolarity inhibits the Na+/H+ exchanger isoforms NHE2 and NHE3: an effect opposite to that on NHE1. Am.J.Physiol. 1996;270:G431-41.

24. Moeser AJ, Nighot PK, Ryan KA, Wooten JG, Blikslager AT. Prostaglandin-mediated inhibition of Na+/H+ exchanger isoform 2 stimulates recovery of barrier

function in ischemia-injured intestine. Am.J.Physiol.Gastrointest.Liver Physiol. 2006;291:G885-94.

25. Kiela PR, Xu H, Ghishan FK. Apical NA+/H+ exchangers in the mammalian gastrointestinal tract. J.Physiol.Pharmacol. 2006;57 Suppl 7:51-79.

26. Schultheis PJ, Clarke LL, Meneton P, Harline M, Boivin GP, Stemmermann G, Duffy JJ, Doetschman T, Miller ML, Shull GE. Targeted disruption of the murine Na+/H+ exchanger isoform 2 gene causes reduced viability of gastric parietal cells and loss of net acid secretion. J.Clin.Invest. 1998;101:1243-1253.

27. Gawenis LR, Stien X, Shull GE, Schultheis PJ, Woo AL, Walker NM, Clarke LL. Intestinal NaCl transport in NHE2 and NHE3 knockout mice. Am.J.Physiol.Gastrointest.Liver Physiol. 2002;282:G776-84.

28. Ledoussal C, Woo AL, Miller ML, Shull GE. Loss of the NHE2 Na(+)/H(+) exchanger has no apparent effect on diarrheal state of NHE3-deficient mice. Am.J.Physiol.Gastrointest.Liver Physiol. 2001;281:G1385-96.

29. Spicer Z, Clarke LL, Gawenis LR, Shull GE. Colonic H(+)-K(+)-ATPase in K(+) conservation and electrogenic Na(+) absorption during Na(+) restriction. Am.J.Physiol.Gastrointest.Liver Physiol. 2001;281:G1369-77.

30. Guan Y, Dong J, Tackett L, Meyer JW, Shull GE, Montrose MH. NHE2 is the main apical NHE in mouse colonic crypts but an alternative Na+-dependent acid

extrusion mechanism is upregulated in NHE2-null mice. Am.J.Physiol.Gastrointest.Liver Physiol. 2006;291:G689-99.

31. Michail S, Collins JF, Xu H, Kaufman S, Vanderhoof J, Ghishan FK. Abnormal expression of brush-border membrane transporters in the duodenal mucosa of two patients with microvillus inclusion disease. J.Pediatr.Gastroenterol.Nutr. 1998;27:536-542.

32. Muller T, Wijmenga C, Phillips AD, Janecke A, Houwen RH, Fischer H, Ellemunter H, Fruhwirth M, Offner F, Hofer S, Muller W, Booth IW, Heinz-Erian P. Congenital sodium diarrhea is an autosomal recessive disorder of sodium/proton exchange but unrelated to known candidate genes. Gastroenterology 2000;119:1506-1513.

33. McSwine RL, Musch MW, Bookstein C, Xie Y, Rao M, Chang EB. Regulation of apical membrane Na+/H+ exchangers NHE2 and NHE3 in intestinal epithelial cell line C2/bbe. Am.J.Physiol. 1998;275:C693-701.

34. Bookstein C, Musch MW, Xie Y, Rao MC, Chang EB. Regulation of intestinal epithelial brush border Na(+)/H(+) exchanger isoforms, NHE2 and NHE3, in C2bbe cells. J.Membr.Biol. 1999;171:87-95.

35. Cha B, Oh S, Shanmugaratnam J, Donowitz M, Yun CC. Two histidine residues in the juxta-membrane cytoplasmic domain of Na+/H+ exchanger isoform 3 (NHE3) determine the set point. J.Membr.Biol. 2003;191:49-58.

36. Lee-Kwon W, Kim JH, Choi JW, Kawano K, Cha B, Dartt DA, Zoukhri D, Donowitz M. Ca2+-dependent inhibition of NHE3 requires PKC alpha which binds to E3KARP to decrease surface NHE3 containing plasma membrane complexes. Am.J.Physiol.Cell.Physiol. 2003;285:C1527-36.

37. Yun CH, Lamprecht G, Forster DV, Sidor A. NHE3 kinase A regulatory protein E3KARP binds the epithelial brush border Na+/H+ exchanger NHE3 and the cytoskeletal protein ezrin. J.Biol.Chem. 1998;273:25856-25863.

38. Yun CH, Oh S, Zizak M, Steplock D, Tsao S, Tse CM, Weinman EJ, Donowitz M. cAMP-mediated inhibition of the epithelial brush border Na+/H+ exchanger, NHE3, requires an associated regulatory protein. Proc.Natl.Acad.Sci.U.S.A. 1997;94:3010-3015.

39. Barrett KE. New ways of thinking about (and teaching about) intestinal epithelial function. Adv.Physiol.Educ. 2008;32:25-34.

40. Donowitz M, Cha B, Zachos NC, Brett CL, Sharma A, Tse CM, Li X. NHERF family and NHE3 regulation. J.Physiol. 2005;567:3-11.

41. Kurashima K, D'Souza S, Szaszi K, Ramjeesingh R, Orlowski J, Grinstein S. The apical Na(+)/H(+) exchanger isoform NHE3 is regulated by the actin cytoskeleton. J.Biol.Chem. 1999;274:29843-29849.

42. Cha B, Tse M, Yun C, Kovbasnjuk O, Mohan S, Hubbard A, Arpin M, Donowitz M. The NHE3 juxtamembrane cytoplasmic domain directly binds ezrin: dual role

in NHE3 trafficking and mobility in the brush border. Mol.Biol.Cell 2006;17:2661-2673.

43. Cha B, Donowitz M. The epithelial brush border Na(+)/H(+) exchanger NHE3 associates with the actin cytoskeleton by binding to ezrin directly and via PDZ domain containing Na(+)/H(+) exchanger regulatory factor (NHERF) proteins. Clin.Exp.Pharmacol.Physiol. 2008;.

44. Chow CW, Woodside M, Demaurex N, Yu FH, Plant P, Rotin D, Grinstein S, Orlowski J. Proline-rich motifs of the Na+/H+ exchanger 2 isoform. Binding of Src homology domain 3 and role in apical targeting in epithelia. J.Biol.Chem. 1999;274:10481-10488.

45. Mailander J, Muller-Esterl W, Dedio J. Human homolog of mouse tescalcin associates with Na(+)/H(+) exchanger type-1. FEBS Lett. 2001;507:331-335.

46. Gens JS, Du H, Tackett L, Kong SS, Chu S, Montrose MH. Different ionic conditions prompt NHE2 and NHE3 translocation to the plasma membrane. Biochim.Biophys.Acta 2007;1768:1023-1035.

47. Silviani V, Colombani V, Heyries L, Gerolami A, Cartouzou G, Marteau C. Role of the NHE3 isoform of the Na+/H+ exchanger in sodium absorption by the rabbit gallbladder. Pflugers Arch. 1996;432:791-796.

48. Chow CW, Khurana S, Woodside M, Grinstein S, Orlowski J. The epithelial Na(+)/H(+) exchanger, NHE3, is internalized through a clathrin-mediated pathway. J.Biol.Chem. 1999;274:37551-37558.

49. Li X, Galli T, Leu S, Wade JB, Weinman EJ, Leung G, Cheong A, Louvard D, Donowitz M. Na+-H+ exchanger 3 (NHE3) is present in lipid rafts in the rabbit ileal brush border: a role for rafts in trafficking and rapid stimulation of NHE3. J.Physiol. 2001;537:537-552.

50. Zhao H, Wiederkehr MR, Fan L, Collazo RL, Crowder LA, Moe OW. Acute inhibition of Na/H exchanger NHE-3 by cAMP. Role of protein kinase a and NHE-3 phosphoserines 552 and 605. J.Biol.Chem. 1999;274:3978-3987.

51. Wiederkehr MR, Zhao H, Moe OW. Acute regulation of Na/H exchanger NHE3 activity by protein kinase C: role of NHE3 phosphorylation. Am.J.Physiol. 1999;276:C1205-17.

52. Yip JW, Ko WH, Viberti G, Huganir RL, Donowitz M, Tse CM. Regulation of the epithelial brush border Na+/H+ exchanger isoform 3 stably expressed in fibroblasts by fibroblast growth factor and phorbol esters is not through changes in phosphorylation of the exchanger. J.Biol.Chem. 1997;272:18473-18480.

53. Muller YL, Collins JF, Bai L, Xu H, Ghishan FK. Molecular cloning and characterization of the rat NHE-2 gene promoter. Biochim.Biophys.Acta 1998;1442:314-319.

54. Malakooti J, Memark VC, Dudeja PK, Ramaswamy K. Molecular cloning and functional analysis of the human Na(+)/H(+) exchanger NHE3 promoter. Am.J.Physiol.Gastrointest.Liver Physiol. 2002;282:G491-500.

55. Kandasamy RA, Orlowski J. Genomic organization and glucocorticoid transcriptional activation of the rat Na+/H+ exchanger Nhe3 gene. J.Biol.Chem. 1996;271:10551-10559.

56. Malakooti J, Dahdal RY, Dudeja PK, Layden TJ, Ramaswamy K. The human Na(+)/H(+) exchanger NHE2 gene: genomic organization and promoter characterization. Am.J.Physiol.Gastrointest.Liver Physiol. 2001;280:G763-73.

57. Yun CH, Gurubhagavatula S, Levine SA, Montgomery JL, Brant SR, Cohen ME, Cragoe EJ,Jr, Pouyssegur J, Tse CM, Donowitz M. Glucocorticoid stimulation of ileal Na+ absorptive cell brush border Na+/H+ exchange and association with an increase in message for NHE-3, an epithelial Na+/H+ exchanger isoform. J.Biol.Chem. 1993;268:206-211.

58. Xu H, Collins JF, Bai L, Kiela PR, Lynch RM, Ghishan FK. Epidermal growth factor regulation of rat NHE2 gene expression. Am.J.Physiol.Cell.Physiol. 2001;281:C504-13.

59. Doble MA, Tola VB, Chamberlain SA, Cima RR, Van Hoek A, Soybel DI. Luminal regulation of Na(+)/H(+) exchanger gene expression in rat ileal mucosa. J.Gastrointest.Surg. 2002;6:387-395.

60. Thwaites DT, Ford D, Glanville M, Simmons NL. H(+)/solute-induced intracellular acidification leads to selective activation of apical Na(+)/H(+) exchange in human intestinal epithelial cells. J.Clin.Invest. 1999;104:629-635.

61. Turner JR, Black ED. NHE3-dependent cytoplasmic alkalinization is triggered by Na(+)-glucose cotransport in intestinal epithelia. Am.J.Physiol.Cell.Physiol. 2001;281:C1533-41.

62. Lucioni A, Womack C, Musch MW, Rocha FL, Bookstein C, Chang EB. Metabolic acidosis in rats increases intestinal NHE2 and NHE3 expression and function. Am.J.Physiol.Gastrointest.Liver Physiol. 2002;283:G51-6.

63. Repishti M, Hogan DL, Pratha V, Davydova L, Donowitz M, Tse CM, Isenberg JI. Human duodenal mucosal brush border Na(+)/H(+) exchangers NHE2 and NHE3 alter net bicarbonate movement. Am.J.Physiol.Gastrointest.Liver Physiol. 2001;281:G159-63.

64. Gawenis LR, Franklin CL, Simpson JE, Palmer BA, Walker NM, Wiggins TM, Clarke LL. cAMP inhibition of murine intestinal Na/H exchange requires CFTR-mediated cell shrinkage of villus epithelium. Gastroenterology 2003;125:1148-1163.

65. Busche R, Bartels J, Genz AK, von Engelhardt W. Effect of SCFA on intracellular pH and intracellular pH regulation of guinea-pig caecal and colonic

enterocytes and of HT29-19a monolayers. Comp.Biochem.Physiol.A Physiol. 1997;118:395-398.

66. Musch MW, Bookstein C, Xie Y, Sellin JH, Chang EB. SCFA increase intestinal Na absorption by induction of NHE3 in rat colon and human intestinal C2/bbe cells. Am.J.Physiol.Gastrointest.Liver Physiol. 2001;280:G687-93.

67. Krishnan S, Rajendran VM, Binder HJ. Apical NHE isoforms differentially regulate butyrate-stimulated Na absorption in rat distal colon. Am.J.Physiol.Cell.Physiol. 2003;285:C1246-54.

68. Gill R, Nazir TM, Wali R, Sitrin M, Brasitus TA, Ramaswamy K, Dudeja PK. Regulation of rat ileal NHE3 by 1,25(OH)2-vitamin D3. Dig.Dis.Sci. 2002;47:1169-1174.

69. Kruszewska D, Kiela P, Ljungh A, Erlwanger KH, Westrom BR, Linderoth A, Pierzynowski SG. Enteral crude red kidney bean (Phaseolus vulgaris) lectin--phytohemagglutinin--induces maturational changes in the enterocyte membrane proteins of suckling rats. Biol.Neonate 2003;84:152-158.

70. Falcone RA,Jr, Shin CE, Stern LE, Wang Z, Erwin CR, Soleimani M, Warner BW. Differential expression of ileal Na(+)/H(+) exchanger isoforms after enterectomy. J.Surg.Res. 1999;86:192-197.

71. Cho JH, Musch MW, DePaoli AM, Bookstein CM, Xie Y, Burant CF, Rao MC, Chang EB. Glucocorticoids regulate Na+/H+ exchange expression and activity in region- and tissue-specific manner. Am.J.Physiol. 1994;267:C796-803.

72. Kiela PR, Guner YS, Xu H, Collins JF, Ghishan FK. Age- and tissue-specific induction of NHE3 by glucocorticoids in the rat small intestine. Am.J.Physiol.Cell.Physiol. 2000;278:C629-37.

73. Janecki AJ, Janecki M, Akhter S, Donowitz M. Basic fibroblast growth factor stimulates surface expression and activity of Na(+)/H(+) exchanger NHE3 via mechanism involving phosphatidylinositol 3-kinase. J.Biol.Chem. 2000;275:8133-8142.

74. Li X, Zhang H, Cheong A, Leu S, Chen Y, Elowsky CG, Donowitz M. Carbachol regulation of rabbit ileal brush border Na+-H+ exchanger 3 (NHE3) occurs through changes in NHE3 trafficking and complex formation and is Src dependent. J.Physiol. 2004;556:791-804.

75. De La Horra MC, Cano M, Peral MJ, Calonge ML, Ilundain AA. Hormonal regulation of chicken intestinal NHE and SGLT-1 activities. Am.J.Physiol.Regul.Integr.Comp.Physiol. 2001;280:R655-60.

76. Gill RK, Saksena S, Tyagi S, Alrefai WA, Malakooti J, Sarwar Z, Turner JR, Ramaswamy K, Dudeja PK. Serotonin inhibits Na+/H+ exchange activity via 5-

HT4 receptors and activation of PKC alpha in human intestinal epithelial cells. Gastroenterology 2005;128:962-974.

77. Magro F, Fraga S, Soares-da-Silva P. Short-term effect on intestinal epithelial Na(+)/H(+) exchanger by Gi(alpha1,2)-coupled 5-HT(1A) and G(q/11)-coupled 5-HT(2) receptors. Life Sci. 2007;81:560-569.

78. Anderson CM, Mendoza ME, Kennedy DJ, Raldua D, Thwaites DT. Inhibition of intestinal dipeptide transport by the neuropeptide VIP is an anti-absorptive effect via the VPAC1 receptor in a human enterocyte-like cell line (Caco-2). Br.J.Pharmacol. 2003;138:564-573.

79. Musa-Aziz R, Mello-Aires M. Action of ANG II and ANP on colon epithelial cells. Pflugers Arch. 2005;450:405-414.

80. Clayburgh DR, Musch MW, Leitges M, Fu YX, Turner JR. Coordinated epithelial NHE3 inhibition and barrier dysfunction are required for TNF-mediated diarrhea in vivo. J.Clin.Invest. 2006;116:2682-2694.

81. Rocha F, Musch MW, Lishanskiy L, Bookstein C, Sugi K, Xie Y, Chang EB. IFN-gamma downregulates expression of Na(+)/H(+) exchangers NHE2 and NHE3 in rat intestine and human Caco-2/bbe cells. Am.J.Physiol.Cell.Physiol. 2001;280:C1224-32.

82. Barmeyer C, Harren M, Schmitz H, Heinzel-Pleines U, Mankertz J, Seidler U, Horak I, Wiedenmann B, Fromm M, Schulzke JD. Mechanisms of diarrhea in the

interleukin-2-deficient mouse model of colonic inflammation. Am.J.Physiol.Gastrointest.Liver Physiol. 2004;286:G244-52.

83. Nemeth ZH, Deitch EA, Szabo C, Mabley JG, Pacher P, Fekete Z, Hauser CJ, Hasko G. Na+/H+ exchanger blockade inhibits enterocyte inflammatory response and protects against colitis. Am.J.Physiol.Gastrointest.Liver Physiol. 2002;283:G122-32.

84. Hecht G, Hodges K, Gill RK, Kear F, Tyagi S, Malakooti J, Ramaswamy K, Dudeja PK. Differential regulation of Na+/H+ exchange isoform activities by enteropathogenic E. coli in human intestinal epithelial cells. Am.J.Physiol.Gastrointest.Liver Physiol. 2004;287:G370-8.

85. Hodges K, Gill R, Ramaswamy K, Dudeja PK, Hecht G. Rapid activation of Na+/H+ exchange by EPEC is PKC mediated. Am.J.Physiol.Gastrointest.Liver Physiol. 2006;291:G959-68.

86. Hodges K, Alto NM, Ramaswamy K, Dudeja PK, Hecht G. The enteropathogenic Escherichia coli effector protein EspF decreases sodium hydrogen exchanger 3 activity. Cell.Microbiol. 2008;.

87. Hayashi H, Szaszi K, Coady-Osberg N, Furuya W, Bretscher AP, Orlowski J, Grinstein S. Inhibition and redistribution of NHE3, the apical Na+/H+ exchanger, by Clostridium difficile toxin B. J.Gen.Physiol. 2004;123:491-504.

88. Cetin S, Dunklebarger J, Li J, Boyle P, Ergun O, Qureshi F, Ford H, Upperman J, Watkins S, Hackam DJ. Endotoxin differentially modulates the basolateral and apical sodium/proton exchangers (NHE) in enterocytes. Surgery 2004;136:375-383.

89. Subramanya SB, Rajendran VM, Srinivasan P, Nanda Kumar NS, Ramakrishna BS, Binder HJ. Differential regulation of cholera toxin-inhibited Na-H exchange isoforms by butyrate in rat ileum. Am.J.Physiol.Gastrointest.Liver Physiol. 2007;293:G857-63.

90. Xu H, Chen R, Ghishan FK. Subcloning, localization, and expression of the rat intestinal sodium-hydrogen exchanger isoform 8. Am.J.Physiol.Gastrointest.Liver Physiol. 2005;289:G36-41.

91. Xu H, Chen H, Dong J, Lynch R, Ghishan FK. Gastrointestinal distribution and kinetic characterization of the sodium-hydrogen exchanger isoform 8 (NHE8). Cell.Physiol.Biochem. 2008;21:109-116.

92. Lamprecht G, Seidler U. The emerging role of PDZ adapter proteins for regulation of intestinal ion transport. Am J Physiol Gastrointest Liver Physiol. 2006;291:G766-77.

CHAPTER III

ClC-2 IS REQUIRED FOR RAPID RESTORATION OF EPITHELIAL TIGHT JUNCTIONS IN ISCHEMIC-INJURED ILEUM.

Abstract. Intestinal barrier function is compromised by ischemic injury. Involvement of ion transporters in barrier recovery has been described in recent studies. The aim of the present study was to investigate mechanisms of intestinal barrier repair following ischemic injury in ClC-$2^{-/-}$ mice. Wild type, ClC-2 heterozygous and ClC-2 null murine ileal mucosa was subjected to complete ischemia, after which recovery of barrier function was monitored by measuring *in vivo* blood-to-lumen clearance of mannitol. Tissues were examined by light and electron microscopy. The role of ClC-2 in reassembly of the tight junction during barrier recovery was studied by immunoblotting, immunolocalization and immunoprecipitation. Following ischemic injury, ClC-$2^{-/-}$ mice were found to have impaired barrier recovery compared to wild type mice, defined by increases in epithelial paracellular permeability that were independent of epithelial restitution. The recovering ClC-$2^{-/-}$ mucosa also had evidence of ultrastructural paracellular defects. The tight junction proteins occludin and claudin-1 shifted significantly to the detergent soluble membrane fraction during post-ischemic recovery in ClC-$2^{-/-}$ mice whereas wild type mice had a greater proportion of junctional proteins in the detergent insoluble fraction. Occludin was co-immunoprecipitated with ClC-2 in uninjured wild type mucosa, and the association between occludin and ClC-2 was re-established during ischemic recovery. Based on immunofluorescence studies, re-localization of occludin from diffuse sub apical areas to apical tight junctions was dramatically impaired in ClC-$2^{-/-}$ mice. These data demonstrate a pivotal role of ClC-2 in recovery of the intestinal epithelium barrier by anchoring assembly of tight junctions following ischemic injury.

Keywords: Tight junction, Intestinal permeability, Ischemia, ClC-2

Introduction.

The single layer of epithelium lining the gastrointestinal tract selectively transports solutes while preventing the entrance of noxious luminal contents. This gut barrier function is largely attributable to the apical intraepithelial tight junctions (TJ). The tight junctions consist of an array of membrane spanning proteins (e.g. occludin and claudins) linked by cytoplasmic plaque proteins such as zonula occludens-1 to the cytoskeleton.[1,2] Recent studies emphasizing the dynamic nature of tight junctions have shown that tight junctions can be regulated to alter solute absorption and barrier properties.[1,3-4] With ever increasing knowledge of the constituents of the tight junctional complex, tight junctions are now considered as a signaling platform for diverse processes such as cell polarity, proliferation, and differentiation.[5]

Intestinal ischemic injury is a leading cause of death in critically ill patients because of the onset of sepsis as the damaged intestinal barrier becomes permeable to bacterial toxins.[6,7] After mucosal injury, closing of paracellular space is crucial for recovery of epithelial barrier; epithelial restitution alone is ineffective without closure of paracellular space. Recovery of the epithelial barrier is mostly synonymous with recovery of tight junctions in the small intestine, which is achieved by recruitment of junctional proteins such as occludin to the apical intercellular space.[8-14] In our previous *ex vivo* experiments we have shown that inhibition of ClC-2 impairs recovery of barrier function in ischemic-injured porcine ileum, and the ClC-2 agonist lubiprostone stimulates barrier recovery through assembly of tight junctions.[12,15]

The ClC-2 channel is broadly expressed in a variety of mammalian secretory epithelia and epithelial cell lines but its role in Cl^- transport and fluid secretion is relatively minor.[16-18] ClC-2 is a member of ClC family of anion channels, and is activated upon hyperpolarization, acidic extracellular pH, and osmotic cell swelling.[18-20] The ubiquitously expressed ClC-2 channels serve organ and tissue specific functional roles e.g. inhibitory GABA responses in neurons or gastric chloride secretion.[21-22] ClC-2 deficient mice lack overt abnormalities except retinal and testicular degeneration; both tissue types depend heavily on supporting cells (retinal pigment epithelium and Sertoli cells, respectively) suggesting a role of ClC-2 in ionic homeostasis.[23] ClC-2 was originally of interest in intestinal disease as a candidate rescue channel for cystic fibrosis. However, disruption of ClC-2 Cl^- channel expression in CFTR mouse models did not exacerbate cystic fibrosis phenotype.[24] This data was based on a putative basolateral location of ClC-2 in large intestine as suggested by using chamber experiments. Evidence is now emerging about regulation of ClC-2 under various physiological and pathophysiological conditions. ClC-2 activity reportedly increases in response to acute oxidative or metabolic stress and is regulated by the cholesterol membrane environment.[25] The CLH-3 homologue in *C. elegans* and mammalian ClC-2 are suggested to play important roles in cell-cell interactions, communication, and regulation of cell cycle-dependent physiological processes.[26] ClC-2 is expressed predominantly at M phase in cells and is regulated at the post- transcriptional level by phosphorylation-dependent ubiquitination.[27] The role of ClC-2 in tumorigenesis is also being defined. For example, proliferation of a human glioma cell line was inhibited by treatment with CIC-2

siRNA.[28] Thus specific and diverse functions of ClC-2 and its differential regulation are currently being described. In murine small intestine, ClC-2 protein is predominantly localized to the apical tight junction[16,17] and this curious localization is supposed to be advantageous for innate ClC-2 activity as well as its regulatory interactions with signaling molecules in the tight junction complex.[29] The objective of the present experiments was to investigate the role of ClC-2 in mucosal repair in ischemic intestine utilizing ClC-2 knockout mice.

Methods

Experimental Animals.

All studies were approved by the North Carolina State University Institutional Animal Care and Use Committee. ClC-2 null ($ClC\text{-}2^{-/-}$), heterozygous ($ClC\text{-}2^{+/-}$), and wild type ($ClC\text{-}2^{+/+}$) mice 2 to 4 months-of-age were used for this study. The generation of ClC-2 knock out mice is described elsewhere.[30] All mice were maintained on a standard laboratory diet. The progeny mice were genotyped by PCR using primers specific for amplification of either intact or disrupted murine ClC-2 alleles. For amplification of wild type and disrupted alleles, two discriminating forward primers (wild type ClC-2 ; 5'- ATG TAT GGC CGG TAC ACT CAG GAA CTC-3', disrupted ClC-2; 5'- CCT GGA AGG TGC CAC TCC CAC TGT CC-3') and a reverse primer (5'- ACA CCC AGG TCC CTG CCC CAA TCT GG-3') were used simultaneously in PCR to yield a wild type ClC-2 product of 200 bp and disrupted ClC-2 product of 300 bp. PCR was

carried out using a BioRad iCycler and a 25µl reaction volume of Promega GoTaq Green Mastermix, according to the manufacturer's instructions. The final concentration of primers was 2.5µM for each of the wild type and disrupted ClC-2 forward primers, and 5µM of the reverse primer. PCR was performed at the following temperature profiles: initial denaturation at 94^0C for 5-min, denaturation at 94^0C for 30 sec, annealing at 60^0C for 30-sec, and extension at 72^0C for 45-sec. The total number of cycles were 35, followed by a final extension for 2-min at 72^0C. PCR products were separated by agarose gel electrophoresis and visualized under UV light after staining with ethidium bromide.

Experimental Surgery.

Mice had unrestricted access to water but were held off feed six hours prior to the experimental surgery. The mice were subjected to general anesthesia using isoflurane (4% for induction and 1.5% for maintenance), and prepared for surgery using aseptic technique. The mid-ileum was approached via a midline laparotomy incision. Intestinal loops 2cm in length were delineated with Doyen intestinal forceps, and complete ischemia was induced by clamping the mesenteric blood supply with Johns Hopkins Bulldog clamps. Following 45-minutes of ischemia, clamps were removed and the abdomen was closed using 4-0 silk for the midline and staples for the skin. The mice were allowed to recover for either 1.5 or 3-hours in heated cages.

***In vivo* blood-to-lumen ^{3}H-mannitol clearance.**

Following the recovery period, mice were re-anesthetized using the same technique as before, after which the abdomen was opened and ischemic and control intestinal segments were ligated with 4-0 silk. Control and ischemic loops were injected with 0.25ml buffered saline (pH 7.4), followed by 0.2ml buffered saline containing ^{3}H-mannitol (10μCi/ml) into the tail vein. Time zero blood samples (0.3ml) were collected via retro-orbital bleeding into heparinized vials. Throughout the experimental procedures body temperature was maintained by retaining abdominal contents within the body wall, and by using water-circulated heating pads and solar blankets. The body temperature was monitored and maintained at 36.5-37.5^{0}C. Blood samples were taken again after one hour. Mice were euthanized, intestinal segments were weighed and intestinal perfusates from each loop were emptied into microcentrifuge tubes. The volume of intestinal perfusate was recorded and the perfusates were saved in scintillation fluid. The blood samples were centrifuged at 14,000 RPM for 4-minutes and 25μl of plasma was saved in scintillation fluid. The plasma and intestinal perfusate samples were assessed for β emission in a scintillation beta counter, and the ^{3}H mannitol clearance was calculated based on modification of formula provided by Komatsu *et al*.,[31] as:

$$\text{Clearance (ml/hr)} = \frac{\text{(CPM, perfusate) / Volume of perfusate (ml)}}{\text{((CPM, plasma time 0) – (CPM, plasma, 1-hour))/0.025}}$$

Histological and electron microscopic examination.

Tissues from control and ischemic-injured intestinal loops were collected in 10% neutral buffered formalin for histological evaluation. From parallel experiments, tissues were also collected immediately after the ischemic period of 45- minutes. Tissues were sectioned (5μm) and stained with hematoxylin and eosin. For each tissue, 3 sections were evaluated. Three well oriented villi and crypts were identified in each of 3 serial sections. Villus length, villus width, and crypt depth was obtained using a micrometer in the eye piece of a light microscope. The surface area of the villus was calculated using the formula for the surface area of a cylinder. The formula was modified by subtracting the area of the base of the villus, and multiplying by a factor accounting for the variable position at which each villus was cross sectioned. The percentage of the villous surface area that remained denuded was calculated and the percent denuded villous surface area was used as an index of epithelial restitution, as described earlier.[32]

For electron microscopy, ileal tissues were fixed in McDowell's and Trump's 4F:1G fixative and processed for transmission electron microscopy using standard techniques.[33] In brief, after 2 rinses in 0.1M sodium phosphate buffer (pH 7.2), samples were placed in 1% osmium tetroxide in the same buffer for 1hr at room temperature. Samples were rinsed 2 times in distilled water and dehydrated in an ethanolic series culminating in two changes of 100% acetone. Tissues were then placed in a mixture of spurr resin and acetone for 30 min, followed by 2hr in 100% resin with 2 changes. Finally, samples were placed in fresh 100% resin in molds and polymerized at 70^{o} C for 8 hrs to 3 days. Semi-

thin (0.25-0.5 µm) sections were cut with glass knives and stained with 1% toluidine blue-O in 1% sodium borate. Ultra thin (70-90nm) sections were cut with a diamond knife, stained with methanolic uranyl acetate followed by lead citrate and examined with a transmission electron microscope (Phillips/FEICO Model 208s; Hillsboro, OR).

Gel electrophoresis and Western blotting.

Mucosal scrapings from control and ischemic-injured intestinal loops were snap frozen and stored at -70°C before SDS-PAGE. Tissue aliquots were thawed at 4°C and added to chilled lysis buffer, including protease inhibitors (0.5mM Pefabloc, 0.1mM 4-nitrophenyl phosphate, 0.04mM glycerophosphate, 0.1mM Na3VO4, 40µg/ml bestatin, 2µg/ml aprotinin, 0.54µg/ml leupeptin, and 0.7µg/ml pepstatin A) at 4°C. This mixture was homogenized on ice and then centrifuged at 4°C, and the supernatant was saved. Protein analysis of extract aliquots was performed (BCA Protein Assay Kit, Pierce). Tissue extracts (amounts equalized by protein concentration) were mixed with an equal volume of 2 × SDS-PAGE sample buffers and boiled for 4 min. Lysates were loaded on a 10% SDS polyacrylamide gel, and electrophoresis was carried out according to standard protocols. Proteins were transferred to a PVDF membrane (Immobilon, Millipore, Billerica, MA) by using an electroblotting minitransfer apparatus. Membranes were blocked at room temperature for 2-hours in Tris-buffered saline plus 0.05% Tween 20 (TBST) and 5% dry powdered milk, and then incubated overnight in primary antibody at 4^0C. (Goat polyclonal anti-occludin or goat polyclonal claudin-1, Santa Cruz Biotech. Inc, CA). After washings in TBST, membranes were incubated with horseradish

peroxidase conjugated secondary antibody, and developed for visualization of protein with luminol enhancer solution (Pierce, Rockford IL). For preparation of detergent soluble and detergent insoluble fractions of intestinal mucosa, the mucosal samples were extracted in lysis buffer (20mM Tris, 5mM $MgCl_2$, 0.3mM EGTA, 210µg/ml sodium fluoride, 18.5µg/ml sodium orthovandate, 30mM sodium pyrophosphate, and Complete mini Protease inhibitor cocktail tablet (Pierce)). Following brief centrifugation to remove debris, Triton X-100 soluble and insoluble fractions were collected by incubation and centrifugation (50,000rpm for 30 min at 4^0C) with lysis buffer containing 0.5% Triton X-100 and 0.5% SDS, respectively. The samples were processed through SDS sample preparation kit (Pierce) and protein assay was performed before proceeding for western blotting.

Immunoprecipitation.

Tissue extracts were prepared according to the Western blotting protocol described previously. Equal amount of proteins were diluted in PBS (pH 7.4) with Protease Inhibitor cocktail tablet, and pre cleared with protein A/G-agarose beads (Santa Cruz Biotechnology, CA) and normal rabbit IgG. After pelleting the beads, the supernatant was incubated with rabbit polyclonal ClC-2 antibody (Alpha Diagnostics, TX) or normal Rabbit IgG (Santa Cruz Biotechnology) for 2-hours at 4^0C. The antibody- protein complexes were adsorbed from solution with protein A/G Agarose beads by overnight incubation at 4^0C. The pellets were washed three times in ice cold RIPA buffer and PBS each. The pellets were solubilised in 2×SDS-PAGE sample buffer and electrophoresis

was carried out according to standard procedures described previously. Nitrocellulose membranes were incubated with goat polyclonal anti-occludin antibody (Santa cruz Biotech., CA) or rabbit polyclonal ClC-2 antibody (Alpha Diagnostics, TX) followed by appropriate secondary antibodies. The blot images were analyzed by densitometry using Sigma Scan Pro 5.0 (Sigmatstat, San Jose CA).

Immunofluorescence and confocal microscopy.

Intestinal tissues were embedded in OCT media (Tissue Tek, Sakura, Torrance, CA), frozen, sectioned at 5µm, and stored at -80^0C till use. The sections were thawed, fixed in cold acetone, and blocked with normal goat serum. The sections were incubated with mouse anti-occludin (Zymed, San Francisco, CA) and or rabbit polyclonal ClC-2 (Alpha diagnostics, San Antino, Tx) antibodies diluted in 2% normal goat serum for 90-minutes. Following washes in PBS, the sections were incubated for 60-minutes with goat anti mouse-Alexa Fluor 488 and goat anti rabbit-Cy3 (Invitrogen) antibodies diluted in 5% normal goat serum. The slides were washed in PBS, mounted in fluorescent mounting media (DakoCytomation) and examined with a Nikon Eclipse 2000E inverted microscope equipped with Nikon C1 confocal laser scanning system. Duplicate sections stained similarly but with omission of primary antibodies served as controls.

Statistical analysis.

Data were reported as means ± SE. All data were analyzed by using an ANOVA for repeated measures (Sigmastat). A Tukey's test was used to determine differences between treatments following ANOVA ($P<0.05$).

Results

Blood-to-lumen intestinal ^{3}H-mannitol clearance.

Intestinal segments from 4-6 month-old wild type (WT) and knockout ($ClC2^{-/-}$) mice siblings were subjected to *in vivo* complete mesenteric ischemia for 45-minutes. The ischemic intestinal segments were then allowed to recover for either 1.5- or 3-hours after which *in vivo* blood-to-lumen clearance of ^{3}H-mannitol was studied as a measure of intestinal permeability. Complete mesenteric ischemia resulted in increased ^{3}H-mannitol flux in ischemic-injured intestinal segments as compared to control intestinal loops in wild type mice (^{3}H-mannitol clearance = 0.16 ± 0.02 and 0.23 ± 0.08 ml/hr x 100g for control and ischemic intestinal loops at 1.5-hours recovery, and 0.28 ± 0.20 and 0.38 ± 0.22 ml/hr x 100g for control and ischemic intestinal loops, respectively at 3-hours recovery) (Figure 1). Similar clearance values for control and recovering ischemic-injured ileal loops were observed in ClC-2 heterozygote ($ClC\text{-}2^{+/-}$) ileum (data not shown). Alternatively, in $ClC\text{-}2^{-/-}$ mice, ^{3}H-mannitol fluxes in ischemic-injured intestine at 1.5 and 3 hours recovery exceeded that of control intestine by 226% and 122% respectively (^{3}H-mannitol clearance = 0.07 ± 0.03 and 0.24 ± 0.09 ml/hr x 100g for control and ischemic intestine at 1.5 hours, $p<0.01$, and 0.09 ± 0.02 and 0.22 ± 0.06 ml/hr

x 100g for control and ischemic intestine at 3 hours, $p<0.01$). This blood-to-lumen intestinal ^{3}H-mannitol flux study clearly indicated an important role of ClC-2 in recovery of barrier function.

Histological, morphometric, and ultrastuctural analyses.

There were no apparent histological differences in control intestinal tissues from wild type and ClC-2 $^{-/-}$ mice (Figure 2). In both genotypes, 45-minutes of intestinal ischemia resulted in typical sloughing of apical villous enterocytes and contraction of villi. Around 13-14% surface denudation and 25% reduction in villus height was seen in ischemic intestinal loops in both genotypes (data not shown). After 1.5-hours of post-ischemic recovery, the epithelium showed approximately 2% denudation with 50% reduction in villus height in wild type as well as ClC-2$^{-/-}$ ischemic loops. By 3-hour post-ischemic recovery, the epithelium was completely and comparably restituted in wild type and ClC-2 deficient mice. The villus width, crypt depth, and surface area measurements did not differ significantly when comparing control and ischemic-injured tissues of wild type and ClC-2$^{-/-}$ mice at any point of observation. These histological findings led us to conclude that significant differences in blood-to-lumen clearance of ^{3}H-mannitol seen in ClC-2$^{-/-}$ mice was independent of epithelial restitution, and most likely attributable to changes in paracellular permeability. Further electron microscopic examination of intestinal samples revealed that whereas the ischemic-injured segments from wild type mice had tightly opposed tight junctions, ischemic-injured intestinal segments from ClC-2 deficient mice displayed dilatation of the tight junctions (Figure 3). This ultrastructural morphologic

evidence supported the earlier findings that delayed recovery of intestinal barrier function in ClC-$2^{-/-}$ mice during recovery from ischemic injury was independent of epithelial restitution and associated with changes in paracellular permeability.

Expression of ClC-2 protein in uninjured and ischemic-injured tissue.

To further assess the role of ClC-2 in barrier function recovery, we studied its expression in uninjured control and ischemic-injured wild type intestine. Western blot analysis revealed increased expression of ClC-2 in ischemic intestine as compared to uninjured intestine (~30% ~15% after 1.5-hour and 3-hour post ischemic recovery, respectively, based on densitometric analyses, $p< 0.05$) (Figure 4).

Expression of TJ proteins in membrane fractions during epithelial barrier recovery.

To elucidate the role of paracellular defects during recovery from ischemic injury, we sought to study the select tight junction proteins in wild type and ClC-$2^{-/-}$ intestine during barrier recovery. The total expression of the tight junction proteins occludin and claudin-1 in whole tissue extracts was similar in wild type and ClC-$2^{-/-}$, control and ischemic tissues (data not shown). The intestinal mucosa was fractionated into detergent soluble and detergent insoluble components to estimate the proportion of occludin and claudin-1 present in the membrane (detergent insoluble) and cytosol (detergent soluble) respectively, realizing that this technique only gives an estimation of this relationship. In control uninjured intestine of wild type as well as ClC-$2^{-/-}$ mice, most of occludin and claudin-1 protein was expressed in the detergent insoluble fraction (data not shown). In

wild type mice, during early recovery (1.5-hours post-ischemia) occludin and claudin-1 was partially expressed in the detergent soluble fraction (Figure 5). However, both of these proteins were almost completely restored to the detergent insoluble fraction by 3-hours post-ischemic recovery. In ClC-$2^{-/-}$ mice, at 1.5-hour recovery the expression of both occludin and claudin-1 was significantly increased in the detergent soluble fractions as compared to wild type mice. Concurrently, the detergent insoluble fractions from ClC-$2^{-/-}$ mice showed significantly reduced expression of occludin and claudin-1, when compared to wild type mice. At 3-hours post-ischemic recovery, expression of claudin-1 in ClC-$2^{-/-}$ detergent insoluble fractions was comparable to those of wild type detergent insoluble fractions while expression of occludin was still significantly lower in detergent insoluble fractions of ClC-$2^{-/-}$ mice as compared to wild type mice. Thus these results not only shed light on the shift of tight junction proteins during recovery from ischemic injury, but also support the differences in barrier recovery between wild type and ClC-$2^{-/-}$ mice based on blood-to-lumen intestinal ^{3}H-mannitol clearance studies.

Co-immunoprecipitation of ClC-2 with occludin.

In previous experiments utilizing porcine ileum it was shown that the tight junction protein occludin is expressed in ClC-2 immunoprecipitates.[12] To further investigate the link between ClC-2 and the tight junction complex, we studied the dynamics of the association between ClC-2 and occludin during recovery from ischemic injury. ClC-2 was immunoprecipitated from wild type control and post-ischemic intestinal mucosal scrapings and expression of occludin was probed by Western blotting.

Immunoprecipitates obtained using pre-immune serum, served as negative controls and showed no evidence for expression of occludin. However, we found that occludin is expressed in ClC-2 immunoprecipitates from uninjured control as well as post-ischemic intestine (Figure 6). Furthermore, we observed that the reduced expression of occludin in the ClC-2 immunoprecipitates at 1.5-hours post-ischemic recovery was significantly increased by 3-hours recovery. In fact, the expression of occludin in the ClC-2 immunoprecipitates after 3-hour recovery was comparable to that of uninjured control intestine.

ClC-2 and TJ protein occludin co-immunolocalization.

ClC-2 has been shown to be localized to apical tight junction region of murine small intestine.[16,17] To explore the role of ClC-2 in paracellular permeability, we investigated whether ClC-2 co-localizes with the TJ integral membrane protein occludin, and if the absence of ClC-2 leads to differences in post-ischemic tight junction protein cellular localization. This immunofluorescence investigation revealed punctuate fluorescent labeling for occludin mostly confined to the region of the apical tight junction in wild type as well as ClC-2$^{-/-}$ uninjured control intestine (Figure 7). In wild type uninjured intestine, ClC-2 was seen along the apical border, and concentrated at the region of the tight junction. The co-localization of occludin and ClC-2 was clearly visible at the apical tight junction region in the merged figure. Following ischemia intestine showed diffuse occludin labeling that was localized predominantly within the cytoplasm. At the early 1.5-hour recovery point in wild type mice, most of the ClC-2 fluorescence was confined

to the apical membrane and co-localization with occludin was visible to some extent. Alternatively, at 1.5-hours post-ischemia, occludin immunofluorescence appeared to be diffuse and indiscrete in ClC-2$^{-/-}$ intestine. By 3-hour post-ischemic recovery, the normal pattern for occludin (and its co-localization with ClC-2) was predominantly recovered in wild type ischemic intestine. However, in ClC-2$^{-/-}$ intestine the occludin fluorescence remained diffusely present along apical membrane and within the sub-apical region.

Discussion

In the present study we have demonstrated an important role of ClC-2 in the recovery of intestinal mucosal barrier function using an *in vivo* intestinal ischemia model. *In vivo* blood-to-lumen ^{3}H-mannitol clearance in recovering ischemic ileum was significantly higher in ClC-2$^{-/-}$ mice as compared with wild type mice. Intestinal ischemia leads to sloughing of epithelium at tips of villi, followed by a mucosal reparative response including epithelial restitution and contraction of villi. As shown by histologic and histomorphometric studies, these mucosal responses were comparable in post-ischemic recovering tissue from wild type and ClC-2$^{-/-}$ mice. Thus the impaired barrier recovery in ClC-2$^{-/-}$ mice indicated by *in vivo* blood-to-lumen ^{3}H-mannitol clearance was independent of epithelial restitution.

In ultrastructural studies we detected dilated tight junctions in ischemic intestinal tissues from ClC-2$^{-/-}$ mice. This prompted us to explore the role of ClC-2 in conformational change in the tight junction during epithelial barrier recovery. Beside the characteristic

localization of ClC-2 in apical tight junctions in the murine small intestine, not much information is known about the physiological role of ClC-2 in the gut. First we investigated the composition of tight junctions during post-ischemic recovery of barrier function by assessing expression of the tight junction proteins occludin and claudin-1 in detergent soluble and detergent insoluble membrane fractions.[34,35] We found that both occludin and claudin-1 increasingly shifted from detergent soluble to detergent insoluble membrane fractions during barrier recovery in wild type mice. In ClC-$2^{-/-}$ mice, particularly at the 1.5-hour early recovery time point, the expression pattern differed markedly from that of wild type mice. Significantly more expression of occludin and claudin-1 was present in ClC-$2^{-/-}$ detergent soluble fractions than that of wild type mice. These findings provided insight into the mechanism through which ClC-$2^{-/-}$ mice lag in recovery of barrier function as compared to wild type mice.

To further confirm the link between ClC-2 and recovery of the tight junction, co immunoprecipitation experiments were performed. Occludin was expressed in ClC-2 wild type immunoprecipitates obtained from control as well as ischemic recovering epithelium. The expression of occludin in ClC-2 immunoprecipitates at 3-hours post-ischemic recovery was comparable to uninjured control intestine. We further carried out immunolocalization experiments to examine occludin and ClC-2 in control and post-ischemic recovering wild type epithelium. The co-immunofluorescence examination of control wild type intestine revealed co localization of occludin and ClC-2 in the tight junction region. These findings are consistent with earlier studies where ClC-2 was co

localized with zona occludin-1 in murine small intestine.[16] In wild type mice, after 1.5-hours recovery, a proportion of occludin fluorescence was detected in the sub-apical cytoplasmic region, and by 3-hours recovery occludin fluorescence regained its normal pattern. However, ClC-2 immunofluorescence was confined mostly to the apical border during post-ischemic recovery. Oxidative stress has been shown to inhibit dynamin-dependent endocytosis of ClC-2 [36], which may help to explain these findings. In contrast to recovery of the normal occludin fluorescence pattern in wild type mice, occludin fluorescence remained diffuse and indiscrete in ClC-$2^{-/-}$ mice after 3-hours of post-ischemic recovery. In spite of the close proximity of ClC-2 to tight junctions, and the presence of signaling molecules and kinases in this region, *in vivo* regulation of ClC-2 is not well understood. ClC-2 has been shown to be phosphorylated by PKA in TSA 201 cell line without alteration in its activity[37] while PKA and PKC activation leads to decreased amplitude of ClC-2 currents in human T84 cells.[38] Considering the importance of tight junction biogenesis in barrier recovery, it is noteworthy that sustained activation of conventional isoform PKCα leads to barrier dysfunction while activation of the novel PKC isoform PKCε enhances barrier function. [4,39-40]

Overall, the functional, biochemical, and morphological data in the present experiments strongly suggest an important role for ClC-2 in the barrier function recovery through tight junction assembly. Although functional regulation of ClC-2 is not well understood, its localization at the tight junction suggests the possibility of its interaction with signaling molecules densely present in this region as well as the tight junction proteins. In a

previous report, the role of ClC-2 was highlighted in the recovery of barrier function in ischemic-injured porcine ileum.[12] Inhibition of ClC-2 and not CFTR was shown to impair prostaglandin-induced recovery of barrier function. Obviously, the ClC-2 channels concentrated around apical tight junction could have an advantage over alternate Cl^- channels in influencing paracellular permeability following initiation of chloride transport. However, whether or not Cl^- secretion is necessary or merely an indication of activation of critical proteins, including ClC-2, in post-ischemic tissue recovering under the influence of prostanoids is not known. In one study, the stimulatory action of a selective ClC-2 agonist lubiprostone on post-ischemic barrier recovery was shown to stimulate Cl^- secretion and enhance tight junction assembly during the recovery period.[15] In addition, inhibition of epithelial Cl- uptake with the NKCC1 inhibitor bumetanide or removal of Cl^- in porcine ischemic-injured tissues prevented recovery.[10] However, there is evidence in our post-ischemic barrier recovery model that select signaling molecules play a role in repair without an effect on Cl^- secretion. For example, inhibition of PI3K impairs recovery of transepithelial resistance without affecting Cl^- secretion.[13]

The failure of tight junction recovery in the ClC-$2^{-/-}$ mice, as demonstrated in the present study, is compatible with our previous findings and suggests that ClC-2 is selectively targeted in the assembly of tight junctions. These tight junctions regulate paracellular resistance and are therefore critical to recovery of epithelial barrier function. We speculate that ClC-2 could act as a scaffold protein recruiting key tight junction proteins

to the apical paracellular membrane. However, the signaling mechanisms in this intriguing process will require further study.

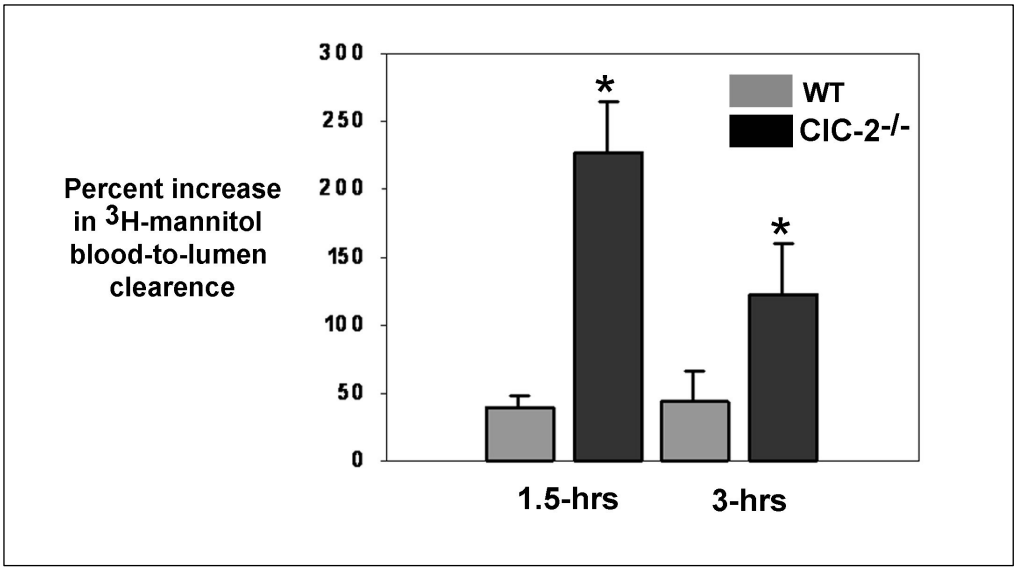

Figure 1. Blood-to-lumen ^{3}H-mannitol clearance following 1.5 and 3 hours of post-ischemic recovery in wild type and ClC-2-/- mice . The percent increase in blood-to-lumen ^{3}H- mannitol clearance was calculated in ischemic-injured intestinal loops over the control loops of wild type and ClC-2$^{-/-}$ mice following 1.5 and 3-hour recovery periods. The ClC-2$^{-/-}$ mice showed approximately 225% and 125% increase in blood-to-lumen ^{3}H-mannitol clearance in ischemic loops over the control loops, at 1.5 and 3-hour recovery, respectively. *: $p < 0.05$ as compared to wild type ischemic loops at respective recovery time point. n = 6.

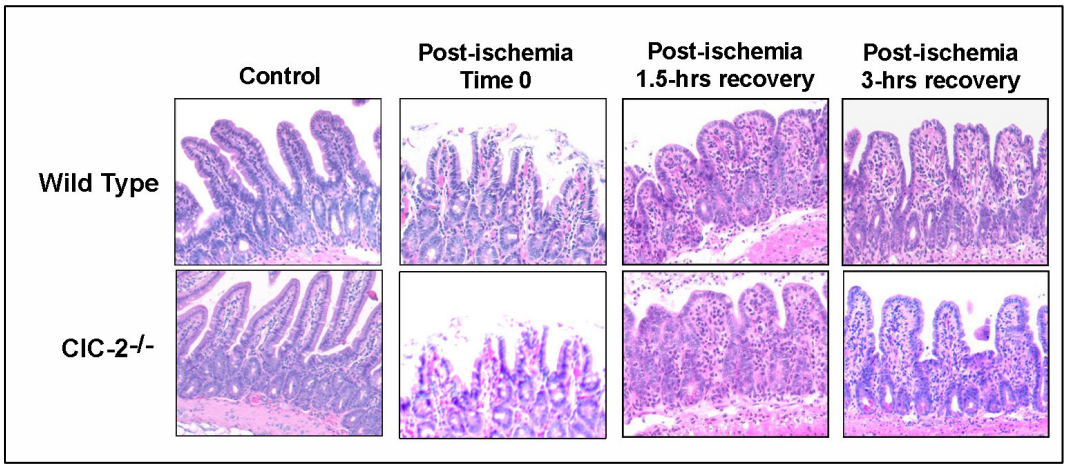

Figure 2. Histological examination of control and ischemic-injured ileal tissues from wild type and ClC-2$^{-/-}$ mice. Ischemia results in epithelial sloughing at the tips of villi and contraction of villi. After 1.5 and 3-hours of post-ischemic recovery the mucosa showed rapid restitution of epithelium that was comparable in wild type and ClC-2$^{-/-}$ mice. H&E Stain, X 100.

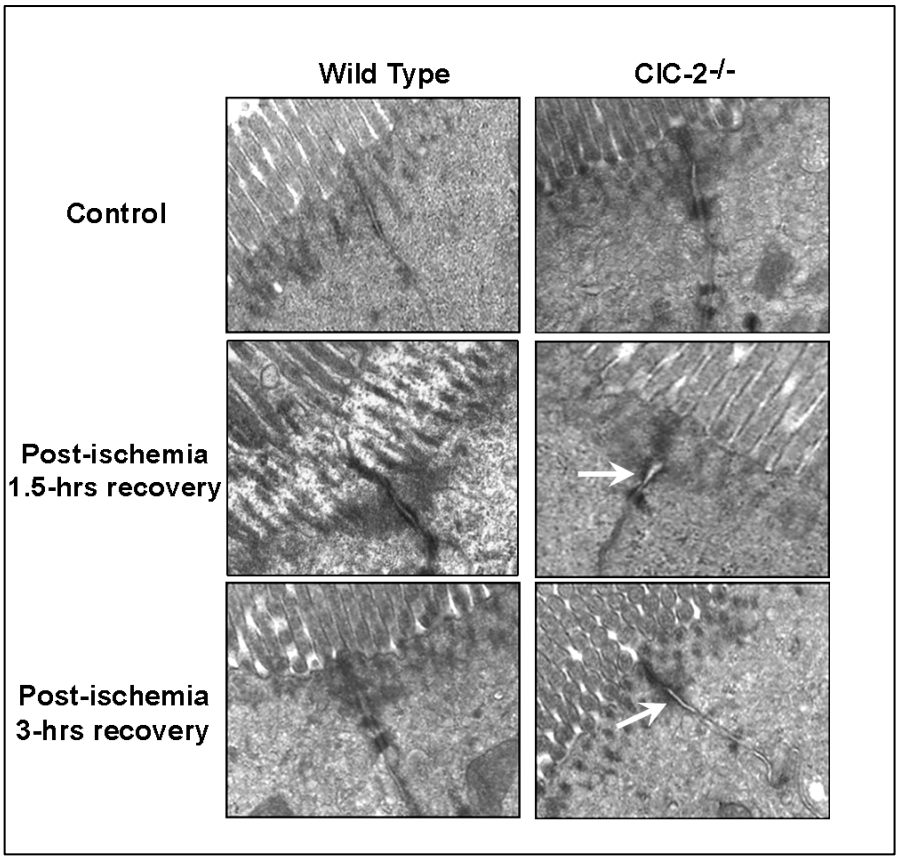

Figure 3. Electron microscopic examination of control and ischemic-injured ileal tissues from wild type and ClC-2$^{-/-}$ mice. In uninjured control wild type (left panel) and ClC-2$^{-/-}$ mice (right panel) intestinal epithelium the tight junctions were closely opposed to each other. However, during post-ischemic recovery, in contrast to wild type, ClC-2$^{-/-}$ epithelium revealed tight junction dilation (arrow). X 28,000.

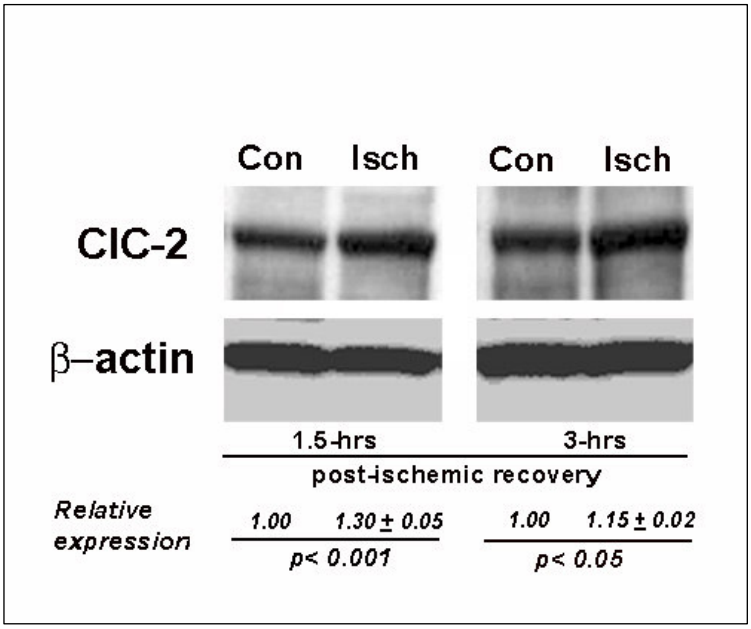

Figure 4. Expression of ClC-2 in uninjured and ischemic-injured tissue. Whole tissue extracts of the control and ischemic mucosa were studied for expression of ClC-2 by Western blotting. The ischemic-injured mucosa (Isch) showed significant increases in expression of ClC-2 at 1.5 and 3-hours of recovery when compared to control mucosa (Con). Densitometry was performed to quantify relative expression utilizing expression of β-actin as loading controls for respective lanes. The blots are representative of at least 3 experiments.

Figure 5. Expression of TJ proteins in membrane fractions during epithelial barrier recovery. Following the post-ischemic recovery period of 1.5 and 3-hours, mucosal extracts from wild type and ClC-$2^{-/-}$ mice were separated into detergent soluble and detergent insoluble fractions (using Triton X-100 and SDS buffers as described in methods). These fractions were subsequently analyzed by Western blotting using anti-occludin and anti-claudin-1 antibodies. There was increased expression of both occludin and claudin-1 in the detergent soluble (DS) fraction of ClC-$2^{-/-}$ mice following ischemia. For the same group, there was reduced expression of occludin and claudin-1 in detergent insoluble (DIS) fraction, as compared to wild type mice, suggesting movement of tight junction proteins to the cytosol. The blots are representative of at least 3 experiments. The β-actin blots are shown as loading controls and were used for densitometric analyses. Densitometry readings in wild type group were adjusted to one to express relative expression in ClC-$2^{-/-}$ group (mean ± S.E.).

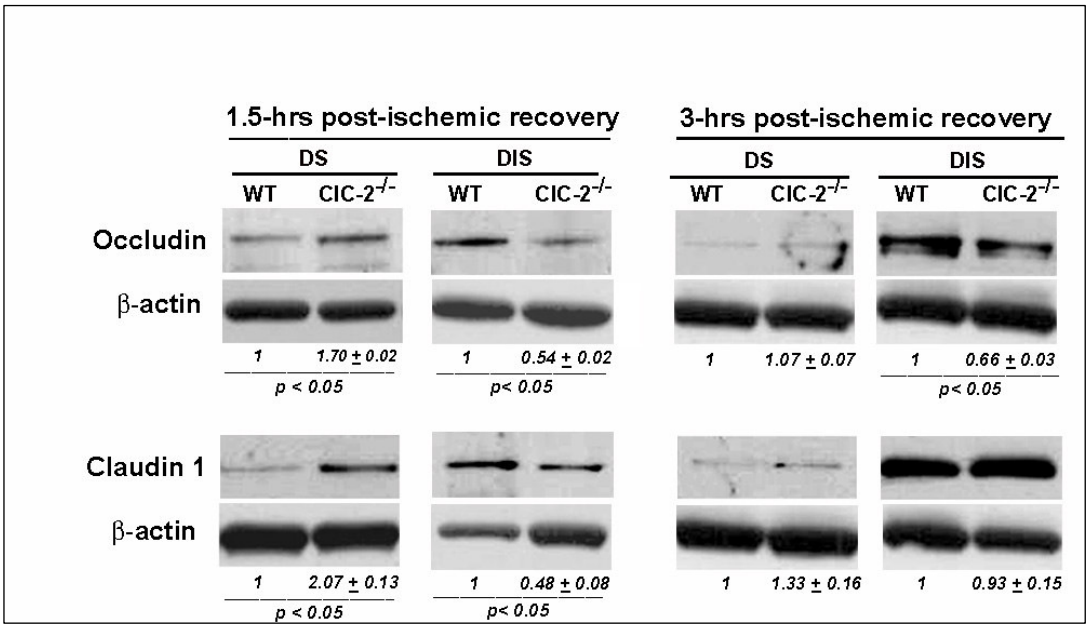
1.5-hrs post-ischemic recovery
3-hrs post-ischemic recovery
DS
DIS
DS
DIS
WT
CIC-2-/-
WT
CIC-2-/-
WT
CIC-2-/-
WT
CIC-2-/-
Occludin
β-actin
1
1.70 ± 0.02
p < 0.05
1
0.54 ± 0.02
p< 0.05
1
1.07 ± 0.07
1
0.66 ± 0.03
p< 0.05
Claudin 1
β-actin
1
2.07 ± 0.13
p < 0.05
1
0.48 ± 0.08
p< 0.05
1
1.33 ± 0.16
1
0.93 ± 0.15

Figure 6. Co-immunoprecipitation of TJ protein occludin with ClC-2. A. ClC-2 was immunoprecipitated from either uninjured control or post-ischemic recovering mucosa of wild type mice. The immunoprecipitates were probed for expression of occludin by Western blotting. Occludin was detected as a band of around 65 kD molecular mass in ClC-2 immunoprecipitates obtained from control mucosa, but not in immunoprecipitates obtained using normal serum. The reduced expression of occludin in the ClC-2 immunoprecipitates at 1.5-hour recovery was found to be increased at 3-hour post-ischemic recovery. The blots of ClC-2 (bands between 95-100 KD mass) for respective lanes are shown as loading control. The blots are representative of at least 3 experiments. B. Densitometry analysis showed comparable expression of occludin in the ClC-2 immunoprecipitates of control and post-ischemic recovered mucosa (mean ± S.E.) (*: significantly different from control and 3-hrs post-ischemic recovery, $p < 0.05$).

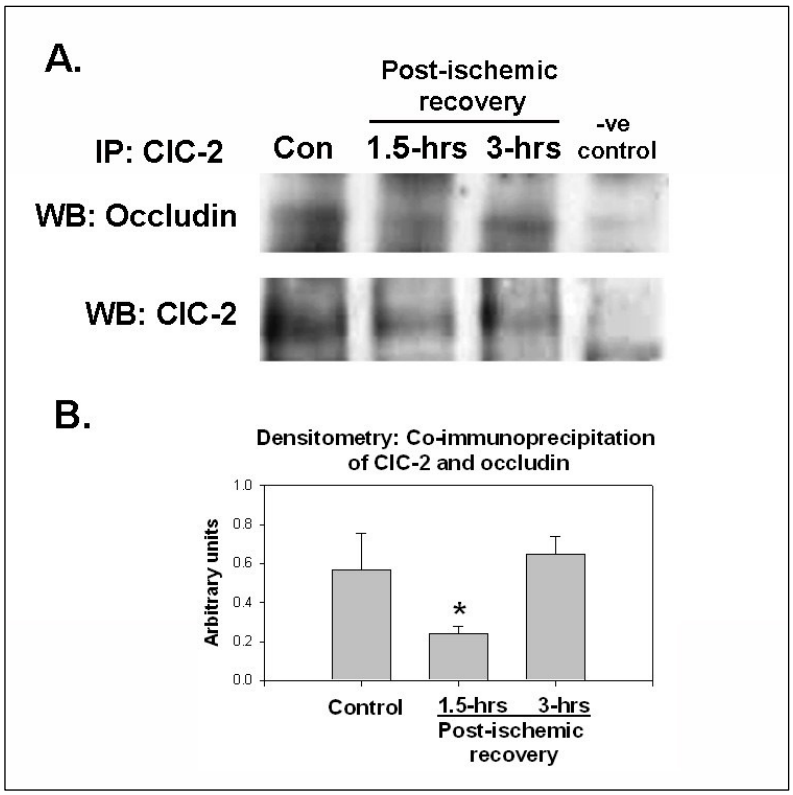
A.
Post-ischemic recovery
IP: CIC-2
Con
1.5-hrs
3-hrs
-ve control
WB: Occludin
WB: CIC-2
B.
Densitometry: Co-immunoprecipitation of CIC-2 and occludin
Arbitrary units
1.0
0.8
0.6
0.4
0.2
0.0
*
Control
1.5-hrs
3-hrs
Post-ischemic recovery

Figure 7. ClC-2 and occludin co-localization using confocal immunofluorescence. In wild type as well as ClC-$2^{-/-}$ mice control intestine, occludin (green) was localized at apical tight junctions (first row). In wild type control intestine ClC-2 (red) was localized along the apical border, concentrated around the tight junction region, and co-localized with occludin (yellow color in the merged figure). During post-ischemic recovery, occludin fluorescence was diffuse, often in the sub-apical region, but regained its normal distribution after 3-hours of recovery in wild type mice (middle and lower row). However in ClC-$2^{-/-}$ mice, occludin showed diffuse and indiscrete localization even after 3-hours of recovery (extreme right panel). Nuclei (blue) were stained with DRAQ5 (Biostatus Ltd.). All images were viewed with a 60 X objective and 1.5X zoom.

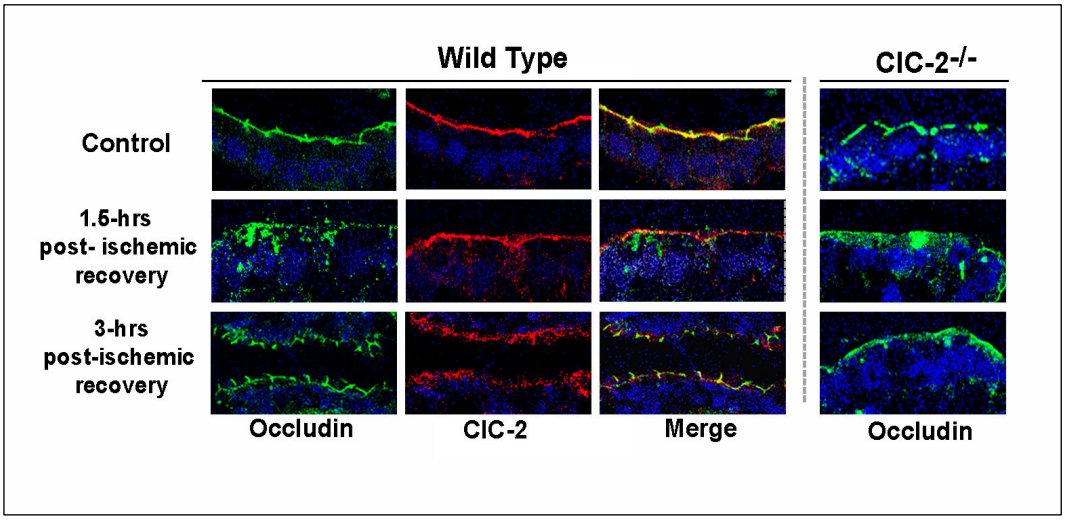
Wild Type
ClC-2-/-
Control
1.5-hrs post- ischemic recovery
3-hrs post-ischemic recovery
Occludin
ClC-2
Merge
Occludin

References:

1. Turner JR, Rill BK, Carlson SL, Carnes D, Kerner R, Mrsny RJ, Madara JL. Physiological regulation of epithelial tight junctions is associated with myosin light-chain phosphorylation. Am J Physiol 1997;273:C1378-C1385.

2. Turner JR. Molecular basis of epithelial barrier regulation: from basic mechanisms to clinical application. Am J Pathol 2006;169:1901-1909.

3. Turner JR, Angle JM, Black ED, Joyal JL, Sacks DB, Madara JL. PKC-dependent regulation of transepithelial resistance: roles of MLC and MLC kinase. Am J Physiol 1996;277:C554-C562.

4. Yoo J, Nichols A, Mammen J, Calvo I, Song JC, Worrell RT, Matlin K, Matthews JB. Bryostatin-1 enhances barrier function in T84 epithelia through PKC-dependent regulation of tight junction proteins. Am J Physiol Cell Physiol 2003;285:C300-C309.

5. Shin K, Fogg V C, Margolis B. Tight junctions and cell polarity. Annu Rev Cell Dev Biol 2006;22:207-235.

6. Deitch EA, Rutan R, Waymack JP. Trauma, shock, and gut translocation. New Horiz 1999;4:289-299.

7. Stechmiller JK, Treloar D, Allen N. Gut dysfunction in critically ill patients: a review of the literature. Am J Crit Care 1997;6:204-209.

8. Moore R, Carlson S, Madara JL. Rapid barrier restitution in an in vitro model of intestinal epithelial injury. Lab Invest 1989;60:237-244.

9. Blikslager AT, Roberts MC, Rhoads JM, Argenzio RA. Prostaglandins I2 and E2 have a synergistic role in rescuing epithelial barrier function in porcine ileum. J Clin Invest 1997;100:1928-1933.

10. Blikslager AT, Roberts MC, Argenzio RA. Prostaglandin-induced recovery of barrier function in porcine ileum is triggered by chloride secretion. Am J Physiol 1999;276:G28-G36.

11. Gookin JL, Galanko, JA, Blikslager AT, Argenzio RA. PG-mediated closure of paracellular pathway and not restitution is the primary determinant of barrier recovery in acutely injured porcine ileum. Am J Physiol Gastrointest Liver Physiol 2003;285:G967-G979.

12. Moeser AJ, Haskell MM, Shifflett DE, Little D, Schultz BD, Blikslager AT. ClC-2 chloride secretion mediates prostaglandin-induced recovery of barrier function in ischemia-injured porcine ileum. Gastroenterology 2004;127:802-815.

13. Little D, Dean RA, Young KM, McKane SA, Martin LD, Jones SL, Blikslager AT. PI3K signaling is required for prostaglandin induced mucosal recovery in ischaemia-injured porcine ileum. Am J Physiol Gastrointest Liver Physiol 2003; 284:G46-G56.

14. Moeser AJ, Nighot PK, Ryan KA, Wooten JG, Blikslager AT. Prostaglandin-Mediated Inhibition of the Na+/H+ Exchanger Isoform 2 Stimulates Recovery of Barrier Function in Ischemia- Injured Intestine. Am J Physiol Gastrointest Liver Physiol 2006;291:G885-G894.

15. Moeser AJ, Nighot PK, Engelke KJ, Ueno R, Blikslager AT. Recovery of mucosal barrier function in ischemic porcine ileum and colon is stimulated by a novel agonist of the ClC-2 chloride channel, lubiprostone. Am J Physiol Gastrointest Liver Physiol 2006;292:G647-G656.

16. Gyömörey K, Yeger H, Ackerly C, Garami E, Bear CE. Expression of the chloride channel ClC-2 in the murine small intestine epithelium. Am J Physiol 2000;279**:**C1787–C1794.

17. Mohammad-Panah R, Gyomorey K, Rommens J, Choudhury M, Li C, Wang Y, Bear CE. ClC-2 contributes to native chloride secretion by a human intestinal cell line, Caco-2. J Biol Chem 2001;276:8306-8313.

18. Thiemann A, Gründer S, Pusch M, Jentsch TJ. A chloride channel widely expressed in epithelial and non-epithelial cells. Nature 1992;356:57–60.

19. Jordt SE, Jentsch TJ. Molecular dissection of gating in the ClC-2 chloride channel. EMBO J 1997;16:1582–1592.

20. Gründer S, Thiemann A, Pusch M, Jentsch TJ. Regions involved in the opening of CIC-2 chloride channel by voltage and cell volume. Nature 1992;360:759–762.

21. Niemeyer MI, Yusef YR, Cornejo I, Flores CA, Sepúlveda FV, Cid LP. Functional evaluation of human ClC-2 chloride channel mutations associated with idiopathic generalized epilepsies. Physiol Genomics 2004;16:74-83.

22. Sherry AM, Malinowska DH, Morris RE, Ciraolo GM, Cuppoletti J. Localization of ClC-2 Cl- channels in rabbit gastric mucosa. Am J Physiol Cell Physiol 2001;280:C1599-C1606.

23. Bösl MR, Stein V, Hübner C, Zdebik AA, Jordt SE, Mukhopadhyay AK, Davidoff MS, Holstein A, Jentsch TJ. Male germ cells and photoreceptors, both dependent on close cell–cell interactions, degenerate upon ClC-2 Cl^- channel disruption. EMBO J 2001; 20:1289–1299.

24. Zdebik AA, Cuffe JE, Bertog M, Korbmacher C, Jentsch TJ. Additional disruption of the ClC-2 Cl(-) channel does not exacerbate the cystic fibrosis phenotype of cystic fibrosis transmembrane conductance regulator mouse models. J Biol Chem 2004;279:22276-22283.

25. Hinzpeter A, Fritsch J, Borot F, Trudel S, Vieu DL, Brouillard F, Baudouin-Legros M, Clain J, Edelman A, Ollero M. Membrane cholesterol content modulates ClC-2 gating and sensitivity to oxidative stress. J Biol Chem 2007;282:2423-2432.

26. Rutledge E, Denton J, Strange K. Cell cycle- and swelling-induced activation of a Caenorhabditis elegans ClC channel is mediated by CeGLC-7alpha/beta phosphatases. J Cell Biol 2002;158:435-444.

27. Zheng YJ, Furukawa T, Ogura T, Tajimi K, Inagaki N. M phase-specific expression and phosphorylation-dependent ubiquitination of the ClC-2 channel. J Biol Chem 2002;277:32268-32273.

28. Yang XY, Lai XG, Zhang Y, Pei JM, Yang AG, Zhou SS. siRNA-mediated silencing of ClC-2 gene inhibits proliferation of human U-87 glioma cells. Ai Zheng 2006;25:805-810.

29. Kirk KL. Chloride channels and tight junctions focus on "Expression of the chloride channel ClC-2 in the murine small intestine epithelium". Am J Physiol 2000;279:C1675–C1676.

30. Nehrke K, Arreola J, Nguyen HV, Pilato J, Richardson L, Okunade G, Baggs R, Shull GE, Melvin JE. Loss of hyperpolarization-activated Cl (-) current in salivary acinar cells from Clcn2 knockout mice. J Biol.Chem 2002;277:23604-23611.

31. Komatsu S, Grisham MB, Russell JM, Granger DN. Enhanced mucosal permeability and nitric oxide synthase activity in ileum of mast cell deficient mice. Gut 1997;41:636-641.

32. Argenzio RA, Lecce J, Powell DW. Prostanoids inhibit intestinal NaCl absorption in experimental porcine cryptosporidiosis. Gastroenterology 1993;104**:**440–471.

33. Dykstra MJ. A manual of applied techniques for biological electron microscopy. 1993, Plenum Press, New York.

34. Tsukamoto T, Nigam SK**.** Tight junction proteins form large complexes and associate with the cytoskeleton in an ATP depletion model for reversible junction assembly. J Biol Chem 1997;272:16133–16139.

35. Blikslager AT, Moeser AJ, Gookin JL, Jones SL, Odle J. Restoration of barrier function in injured intestinal mucosa. Physiol Rev 2007;87:545-64.

36. Dhani SU, Mohammad-Panah R, Ahmed N, Ackerley C, Ramjeesingh M, Bear CE. Evidence for a functional interaction between the ClC-2 chloride channel and the retrograde motor dynein complex. J Biol Chem 2003;278:16262-16270.

37. Park K, Begenisich T, Melvin JE. Protein Kinase A Activation Phosphorylates the Rat ClC-2 Cl− Channel but Does Not Change Activity J Membrane Biol 2001;182: 31–37.

38. Fritsch, J., Edelman, A. Modulation of the hyper polarization- activated Cl– current in human intestinal T84 epithelial cells by phosphorylation. J. Physiol 1996;490:115–128.

39. Farhadi A, Keshavarzian A, Ranjbaran Z, Fields JZ, Banan A. Role of PKC isoforms in modulation of injury and repair of the intestinal barrier. Journal of Pharmacology And Experimental Therapeutics 2006;316:1-7.

40. Um JW, Matthews J, Jaekyung C, Song MS, Mun EC. Role of protein kinase C in intestinal ischemic preconditioning. Journal of Surgical Research 2005;124:289-296.

CHAPTER IV

MICE LACKING THE SODIUM CHANNEL NHE2 HAVE IMPAIRED RECOVERY OF INTESTINAL BARRIER FUNCTION

Abstract: Ischemia results in breakdown of the intestinal barrier. Recent studies indicate that ion transporters are involved in barrier recovery via a process involving closure of interepithelial tight junctions. The aim of present study was to determine if Sodium Hydrogen Exchanger NHE2, via a link to the tight junction, is critical to recovery of intestinal barrier function. Wild type, NHE2 heterozygous and NHE2 null murine jejunal mucosa was subjected to complete ischemia, after which recovery of barrier function was monitored by measuring blood-to-lumen clearance of mannitol. Tissues were assessed for expression of select junctional proteins. NHE2 null ($NHE2^{-/-}$) mice had significant increases in permeability to mannitol during the post-ischemic recovery process compared to NHE2 heterozygous ($NHE2^{+/-}$) and wild-type mice and this process was independent of epithelial restitution. The tight junction proteins occludin and claudin-1 were poorly localized and displayed shift to Triton-X soluble membrane fraction in $NHE2^{-/-}$ mice. Occludin and claudin-1 were co-immunoprecipitated with NHE2 in wild type mice and were found more serine phosphorylated during recovery compared to NHE2 null mice. Furthermore, ezrin binding phosphoprotein 50 (EBP50) which facilitates phosphorylation of NHE proteins and is involved in tight junction formation via ezrin, was found expressed in NHE2 immunoprecipitate. These data indicate that NHE2 is intimately involved in recovery of barrier function during recovery from ischemic injury, mediating re-assembly of tight junctions.

Keywords: Tight junction, Intestinal permeability, Ischemia, Na^+/H^+ exchange

Introduction

The gastrointestinal tract is lined by a single layer of epithelial cells connected by a series of interepithelial junctions. Collectively, the epithelial monolayer can selectively transport solutes, but also prevent the entrance of noxious luminal contents. The latter function is termed gut barrier function. The barrier properties of the epithelium are regulated by the apical tight junctions (TJ) which consist of an array of membrane-spanning proteins (e.g. occludin and claudins) linked by cytoplasmic plaque proteins such as zonula occludens-1 to the cytoskeleton.[1,2] Recent studies have shown that tight junctions are not static structures, but can be regulated to alter solute absorption and barrier properties.[2-4] For example, NHE3 activity is involved in a signaling cascade that results in increased transepithelial resistance during Na^+-glucose co-transport as a result of tight junction alteration.[5]

Intestinal ischemic injury is a leading cause of death in critically ill patients because of the onset of sepsis as the damaged intestinal barrier becomes permeable to bacterial toxins.[6,7] Injured mucosa is initially repaired by restitution, during which viable epithelial cells adjacent to the wound migrate to cover denuded basement membrane.[8] However, loss of TJ architecture must also be addressed to fully restore barrier function.[9-11] Although epithelial restitution is major phenomenon, barrier function was predominantly restored by restoration of tight junctions. This was associated with recruitment of junctional proteins such as occludin to the apical intercellular space.[12,13] Pharmacological approaches indicated that a large component of the recovery of intestinal barrier function

following ischemic injury was attributable to NHE function. In particular, NHE2, rather than NHE3, played a major role in recovery of barrier function.[13]

Currently, the exact role of NHE2 in gastrointestinal function remains obscure. Most of the electro neutral Na^+ absorption that occurs between meals has been shown to be mediated through NHE3 whereas NHE2 is thought to have a minor contribution.[14] Investigators have demonstrated that NHE3 KO mice develop diarrhea and electrolyte abnormalities, indicative of the importance of this transporter in intestinal absorption. Alternatively, NHE2 KO mice do not exhibit any noticeable clinical or electrophysiological abnormalities.[14,15] In double knockout experiments, mice with targeted deletion of both NHE2 and NHE3 did not exhibit differences in Na^+ malabsorption or severity of diarrhoeal disease compared with NHE3 Knockout mice, suggesting that NHE2 does not have a compensatory role in these mice.[16] However, there is increasing evidence that NHE2 may play an important role in the large intestine. In addition, there are considerable species differences with regard to the contribution of NHE2 to electro neutral Na^+/H^+ exchange.[17,18] The objective of the present experiments was to investigate the role of NHE2 in mucosal repair in ischemic intestine utilizing NHE2 knockout mice.

Methods

Experimental Animals

All studies were approved by the North Carolina State University Institutional Animal Care and Use Committee. NHE2 null ($NHE2^{-/-}$), heterozygous ($NHE2^{+/-}$), and wild type ($NHE2^{+/+}$) mice 2 to 4 months-of-age were used for this study. All mice were maintained on a standard laboratory diet. The progeny mice were genotyped by PCR using primers specific for amplification of either intact or disrupted murine NHE2 alleles, as described previously.[14] For amplification of wild type and disrupted alleles, two discriminating forward primers (wild type NHE2; 5'-CATCTCTATCACAAGTTGCCCACAATCGTG-3', disrupted NHE2; 5'-GACAATAGCAGCCATGCTGG-3') and a conversed reverse primer (5'-GTGACTTCGTTGAGCAGAGACTCG-3') were used simultaneously in PCR to yield a wild type NHE2 product of 450 bp and disrupted NHE2 product of 220 bp. PCR was carried out using a BioRad iCycler in a 50µl reaction volume of PCR buffer II (Perkin-Elmer; Foster City CA) containing 2.5mM$MgCl_2$, 2.5U AmpliTaq Gold DNA Polymerase, 100pMol of each forward primer, 200pMol reverse primer, 20µM each deoxynucleotide diphosphate and 5µl DNA template. PCR was performed at the following temperature profiles: initial denaturation at 94^0C for 5-min; denaturation at 94^0C for 30 sec, annealing at 60^0C for 30-sec, and extension at 72^0C for 30-sec. Total number of cycles were 40, followed by a final extension for 5-min at 72^0C. PCR products were separated by agarose gal electrophoresis and visualized under UV light after staining with ethidium bromide.

Experimental Surgery

Mice had unrestricted access to water but not feed six hours prior to the experimental surgery. The mice were subjected to general anesthesia using isoflurane (4% for induction and 1.5% for maintenance), and prepared for surgery using aseptic technique. The mid-jejunum was approached via a midline laporotomy incision. Intestinal loops 2 cm in length were delineated with Doyen intestinal forceps, and complete ischemia was induced by clamping the mesenteric blood supply with Johns Hopkins Bulldog clamps. Following 45 minutes of ischemia, clamps were removed and the abdomen was closed using 4-0 silk for the midline and staples for the skin. The mice were allowed to recover for 1.5 or 3-hours in heated cages.

Blood-to-lumen ^{3}H-mannitol clearance

Following the 1.5 or 3-hour recovery period, mice were re-anesthetized using the same technique as before, after which the abdomen was opened and ischemic and control intestinal segments were ligated with 4-0 silk. Control and ischemic loops were injected with 0.25ml buffered saline (pH 7.4), followed by 0.2ml buffered saline containing ^{3}H-mannitol (10μCi/ml) into the tail vein. Time zero blood samples (0.3ml) were collected via retro-orbital bleeding into heparinized vials. Throughout the experimental procedures body temperature was maintained by retaining abdominal contents within the body wall, and by using water-circulated heating pads and solar blankets. The body temperature was monitored and maintained at 36.5-37.5^{0}C. Blood samples were taken again after one hour. Mice were euthanized, intestinal segments were weighed and intestinal perfusates

from each loop were emptied into micro centrifuge tubes. The volume of intestinal perfusate was recorded and the perfusates were saved in scintillation fluid. The blood samples were centrifuged at 14,000 RPM for 4-minutes and 25µl of plasma was saved in scintillation fluid. The plasma and intestinal perfusate samples were assessed on a scintillation beta counter to study ^{3}H activity, and the ^{3}H –Mannitol clearance was calculated based on modification of formula provided by Komatsu *et al*[19] as:

$$\text{Clearance (ml/hr)} = \frac{\text{(CPM, perfusate) / Volume of perfusate (ml)}}{\text{((CPM, plasma time 0) – (CPM, plasma, 1-hour))/0.025}}$$

where CPM is counts per minute per ml of perfusate or plasma, and wt is weight in grams of the jejunal segment.

Ussing chamber studies.

Following the 45-minutes of ischemic period jejunal tissues were harvested, and mounted in 0.13-cm^2 aperture Ussing chambers, as described in a previous study.[9] Tissues were bathed on the serosal and mucosal sides with 8 ml Ringer solution. The serosal bathing solution contained 10 mM glucose and was osmotically balanced on the mucosal side with 10 mM mannitol. Bathing solutions were oxygenated (95% O_2-5% CO_2) and circulated in water-jacketed reservoirs. The spontaneous potential difference (PD) was measured using Ringer-agar bridges connected to calomel electrodes, and the PD was short circuited through Ag-AgCl electrodes using a voltage clamp that was corrected for fluid resistance. Following 30-minutes of equilibration period, a set of duplicate control

and ischemic tissue was treated on mucosal side with HOE-694 (25 μM). TER ($\Omega \cdot cm^2$) was calculated from the spontaneous PD and short-circuit current (I_{sc}) recorded at 15-min intervals over a 3-hours experiment.

Histological examination

Tissues from control and ischemic intestinal loops were collected in 10% neutral buffered formalin for histological evaluation. Tissues were sectioned (5μm) and stained with hematoxylin and eosin. For each tissue, 3 sections were evaluated. Three well oriented villi and crypts were identified in each of 3 serial sections. Villus length, villus width, and crypt depth was obtained using a micrometer in the eye piece of a light microscope. The surface area of the villus was calculated using the formula for the surface area of a cylinder. The formula was modified by subtracting the area of the base of the villus, and multiplying by a factor accounting for the variable position at which each villus was cross sectioned.[20] The percentage of the villous surface area that remained denuded was calculated and the percent denuded villous surface area was used as an index of epithelial restitution.

Immuno-localization of TJ proteins

Intestinal tissues were embedded in OCT media (Tissue Tek, Sakura, Torrance, CA), frozen, sectioned at 5μm, and stored at -80^0C. Sectioned tissues were fixed in cold acetone, and blocked with normal goat serum. The sections were incubated with rabbit polyclonal occludin, or claudin-1 (Zymed, San Francisco, CA) antibodies diluted in 5%

normal goat serum for 90-minutes. Following washes in PBS, the sections were incubated for 60-minutes with goat anti rabbit IgG conjugated with FITC or Cy3 (Zymed) diluted in 5% normal goat serum. The slides were washed in PBS and mounted in media with DAPI (Vectashield, Vector Laboratories Inc., CA), and examined with a microscope capable of detecting epifluorescence. Duplicate sections stained similarly but with omission of primary antibodies served as controls.

TJ protein and phospho-serine analysis

Intestinal mucosal scrapings from control and ischemic-injured mucosa were snap frozen and stored at -70°C before SDS-PAGE (sodium dodecyl sulphate-polyacramide gel electrophoresis). Triton X soluble and insoluble fractions were extracted using respective buffers (Triton X soluble extraction buffer: 0.5% Triton X-100, 50mM Tris-HCl,140mM EGTA, 30mM Sodium Pyrophosphate, 50mM Sodium Fluoride, 100µM Sodium Orthovanadate, Complete Protease Inhibitor cocktail tablet from Roche; Triton X insoluble extraction buffer: 1% SDS, 50mM Tris-HCl, 140mM EGTA, 30mM Sodium Pyrophosphate, 50mM Sodium Fluoride, 100µM Sodium Orthovanadate, Complete Protease Inhibitor cocktail tablet from Roche). Protein analysis of extract aliquots was performed (DC protein assay; Bio-Rad, Hercules, CA). Tissue extracts (amounts equalized by protein concentration) were mixed with an equal volume of 2× SDS-PAGE sample buffer and boiled for 4 min. Lysates were loaded on a 10% SDS polyacrylamide gel, and electrophoresis was carried out according to standard protocols. Proteins were transferred to a PVDF membrane (Immobilon, Millipore, Billerica, MA) by using an

electro blotting minitransfer apparatus. Membranes were blocked at room temperature for 60-min in Tris-buffered saline plus 0.05% Tween 20 (TBST) and 5% dry powdered milk, and then incubated for 60-minutes in primary antibody (rabbit polyclonal occludin, claudin-1 (Zymed, San Franscico, CA). After washings in TBST, membranes were incubated with horseradish peroxidase-conjugated secondary antibody, and developed for visualization of protein with chemiluminance enhancer solution (Pierce, Rockford IL). For analysis of phosphorylated proteins, tissue aliquots were thawed at 4°C and added to 3ml chilled lysis buffer, including protease inhibitors (0.5mM Pefabloc, 0.1mM 4-nitrophenyl phosphate, 0.04mM β-glycerophosphate, 0.1mM Na3VO4, 40 µg/ml bestatin, 2µg/ml aprotinin, 0.54µg/ml leupeptin, and 0.7µg/ml pepstatin A) at 4°C. This mixture was homogenized on ice and then centrifuged at 4°C, and the supernatant was saved. Extracted proteins (1mg) were solubilised in RIPA buffer (50mM Tris-Cl, pH 7.4, 150mM NaCl, 1mM EDTA, 0.1% (w/v) SDS, 1% Triton X-100 with protease inhibitors), pre cleared with protein A/G-agarose beads (Santa Cruz Biotechnology, CA) and incubated with either NHE2 or NHE3 anti goat polyclonal antibodies or normal goat pre-immune serum (Santa Cruz Biotechnology) for 1-hour at 37^0 C. The antibody-protein complexes were adsorbed from solution with protein A/G-agarose beads. Protein samples were washed 3X in ice cold RIPA buffer and centrifuged at 2,500 rpm for 2-min at 4^0C. Protein pellets were solubilised in 2×SDS-PAGE sample buffer and electrophoresis and transfer to membrane was carried out according to standard procedures described previously. The blots were probed for respective proteins, then treated with stripping

buffer, washed in TBS, and probed with anti-phosphoserine antibodies (Chemicon, Billerica, MA).

Co-immunoprecipitation experiments

For co-immunoprecipitation experiments, immunoprecipitated NHE2 or NHE3 was subjected to SDS-PAGE and probed using a rabbit polyclonal occludin, claudin-1 (Zymed, San Franscico, CA), or EBP50 antibody (Abcam Inc, Cambridge, MA). Immunoprecipitates obtained using normal pre immune serum served as negative control. The experiments were repeated more than three times and the blot images were analyzed by densitometry using SigmaScan Pro 5.0 (Sigmastat, San Jose CA, USA).

Statistics

Data were reported as means ± SE. All data were analyzed by using an ANOVA for repeated measures using a standard one-way ANOVA (Sigmastat, Systat Software Inc, San Jose, CA, USA). A Tukey's test was used to determine differences between treatments following ANOVA ($p<0.05$).

Results

NHE2$^{-/-}$ mice had increased blood-to-lumen intestinal ^{3}H-mannitol clearance

Complete mesenteric ischemia followed by a 3-hour recovery period resulted in a significant 1.7-fold increase ($p<0.05$) in blood-to-lumen ^{3}H-Mannitol clearance rate compared to non-ischemic control loops in NHE2$^{+/+}$ mice (0.646±0.2 vs. 1.08±0.3 ml/hr

x 100g in control and ischemic loops, respectively; Figure 1). Similar clearance values for control and ischemic ileal loops were observed in NHE2 heterozygote ($NHE2^{+/-}$) ileum (data not shown). Blood-to-lumen ^{3}H-mannitol clearance in $NHE^{-/-}$ ileal segments following a 3-hour recovery period was 6.2-fold greater than respective non-ischemic control loops (0.722±0.19 vs. 4.52±1.53 ml/hr x100g in control and ischemic loops respectively, $p< 0.01$) and significantly greater ($p<0.05$) when compared with $NHE2^{+/+}$ ischemic loops, indicating an important role of NHE2 in recovery of barrier function.

Recovery of Transepithelial Resistance (TER) is impaired by selective inhibition of NHE2.

Following increased *in vivo* blood-to-lumen intestinal ^{3}H-mannitol clearance in NHE2 deficient mice, we investigated whether pharmacological inhibition of NHE2 in wild type mice would have similar effect on intestinal barrier recovery. Therefore, the ischemia-injured jejunal mucosa from wild type mice was treated with the selective NHE2 isoform inhibitor HOE-694 and TER was monitored over a 3-hour period on Ussing chambers. Application of HOE-694 (25 μM) to the mucosal surface of the ischemia-injured mucosa led to reduction in TER compared with ischemia-injured controls, suggesting an significant role of NHE2 in the recovery of intestinal barrier after ischemic injury (Figure 2).

Barrier defects in NHE2$^{-/-}$ mice were independent of epithelial restitution

There were no apparent histological differences when examining intestinal tissues from wild type and NHE2$^{-/-}$ mice. In both genotypes, 45-minutes of intestinal ischemia resulted in sloughing of apical villous enterocytes and contraction of villi (Figure 3). After 1.5-hour of post-ischemic recovery the villi were found contracted and epithelium was almost restituted in NHE2$^{+/+}$ and NHE2 deficient mice. Following a 3-hour recovery period, the epithelium was completely restituted in NHE2$^{+/+}$ and NHE2 deficient mice. The villus width and crypt depth measurements were comparable in control and ischemic tissues of wild type and NHE2 deficient mice (Table 1). These histological findings led us to conclude that the increased blood-to-lumen clearance of ^{3}H-mannitol noted with both genotypes of mice, particularly NHE2$^{-/-}$ mice, is independent of epithelial restitution, and more likely attributable to changes in paracellular permeability.

TJ protein expression in NHE2$^{+/+}$ and NHE2$^{-/-}$ mice

To determine if impaired mucosal barrier recovery in NHE2$^{-/-}$ mice was associated with changes in TJ composition, we performed Western blot analyses for core TJ proteins occludin and claudin-1. Western analyses revealed minimum expression of occludin and claudin-1 in Triton-X soluble fractions of NHE2$^{+/+}$ mice after 3-hours of post-ischemic recovery, and most of these two proteins were concentrated in Triton-X insoluble fraction (Figure 4, *panel A*). Alternatively, Triton-X soluble fractions from NHE2$^{-/-}$ mice showed increased expression of occludin and claudin-1. The expression of both these proteins was reduced in Triton-X insoluble fractions of NHE2$^{-/-}$ mice. Thus there was increased

shift of occludin and claudin-1 from Triton-X insoluble fractions towards Triton-X soluble fraction in $NHE2^{-/-}$ mice as compared to $NHE2^{+/+}$ mice. The total expression of occludin and claudin-1 was comparable in control and ischemic tissues of wild type and $NHE2^{-/-}$ mice, as revealed by western analysis of respective whole tissue lysates (Figure 4, *panel B*)

Localization of TJ proteins

We further investigated TJ structure by performing immunofluorescence (IF) labeling for occludin and claudin-1 in $NHE2^{+/+}$ and $NHE2^{-/-}$ ischemic mucosa. IF analyses revealed uniform, punctuate, fluorescence for occludin that was confined to region of the apical tight junction in $NHE2^{+/+}$ recovering ischemic mucosa. Likewise for claudin-1, the normal chicken wire pattern was seen in cross sections from $NHE2^{+/+}$ ileal tissues (Figure 5). In contrast, IF analyses for occludin and claudin-1 from ischemic tissues from $NHE2^{-/-}$ mice showed a disrupted and diffuse staining pattern.

Expression of phosphorylated tight junction proteins in control and ischemic tissues

To further assess NHE2 mediated barrier function recovery, we studied the phosphorylation status of tight junction protein in mouse tissues. Western blot analyses of immunoprecipitated occludin and claudin-1 showed significantly increased phosphoserine expression of both junctional proteins in ischemic intestine of $NHE2^{+/+}$ mice but not NHE2 deficient mice (Figure 6).

Co-immunoprecipitation of NHE2 with tight junction proteins and Na^+/H^+ regulatory factor 1, EBP50.

In previous experiments utilizing porcine ileum it was shown that the cytosolic scaffold protein EBP50 was expressed in both NHE2 and NHE3 immunoprecipitates. Moreover, ischemic injury resulted in increased expression of EBP50 in NHE2 immunoprecipitates whereas its expression in ischemic NHE3 immunoprecipitates remained unchanged.[13] We speculated that interaction of NHE2 with EBP50 may serve as a potential link to the TJs. Therefore NHE2 and NHE3 protein from control and post-ischemic $NHE2^{+/+}$ wild type mice ileum was immunoprecipitated and western blots were probed using antibodies for EBP50, occludin, and claudin-1. As shown in Figure 7, EBP50 was expressed in both NHE2 and NHE3 immunoprecipitates in control and post-ischemic ileum. As in porcine tissues, ischemia appeared to up regulate EBP50 expression in NHE2 immunoprecipitates ($p<0.05$) and not NHE3 immunoprecipitates. This may provide an important piece of evidence that reveals how NHE2 is involved in TJ regulation. In subsequent experiments, NHE2 and NHE3 immunoprecipitates were probed for expression of TJ proteins occludin and claudin-1. Occludin and claudin-1 were expressed in both NHE2 and NHE3 immunoprecipitates in uninjured control and ischemic tissues; their expression did not change significantly in ischemic tissues.

Discussion

The present studies demonstrate an important role for NHE2 in repair of mucosal barrier function in ischemic mouse ileum. *In vivo* blood-to-lumen ^{3}H-mannitol clearance in recovering ischemic ileum was 4-fold greater in NHE2$^{-/-}$ ileum compared with NHE2$^{+/+}$ ileum. Histological examination of the ischemic tissues revealed that epithelial restitution was complete by the 3-hour post-ischemic period, indicating that increased ^{3}H-mannitol clearance in NHE2$^{-/-}$ mice was attributable to increased paracellular permeability, as has been shown in previous studies. The link between NHE2 and epithelial barrier function has been demonstrated previously. For example, Nowak *et al* showed that inhibition of NHE2 in Caco2 cell monolayer resulted in elevations in transepithelial resistance.[21] Furthermore, the authors showed that an NHE2 inhibitor prevented PMA-induced disruption of tight junction proteins and barrier properties. It is unclear why pharmacological inhibition of NHE2 enhances barrier function, as shown in our prior in-vitro pharmacological experiments in porcine model[13] whereas the genetic lack of NHE2 expression is deleterious to recovery of barrier function in mice. However, the present experiments clearly indicate that NHE2 protein expression is required for optimal recovery. The experiment with pharmacological inhibition of NHE2 in wild type mice also supported the *in vivo* findings. Inhibition of NHE2 with HOE-694 in ischemic mucosa led to reductions in the TER as compared to untreated ischemic mucosa. Though the similarity in results obtained after pharmacological modulation of a protein and

deleting the same protein through out development is known,[22-24] the difference in results of pharmacological experiments with porcine mucosa and murine mucosa appears to be species specific phenomenon.

Impaired barrier recovery in ischemic $NHE2^{-/-}$ mouse ileum was associated with a marked disruption of occludin and claudin-1 localization and a shift in expression of these proteins to the cytosol, suggesting that loss of NHE2 impairs the ability of the TJ repair. The signaling events associated with impaired TJ recovery in $NHE2^{-/-}$ mouse ileum are not known. However, it is known that TJs are regulated by phosphorylation events during repair or biogenesis that represents critical signaling events in TJ repair.[25-27] For example, recovery of barrier function and occludin localization to the TJs in Madin-Darby canine kidney cells coincided with the phosphorylation status of occludin.[27] In the present study, occludin and claudin-1 phosphorylation was increased in recovering ischemic ileum of $NHE2^{+/+}$ mice and not $NHE2^{-/-}$ mouse ileum thus suggesting that signaling events that result in phosphorylation of TJs are disrupted in the absence of NHE2. The mechanisms coordinating these events remain to be elucidated.

In the present study, co-immunoprecipitation experiments revealed that the TJ proteins occludin and claudin-1 were expressed in NHE2 and 3 immunoprecipitates, indicating their close proximity. Intracellular trafficking of NHE2 is not studied in details. None the less, as compared to NHE3 that has greater membrane turnover,[28,29] NHE2 is considered as resident of plasma membrane and this may provide opportunity

for NHE2-junctional protein complexes to form. Recent work has demonstrated rapid recruitment of NHE2 to the plasma membrane in response to lower cytosolic pH.[30]

Several studies clearly indicate that apical NHE are regulated by phosphorylation, and this phosphorylation is in large part facilitated by accessory protein such as EBP50.[31,32] The linkage between EBP50 and NHE isoforms appears to occur via PDZ domains, and allows access of kinases such as PKA to the cytosolic tail of NHE.[29] Although advances have been made in understanding the regulation of NHE3 through interaction with Na^+/H^+ exchange regulatory factors (NHERFs) such as EBP50[33] which in turn links NHE3 to the cytoskeleton via ezrin,[29] little is known about regulation of NHE2. Nonetheless, recent studies have shown that NHE2 is co-expressed with EBP50 in porcine small intestinal tissues.[13] In addition, α spectrin, a cytoskeletal protein, has been shown to interact with a C-terminal proline-rich area of NHE2.[34] In the present studies, we showed that EBP50 was expressed in both NHE2 and NHE3 immunoprecipitates, but there was greater expression of EBP50 in NHE2 immunoprecipitates during recovery from ischemia. Members of the NHERF family have been shown to be involved in cytoskeleton remodeling,[35] but the mechanisms of NHE-EBP50 interactions and their potential role in tight junction repair need to be investigated further.

Our results so far suggest a signal transduction pathway involving NHE2 and reorganization of junctional proteins, leading to closure of TJs following ischemic injury. PKA regulation of NHE2 involves interaction with its c-terminus end,[36] which may in

turn signal the recruitment of junctional proteins to the apical epithelial membrane. The strong role of PKA in phosphorylating NHE may explain in part the reparative effects of prostaglandins, which signal through this pathway. The NHE2 deficient mice used in this study lacks a complete C- terminus, although a truncated N-terminus is produced (personal communication, Dr. Lara Gawenis, Shull lab, University of Cincinnati, USA). It is possible that the phosphorylation of the C-terminus of NHE2 by a PKA agonist, facilitated by a regulatory factor such as EBP50, effects changes in tight junction proteins.

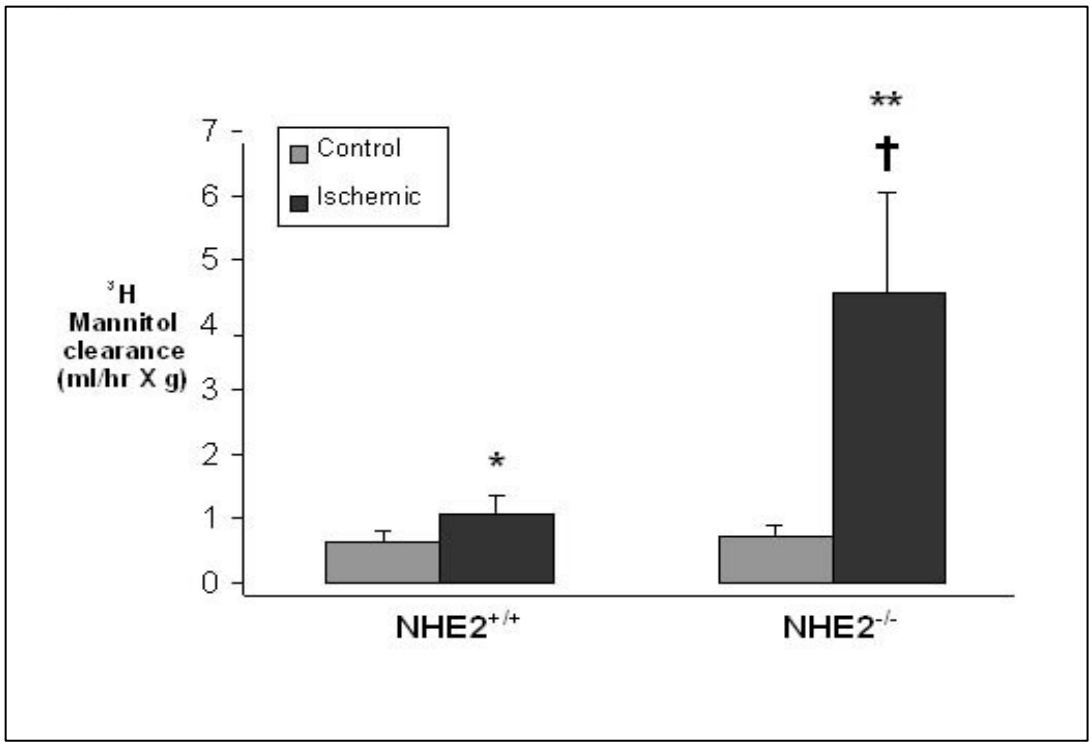

Figure 1. Blood-to-lumen ^{3}H-mannitol clearance following 3-hours of post-ischemic recovery. In NHE2$^{+/+}$ and NHE2$^{-/-}$ mice, there was significant increase in ^{3}H-mannitol clearance in ischemic groups (*, ** $p< 0.05$). However, in NHE2$^{-/-}$ mice, the ischemic loops had dramatically elevated ^{3}H-mannitol clearances as compared to control loops as well as control and ischemic loops of NHE2$^{+/+}$ mice ($^{\dagger}P< 0.01$).

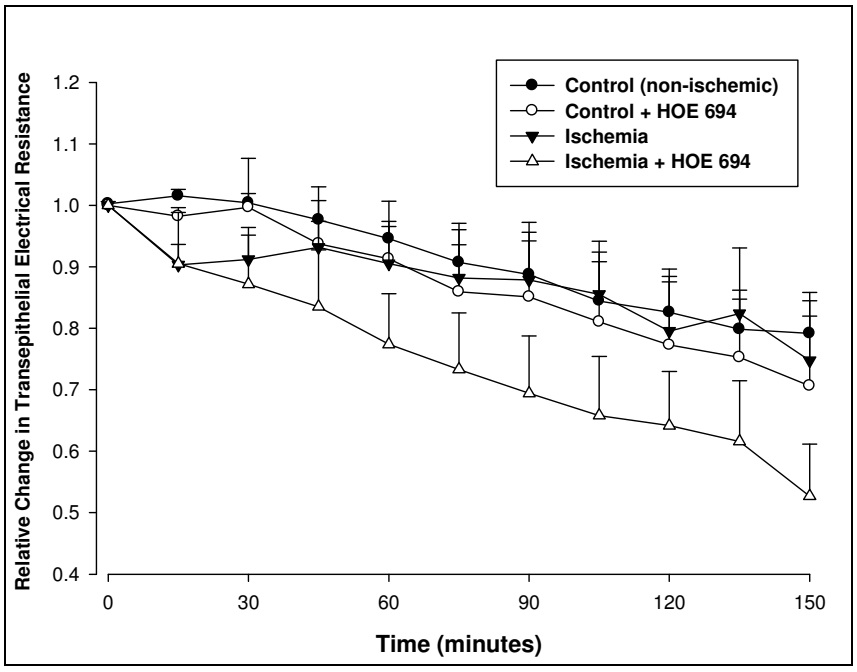

Figure 2. Transepithelial resistance (TER) in ischemia-injured wild type ileum treated with inhibitor of sodium hydrogen exchanger NHE2. Either sham control or 45-minutes of *in vivo* ischemia-injured jejunal mucosa were mounted on Ussing chamber and equilibrated for a period of 30 minutes. Treatment with NHE2 inhibitor HOE-694 (25 μM, added to the mucosal surface) led to significant reduction of TER in ischemic-injured tissues ($p < 0.05$). Values are means ± SE; $n = 4$.

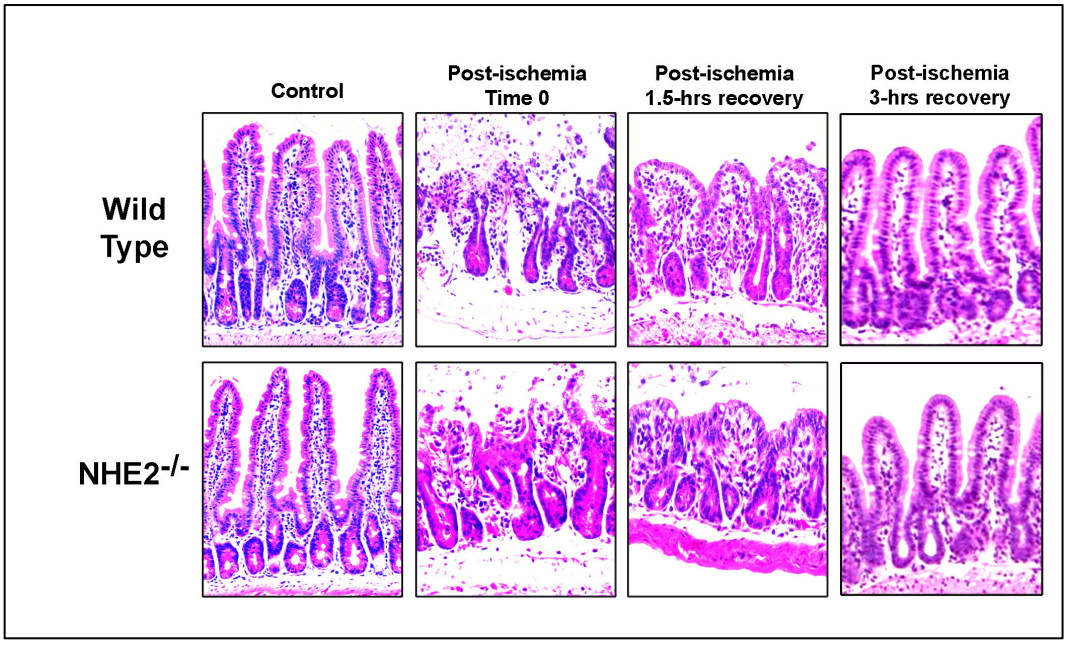

Figure 3. Histological examination of ileal tissues from wild type and NHE2$^{-/-}$ mice subjected to ischemia. Ischemia results in epithelial sloughing at the tips of villi and contraction of villi. After 1.5 and 3-hours of recovery, the epithelial restitution in NHE2$^{-/-}$ mice was comparable to wild type mice. H&E Stain, X 100.

Table 1. Morphometric assessment of ischemic ileal epithelium of wild type and NHE2$^{-/-}$ mice

Genotype	Villous height (µm)		Villous width (µm)		Crypt depth (µm)	
	Control	Ischemic	Control	Ischemic	Control	Ischemic
NHE2$^{+/+}$	162.9±1.6	122.1±1.9	40.83±2.3	44.72±2.7	32.4±7.3	28.4±2.7
NHE2$^{-/-}$	172.2±5.4	131.8±5.9	40.31±1.1	41.8±0.4	34.7±4.2	29.1±3.9

Uninjured and ischemic intestinal segments from NHE2$^{+/+}$ and NHE2 deficient mice were fixed in 10% buffered formalin, and processed for histological examination according to standard protocol. There was no significant difference in villous height, villous width, and crypt depth measurements of ischemic loops of wild type and NHE2$^{-/-}$ mice. Data represented as mean ± SE, n= 6

Figure 4. Western Blot analysis of cell fractions for tight junction proteins. A, following the post-ischemic recovery period of 3 hours, protein extracts from $NHE2^{+/+}$ and $NHE2^{-/-}$ mice were homogenized in a buffer containing Triton X-100 (Triton X-100 soluble) or a more stringent buffer (RIPA, Triton X-100 insoluble). Supernatants were subsequently analyzed using anti-occludin and anti-claudin-1 antibodies. There was increased expression of both occludin and claudin-1 in the Triton X-100 soluble fraction in NHE2 deficient mice following ischemia, suggesting movement of TJ proteins to the cytosol. B, The whole tissue lysates from control and ischemic tissues of wild type and $NHE2^{-/-}$ mice revealed comparable expression of occludin and claudin-1.

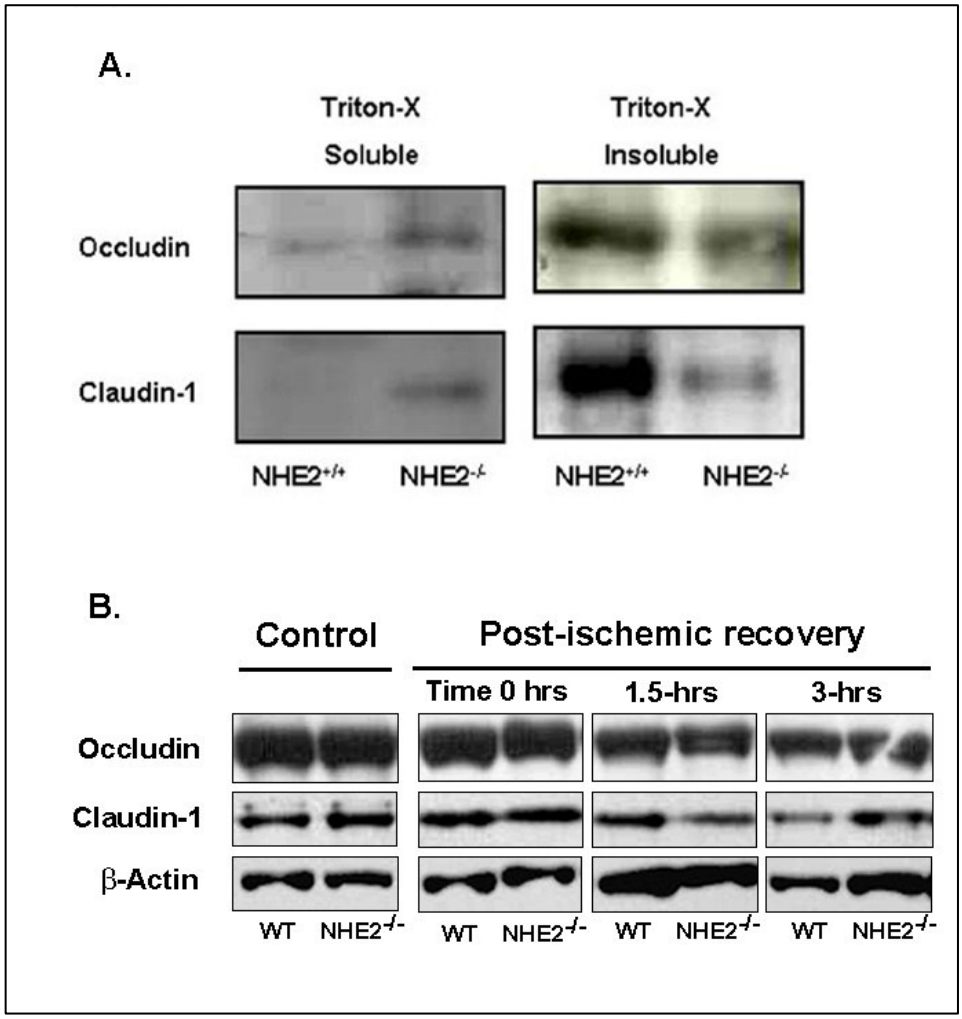
A.
Triton-X
Soluble
Triton-X
Insoluble
Occludin
Claudin-1
NHE2+/+
NHE2-/-
NHE2+/+
NHE2-/-
B.
Control
Post-ischemic recovery
Time 0 hrs
1.5-hrs
3-hrs
Occludin
Claudin-1
β-Actin
WT
NHE2-/-
WT
NHE2-/-
WT
NHE2-/-
WT
NHE2-/-

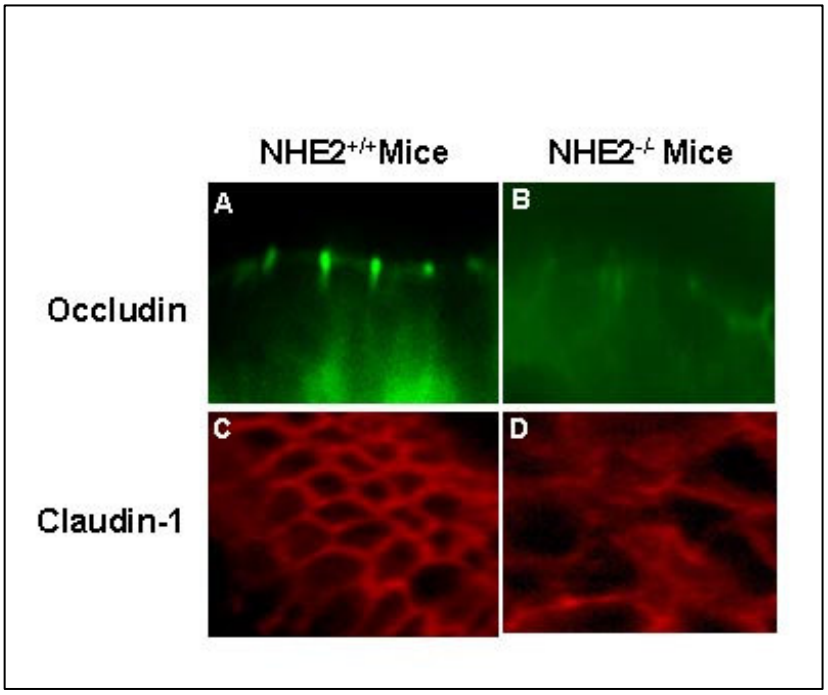

Figure 5. Localization of the tight junction proteins occludin and claudin-1 in control and ischemic injured ileal mucosa of wild type and NHE2$^{-/-}$ mice. After 3-hour post-ischemic recovery intestinal samples were collected and processed for immunofluorescence using rabbit polyclonal occludin and claudin-1 antibodies, followed by goat anti rabbit IgG conjugated with FITC and Cy3 respectively. A, Punctuate localization of occludin to the region of the tight junction was noted in NHE2$^{+/+}$ mice compared to (B) diffuse localization of occludin in NHE2$^{-/-}$ mice. C, An en face view of the immunofluorescence pattern of claudin-1, showing a 'chicken-wire' configuration in NHE2$^{+/+}$ mice, as compared to (D) diffuse staining in NHE2$^{-/-}$ mice.

Figure 6

Phosphorylation of tight junction proteins during post-ischemic recovery. A, The expression of phosphorylated claudin-1 serine residues appears greater in post-ischemic 3-hour recovered tissues from $NHE2^{+/+}$ mice as compared to similar tissues from $NHE2^{-/-}$ mice on a representative Western blots. Lower panel: Densitometry analysis, which accounted for total claudin-1 expression as against phosphorylated claudin-1 in individual lane, revealed around 15% increase in claudin-1 phosphoserine expression in ischemic intestine over control intestine in $NHE2^{+/+}$ mice; n=4, *$p< 0.05$. **B,** The expression of serine phosphorylated occludin appears greater in post-ischemic 3-hour recovered tissues from $NHE2^{+/+}$ mice as compared to similar tissues from $NHE2^{-/-}$ mice on a representative Western blot. Lower panel: Densitometry analysis that also considered total occludin expression in individual lane revealed around 14% increase in occludin phosphoserine expression in ischemic intestine over control intestine in $NHE2^{+/+}$ mice; n=4, *$p< 0.05$. The expression of neither serine phosphorylated claudin-1 or occludin changed significantly in between control and ischemic intestine in $NHE2^{-/-}$ mice.

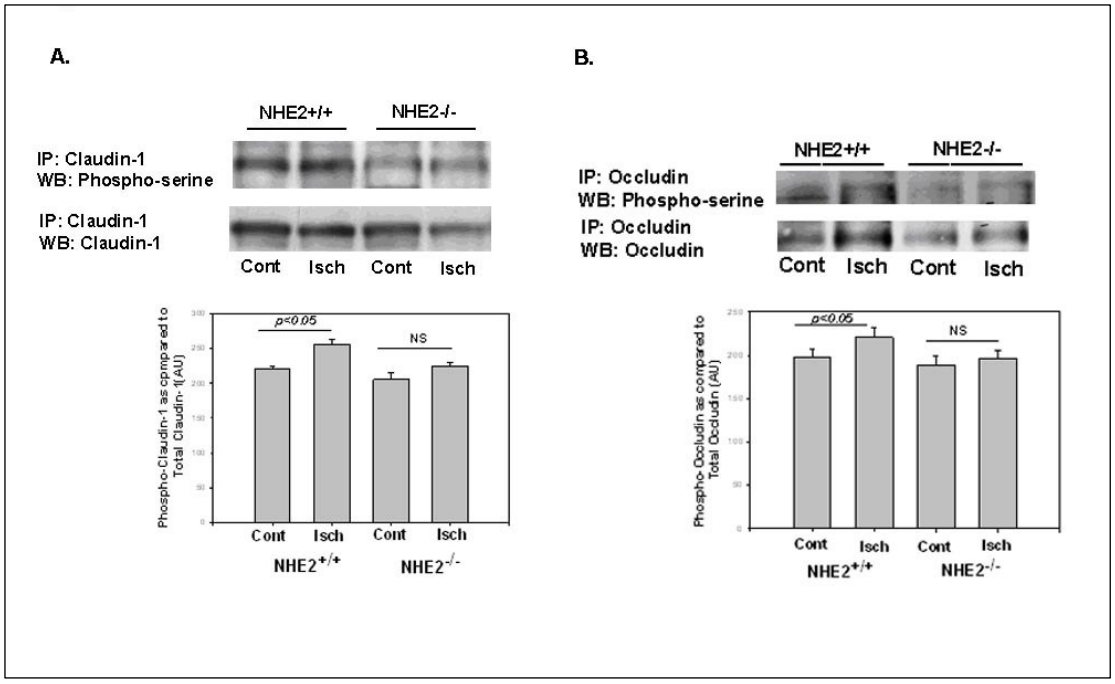
A.
NHE2+/+
NHE2-/-
IP: Claudin-1
WB: Phospho-serine
IP: Claudin-1
WB: Claudin-1
Cont
Isch
Cont
Isch
p<0.05
NS
Phospho-Claudin-1 as cpmpared to Total Claudin-1(AU)
Cont
Isch
Cont
Isch
NHE2+/+
NHE2-/-
B.
NHE2+/+
NHE2-/-
IP: Occludin
WB: Phospho-serine
IP: Occludin
WB: Occludin
Cont
Isch
Cont
Isch
p<0.05
NS
Phospho-Occludin as compared to Total Occludin (AU)
Cont
Isch
Cont
Isch
NHE2+/+
NHE2-/-

Figure 7

EBP50 and junctional protein expression in NHE2 and NHE3 immunoprecipitates from wild-type mice. A. Representative Western blots revealed the relative expression of claudin-1, occludin, and EBP50 in NHE2 and NHE3 immunoprecipitates from control and ischemic intestine of wild type mice. **B.** Based on densitometry analyses (n=3), there was around two-fold increase in the expression of EBP50 in NHE2 immunoprecipitates from ischemic intestine over the control intestine (*$p<0.05$), which may explain in part the regulatory role of NHE2 in recovery of junctional barrier function. The expression of junctional proteins claudin-1 and occludin did not increase significantly in ischemic tissues over the control tissues in NHE2 as well as NHE3 immunoprecipitates, as revealed by densitometry analysis (not shown).

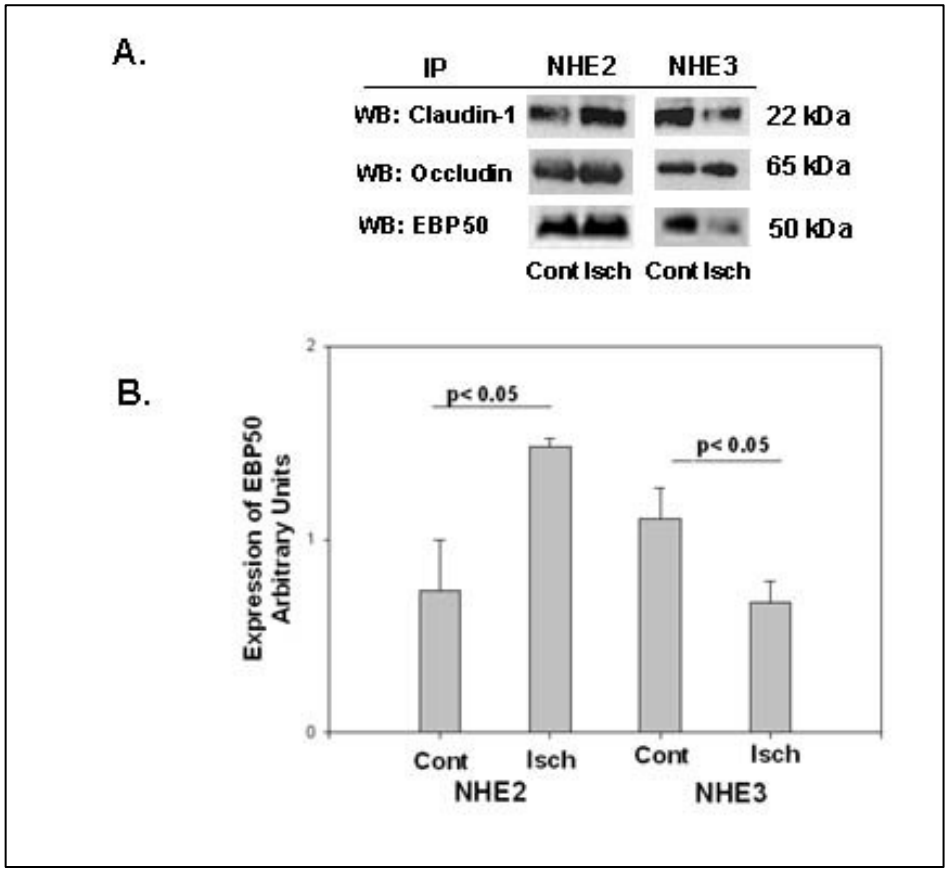
A.
IP
NHE2
NHE3
WB: Claudin-1
22 kDa
WB: Occludin
65 kDa
WB: EBP50
50 kDa
Cont Isch Cont Isch
B.
Expression of EBP50
Arbitrary Units
2
1
0
p< 0.05
p< 0.05
Cont
Isch
Cont
Isch
NHE2
NHE3

References

1. Turner JR. Molecular basis of epithelial barrier regulation: from basic mechanisms to clinical application. Am.J.Pathol. 2006;169:1901-1909.

2. Turner JR, Rill BK, Carlson SL, Carnes D, Kerner R, Mrsny RJ, Madara JL. Physiological regulation of epithelial tight junctions is associated with myosin light-chain phosphorylation. Am.J.Physiol. 1997;273:C1378-85.

3. Turner JR, Angle JM, Black ED, Joyal JL, Sacks DB, Madara JL. PKC-dependent regulation of transepithelial resistance: roles of MLC and MLC kinase. Am.J.Physiol. 1999;277:C554-62.

4. Yoo J, Nichols A, Mammen J, Calvo I, Song JC, Worrell RT, Matlin K, Matthews JB. Bryostatin-1 enhances barrier function in T84 epithelia through PKC-dependent regulation of tight junction proteins. Am.J.Physiol.Cell.Physiol. 2003;285:C300-9.

5. Turner JR, Black ED, Ward J, Tse CM, Uchwat FA, Alli HA, Donowitz M, Madara JL, Angle JM. Transepithelial resistance can be regulated by the intestinal brush-border Na(+)/H(+) exchanger NHE3. Am.J.Physiol.Cell.Physiol. 2000;279:C1918-24.

6. Deitch EA, Rutan R, Waymack JP. Trauma, shock, and gut translocation. New Horiz. 1996;4:289-299.

7. Stechmiller JK, Treloar D, Allen N. Gut dysfunction in critically ill patients: a review of the literature. Am.J.Crit.Care 1997;6:204-209.

8. Moore R, Carlson S, Madara JL. Rapid barrier restitution in an in vitro model of intestinal epithelial injury. Lab.Invest. 1989;60:237-244.

9. Blikslager AT, Roberts MC, Argenzio RA. Prostaglandin-induced recovery of barrier function in porcine ileum is triggered by chloride secretion. Am.J.Physiol. 1999;276:G28-36.

10. Blikslager AT, Roberts MC, Rhoads JM, Argenzio RA. Prostaglandins I2 and E2 have a synergistic role in rescuing epithelial barrier function in porcine ileum. J.Clin.Invest. 1997;100:1928-1933.

11. Gookin JL, Galanko JA, Blikslager AT, Argenzio RA. PG-mediated closure of paracellular pathway and not restitution is the primary determinant of barrier recovery in acutely injured porcine ileum. Am.J.Physiol.Gastrointest.Liver Physiol. 2003;285:G967-79.

12. Little D, Dean RA, Young KM, McKane SA, Martin LD, Jones SL, Blikslager AT. PI3K signaling is required for prostaglandin-induced mucosal recovery in ischemia-injured porcine ileum. Am.J.Physiol.Gastrointest.Liver Physiol. 2003;284:G46-56.

13. Moeser AJ, Nighot PK, Ryan KA, Wooten JG, Blikslager AT. Prostaglandin-mediated inhibition of Na+/H+ exchanger isoform 2 stimulates recovery of barrier

function in ischemia-injured intestine. Am.J.Physiol.Gastrointest.Liver Physiol. 2006;291:G885-94.

14. Gawenis LR, Stien X, Shull GE, Schultheis PJ, Woo AL, Walker NM, Clarke LL. Intestinal NaCl transport in NHE2 and NHE3 knockout mice. Am.J.Physiol.Gastrointest.Liver Physiol. 2002;282:G776-84.

15. Schultheis PJ, Clarke LL, Meneton P, Miller ML, Soleimani M, Gawenis LR, Riddle TM, Duffy JJ, Doetschman T, Wang T, Giebisch G, Aronson PS, Lorenz JN, Shull GE. Renal and intestinal absorptive defects in mice lacking the NHE3 Na+/H+ exchanger. Nat.Genet. 1998;19:282-285.

16. Ledoussal C, Woo AL, Miller ML, Shull GE. Loss of the NHE2 Na(+)/H(+) exchanger has no apparent effect on diarrheal state of NHE3-deficient mice. Am.J.Physiol.Gastrointest.Liver Physiol. 2001;281:G1385-96.

17. Bachmann O, Riederer B, Rossmann H, Groos S, Schultheis PJ, Shull GE, Gregor M, Manns MP, Seidler U. The Na+/H+ exchanger isoform 2 is the predominant NHE isoform in murine colonic crypts and its lack causes NHE3 upregulation. Am.J.Physiol.Gastrointest.Liver Physiol. 2004;287:G125-33.

18. Guan Y, Dong J, Tackett L, Meyer JW, Shull GE, Montrose MH. NHE2 is the main apical NHE in mouse colonic crypts but an alternative Na+-dependent acid extrusion mechanism is upregulated in NHE2-null mice. Am.J.Physiol.Gastrointest.Liver Physiol. 2006;291:G689-99.

19. Komatsu S, Grisham MB, Russell JM, Granger DN. Enhanced mucosal permeability and nitric oxide synthase activity in jejunum of mast cell deficient mice. Gut 1997;41:636-641.

20. Argenzio RA, Lecce J, Powell DW. Prostanoids inhibit intestinal NaCl absorption in experimental porcine cryptosporidiosis. Gastroenterology 1993;104:440-447.

21. Nowak P, Blaheta R, Schuller A, Cinatl J, Wimmer-Greinecker G, Moritz A, Scholz M. The Na+/H+ exchange inhibitor HOE642 prevents stress-induced epithelial barrier dysfunction. Int.J.Mol.Med. 2004;14:175-178.

22. Hodge CW, Raber J, McMahon T, Walter H, Sanchez-Perez AM, Olive MF, Mehmert K, Morrow AL, Messing RO. Decreased anxiety-like behavior, reduced stress hormones, and neurosteroid supersensitivity in mice lacking protein kinase Cepsilon. J.Clin.Invest. 2002;110:1003-1010.

23. Leidenheimer NJ, Chapell R. Effects of PKC activation and receptor desensitization on neurosteroid modulation of GABA(A) receptors. Brain Res.Mol.Brain Res. 1997;52:173-181.

24. Gordon JA. Anxiolytic drug targets: beyond the usual suspects. J.Clin.Invest. 2002;110:915-917.

25. Balda MS, Gonzalez-Mariscal L, Matter K, Cereijido M, Anderson JM. Assembly of the tight junction: the role of diacylglycerol. J.Cell Biol. 1993;123:293-302.

26. Sakakibara A, Furuse M, Saitou M, Ando-Akatsuka Y, Tsukita S. Possible involvement of phosphorylation of occludin in tight junction formation. J.Cell Biol. 1997;137:1393-1401.

27. Wong V. Phosphorylation of occludin correlates with occludin localization and function at the tight junction. Am.J.Physiol. 1997;273:C1859-67.

28. Cavet ME, Akhter S, Murtazina R, Sanchez de Medina F, Tse CM, Donowitz M. Half-lives of plasma membrane Na(+)/H(+) exchangers NHE1-3: plasma membrane NHE2 has a rapid rate of degradation. Am.J.Physiol.Cell.Physiol. 2001;281:C2039-48.

29. Zachos NC, Tse M, Donowitz M. Molecular physiology of intestinal Na+/H+ exchange. Annu.Rev.Physiol. 2005;67:411-443.

30. Gens JS, Du H, Tackett L, Kong SS, Chu S, Montrose MH. Different ionic conditions prompt NHE2 and NHE3 translocation to the plasma membrane. Biochim.Biophys.Acta 2007;1768:1023-1035.

31. Yun CH, Oh S, Zizak M, Steplock D, Tsao S, Tse CM, Weinman EJ, Donowitz M. cAMP-mediated inhibition of the epithelial brush border Na+/H+ exchanger, NHE3, requires an associated regulatory protein. Proc.Natl.Acad.Sci.U.S.A. 1997;94:3010-3015.

32. Zizak M, Lamprecht G, Steplock D, Tariq N, Shenolikar S, Donowitz M, Yun CH, Weinman EJ. cAMP-induced phosphorylation and inhibition of Na(+)/H(+)

exchanger 3 (NHE3) are dependent on the presence but not the phosphorylation of NHE regulatory factor. J.Biol.Chem. 1999;274:24753-24758.

33. Sun F, Hug MJ, Lewarchik CM, Yun CH, Bradbury NA, Frizzell RA. E3KARP mediates the association of ezrin and protein kinase A with the cystic fibrosis transmembrane conductance regulator in airway cells. J.Biol.Chem. 2000;275:29539-29546.

34. Chow CW. Regulation and intracellular localization of the epithelial isoforms of the Na+/H+ exchangers NHE2 and NHE3. Clin.Invest.Med. 1999;22:195-206.

35. Lamprecht G, Weinman EJ, Yun CH. The role of NHERF and E3KARP in the cAMP-mediated inhibition of NHE3. J.Biol.Chem. 1998;273:29972-29978.

36. Nath SK, Kambadur R, Yun CH, Donowitz M, Tse CM. NHE2 contains subdomains in the COOH terminus for growth factor and protein kinase regulation. Am.J.Physiol. 1999;276:C873-82.

CHAPTER V

MECHANISMS OF TURKEYASTROVIRUS TASTV-2-INDUCED DIARRHEA

Abstract

Astrovirus causes enteric disease in several mammalian and avian hosts and is a leading cause of viral gastroenteritis in infants worldwide. The mechanism of astrovirus-induced diarrhea is poorly understood. We studied the pathophysiology of turkey astrovirus type 2 (TAstV-2)-induced diarrhea in an established experimental model using the natural host. Three-day old turkey poults were infected orally with TAstV-2 or the vehicle. Four days post-infection, when infected poults exhibited diarrhea, small intestinal tissues were harvested and studied on Ussing chamber for measurements of ion transport (short circuit current (I_{sc}) and isotopic Na^+ and Cl^- fluxes) and mucosal barrier function (transepithelial electrical resistance (TER) and mucosal to serosal ^{3}H-mannitol flux). Tissues were also processed for histologic and ultra-structural examination, immunofluorescence, and immuno-blotting. Ussing chamber studies revealed similar I_{sc} and TER measurements in TAstV-2 infected and control jejunum. However isotopic flux studies demonstrated impaired electroneutral Na^+ absorption in astrovirus-infected jejunum ($_JNa^+_{net}$ flux = 0.82 ± 0.52 and -1.22 ± 0.53 µeq/cm2/.hfor control and TAstV-2 infected jejunum, respectively, $p< 0.05$). The histological changes in infected intestine were minimal and there was no evidence of a robust inflammatory response. Furthermore, histomorphometry for villus height and surface area, and crypt depth did not differ between control and infected intestine. Paracellular permeability in astrovirus-infected jejunum was not different from control intestine, as judged by mucosal-to-serosal ^{3}H mannitol fluxes performed on Ussing chambers. In electron microscopic examinations neither tight junctions nor paracellular spaces were found to be dilated. However, the

terminal web region displayed frequent dense aggregations in TAstV-2 infected intestine. Immunofluorescence for F-actin revealed rearrangement of apical F-actin in thicker, dense aggregations in TAstV-2 infected intestine. Western analysis was performed to study major apical membrane Sodium Hydrogen Exchangers (NHEs). The total protein expression for NHE3 in astrovirus-infected jejunum was not changed as compared to control. However, a significant shift was observed for expression of NHE3 from detergent insoluble fractions to detergent soluble fractions of TAstV-2 infected jejunum. Alternatively, NHE2 was up-regulated in infected jejunum, possibly as a compensatory response. We concluded that astrovirus TAstV-2 induced malabsorptive diarrhea associated with actin re-arrangement and redistribution of apical membrane NHE3.

Introduction:

Gastrointestinal infections are the outcome of the interaction between pathogen virulence factors and host defense mechanisms resulting in clinical symptoms such as diarrhea or vomiting due to altered gut transport or barrier function. Acute diarrheal disease continues to be a major concern worldwide in humans and animals, and is mostly caused by viral agents including rotavirus, astrovirus, calicivirus and enteric adenovirus.[1]. The impact of diarrheal diseases is marked by significant morbidity and mortality in developing countries and a high cost of treatment and hospitalization due to illness in developed countries.[2,3] With the availability of newer molecular diagnostic tools, astrovirus is now recognized as a leading cause of diarrhea, particularly in infants, as well as immunocompromised patients.[4,5,6] Outbreaks of astrovirus-induced diarrhea also occur

in institutions such as day care centers and hospitals[6,7,8] and are associated with food-related illnesses.[9] Astroviruses are member of the *Astroviridae* family, which is divided into two genera: *Mamastrovirus* (mammalian astroviruses) and *Avastrovirus* (avian astroviruses). Typically the virion (28–41 nm) is non-enveloped and contains a positive single-stranded polyadenylated RNA genome.[10] Astrovirus causes morbidity and enteric infections in a number of mammalian hosts including humans, dogs, cats, lambs, mice, and pigs; morbidity, severity of clinical symptoms and course of infection varies between species.[11]Astroviruses are known to be widely prevalent in commercial chicken and turkey flocks and associated with diarrheal disease.[12-14] Previous reports described diarrhea, growth depression, altered intestinal maltase activity and minimal histologic changes in the intestine of astrovirus-infected juvenile turkeys.[15,16] The turkey astrovirus TAstV-2 used in this study was originally isolated from natural outbreaks of complex diarrheal disease involving multiple organisms, and is reported to cause diarrhea experimentally, in the absence of overt histological changes and enterocyte death.[11]

Continuing investigation into the role of ion transport in infectious diarrhea has established that cholera toxin and the heat-labile and heat-stable enterotoxins of *Escherichia coli* produces pure Cl^- secretory diarrhea.[17] From current research on the complex interaction of rotaviral proteins with intestinal epithelium, it appears that diarrhea is of a mixed type and has malabsorptive as well as secretory components due to impaired activities of intestinal disaccharidases and SGLT1-mediated Na^+-D-glucose symport, and moderate Cl^- secretion regulated by a phospholipase C-dependent calcium

signaling pathway, respectively.[17] Unlike these developments, the pathophysiology and mechanism of diarrhea for astroviruses is largely unknown, and this is attributed to the lack of a small animal model to understand this disease.[18] In this study we investigated the pathophysiology of astrovirus infection in a pre-established *in vivo* model using turkey astrovirus TAstV-2. The genetic and immunological characterization of TAstV-2, kinetics of *in vivo* replication, and host responses to TAstV-2 infection have been described earlier.[11,19,20] The results of the present study indicate that astrovirus infection leads to impaired Na^+ transport associated with actin rearrangement and redistribution of the apical Na^+-H^+ exchanger NHE3 in small intestine.

Methods:

Animals.

One-day-old unvaccinated Turkey poults obtained from a commercial hatchery were randomly divided into two groups and housed in separate 934-1-WP Animal isolators (developed by Southeast Poultry Research Lab, Athens, Georgia, USDA-ARS) with a HEPA filtered inlets and exhausts. Birds had free access to feed and water. After an acclimation period of 3 days, one group of 4-day-old poults was orally inoculated with ~10^6 genomic units of astrovirus in 100µl of phosphate-buffered saline (PBS) as described previously.[11] The control group was sham inoculated with PBS (100 µl). Birds were monitored daily for signs of clinical disease and weighed at 0, 1, 4, 10, and 15 days post infection. At 1, 4, 10, and 15 days post infection, 5 poults per group were randomly

selected and euthanized by cervical dislocation. The duodenum, jejunum, ileum, and cecum were collected. All tissues were stored at -70°C or placed in 10% phosphate-buffered formalin. All animal experiments were approved by the North Carolina State University Animal Care and Use Committee.

Ussing chamber studies.

Immediately after euthanasia, jejunum was harvested from poults and the mucosa was stripped from the seromuscular layer in oxygenated (95% O_2/5% CO_2) avian ringer solution.[21] Tissues then were mounted in 0.13-cm^2 aperture Ussing chambers, as described in previous studies.[22,23] For each Ussing chamber experiment, jejunal tissues from one animal were mounted on duplicate Ussing chambers. Tissues were bathed on the serosal and mucosal sides with 8 ml of oxygenated avian Ringer's solution circulated in water-jacketed reservoirs. The serosal bathing solution contained 10 mM glucose, and was balanced osmotically on the mucosal side with 10 mM mannitol. The spontaneous potential difference (PD) was measured using Ringer-agar bridges connected to calomel electrodes, and the PD was short-circuited through Ag-AgCl electrodes using a voltage clamp that corrected for fluid resistance. Trans-epithelial resistance (TER, $\Omega \cdot cm^2$) was calculated from the spontaneous potential difference and short-circuit current (*I*sc), as previously described. If the spontaneous PD was between –1.0 and +1.0 mV, tissues were current-clamped at ± 25μA for 5-sec and the PD were recorded. I_{sc} and PD were recorded at 15-min intervals.

Isotopic flux studies.

These studies were performed simultaneously with the electrical measurements. To assess transmucosal Na^+ and Cl^- fluxes, ^{22}Na or ^{36}Cl were added to the mucosal or serosal solutions of tissues paired according to their conductance (conductance within 25% of each other). After a 15-min equilibration period, standards were collected from bathing reservoirs and 3 successive 30-min flux periods were performed by taking samples from the bathing reservoirs opposite the side of isotope addition. Samples were counted for ^{22}Na and ^{36}Cl in a liquid scintillation counter. The contribution of ^{22}Na β-counts to ^{36}Cl β-counts was subtracted and the unidirectional fluxes were calculated as previously described.[24]

Mucosal-to-serosal fluxes of [^{3}H] mannitol.

To study paracellular permeability, mucosal-to-serosal fluxes of [^{3}H] mannitol were performed as described above. The mucosal side of Ussing chamber-mounted tissues received 0.2 μCi/ml [^{3}H] mannitol and after a 15-min equilibration period, standards were taken from the mucosal side of each chamber. A 60-min flux period was established by taking 0.5ml samples from the serosal compartment. The presence of ^3H was established by measuring β-emission in a liquid scintillation counter (LKB Wallac, model 1219 Rack Beta, Perkin Elmer Life and Analytical Sciences, Boston, MA).

Histologic examination.

Duodenal, jejunal, ileal, and cecal tissues were fixed in 10% neutral buffer formalin, paraffin embedded, sectioned, and stained with H & E for histologic and histo-morphometric evaluation. Besides epithelial changes, sections were evaluated for morphometric measurements including villus height, villus width, crypt depth, and the number of goblet cells. A minimum of 3 well-oriented villi, each from three sections of each organ, were evaluated at each time point.

Electron microscopy.

For electron microscopy, jejunal tissues were fixed in McDowell's and Trump's 4F:1G fixative and processed for transmission electron microscopy using standard techniques.[25] In brief, after 2 rinses in 0.1M sodium phosphate buffer (pH 7.2), samples were placed in 1% osmium tetroxide in the same buffer for 1hr at room temperature. Samples were rinsed 2 times in distilled water and dehydrated in an ethanolic series culminating in two changes of 100% acetone. Tissues were then placed in a mixture of spurr resin and acetone for 30 min, followed by 2hr in 100% resin with 2 changes. Finally, samples were placed in fresh 100% resin in molds and polymerized at 70^{o} C for 8 hrs to 3 days. Semi-thin (0.25-0.5 µm) sections were cut with glass knives and stained with 1% toluidine blue-O in 1% sodium borate. Ultra thin (70-90 nm) sections were cut with a diamond knife, stained with methanolic uranyl acetate followed by lead citrate and examined with a transmission electron microscope (Phillips/FEICO Model 208s; Hillsboro, OR).

Immunofluorescence.

Jejunal tissues were embedded in OCT media (Tissue Tek, Sakura, Torrance, CA), frozen, sectioned at 5μm, and stored at -80^{0}C till use. The sections were thawed, fixed in cold acetone, and were incubated with phalloidin conjugated with Alexa fluor @ 546 (Molecular probes, Eugene, OR). Following washings in PBS, the slides were mounted in fluorescent mounting media containing DAPI for nuclear staining (Santa cruz Biotech, CA) and examined with a Olympus VANOX AHS-3 epifluorescence photomicroscope.

Gel electrophoresis and Western blotting.

Jejunal mucosal scrapings from control and infected poults were snap frozen and stored at -70°C before SDS-PAGE. Tissue aliquots were thawed at 4°C and added to chilled lysis buffer that includes protease inhibitors (0.5mM Pefabloc, 0.1mM 4-nitrophenyl phosphate, 0.04mM β-glycerophosphate, 0.1mM Na_3VO_4, 40 μg/ml bestatin, 2μg/ml aprotinin, 0.54μg/ml leupeptin, and 0.7μg/ml pepstatin A) at 4°C. This mixture was homogenized on ice and then centrifuged at 4°C, and the supernatant was saved. Protein analysis of extract aliquots was performed (DC protein assay, Bio-Rad, Hercules, CA). Tissue extracts (amounts equalized by protein concentration) were mixed with an equal volume of 2× SDS-PAGE sample buffer and boiled for 4-min. Lysates were loaded on a 10% SDS polyacrylamide gel, and electrophoresis was carried out according to standard protocols. Proteins were transferred to a PVDF membrane (Immobilon, Millipore) by using an electro blotting minitransfer apparatus. Membranes were blocked at room temperature for 60 min in Tris-buffered saline plus 0.05% Tween 20 (TBST) and 5% dry

powdered milk, and then incubated overnight at 4^0C in primary antibody. After washings in TBST, membranes were incubated with horseradish peroxidase-conjugated secondary antibody, and developed for visualization of protein with luminol enhancer solution (Pierce Biotechnology, IL,). Rabbit polyclonal anti-NHE2 and NHE3 antibodies were a generous gift from Dr. Mark Donowitz, The Johns Hopkins University School of Medicine, Baltimore, MD, USA. For preparation of detergent soluble and detergent insoluble fractions of jejunal mucosa, the mucosal samples were extracted in lysis buffer (20mM Tris, 5mM $MgCl_2$, 0.3mM EGTA, 210µg/ml sodium fluoride, 18.5µg/ml sodium orthovandate, 30mM sodium pyrophosphate, and Complete mini Protease inhibitor cocktail tablet (Pierce Biotechnology, IL,). Following brief centrifugation to remove debris, Triton X-100 soluble and insoluble fractions were collected by incubation and centrifugation (50,000rpm for 30 min at 4^0C) with lysis buffer containing 0.5% Triton X-100 and 0.5% SDS, respectively. Before SDS-PAGE analysis, samples were processed through a SDS-PAGE sample preparation kit (Pierce Biotechnology, IL, USA), and protein analysis was performed by BCA Protein Assay (Pierce Biotechnology, IL, USA).

Statistical analysis.

Data were reported as mean ± SE. All data were analyzed by using ANOVA for repeated measures except where the peak response was analyzed by using standard one-way ANOVA (Sigmastat; Jandel Scientific, San Rafael, CA). A Tukey's test was used to determine differences between treatments following ANOVA.

Results:

Clinical signs of TAstV-2-induced disease.

Naïve animals were orally inoculated and monitored for signs of clinical disease and virus replication. Within 3 day of inoculation all animals demonstrated signs of diarrhea as compared to the sham inoculated animals with the most severe clinical signs observed between days 3-7 post inoculation, as previously described.[11] This corresponded with the peak of virus replication as detected by real time RT-PCR (data not shown).

Ion transport and electro-physiology of TAstV-2 infected jejunum.

At four days post infection, uninfected control and TAstV-2 infected jejunum were mounted on Ussing chambers to study electrophysiological and ion transport alterations. The *I*sc values in infected poult jejunum (6.00 ± 2.00 μeq/cm^2/h as compared to 9.52 ±0.90 μeq/cm^2/h in control) reflected no major secretory response (Table 1). The trans-epithelial resistance (TER), which is the inverse function of conductance (G), was lower but not different in TAstV-2 infected poults compared to controls. Simultaneously, we performed Na^+ and Cl^- unidirectional flux experiments to directly examine Na^+ and Cl^- transport (Table 1). TAstV-2 infection did not trigger net secretion of Cl^- that was different from uninfected controls. Alternatively, mucosal-to-serosal and not serosal-to-mucosal Na^+ movement was hampered in TAstV-2 infected poults. Consequently, the net Na^+ absorption was significantly lower in TAstV-2 infected poults (0.82 ± 0.52

μeq/cm^2/h and -1.22 ± 0.53 μeq/cm^2/h in controls and infected group respectively, $p<$ 0.05). Taken together, the *Isc*, TER, and unidirectional flux measurements indicated that Na^+ malabsorption is the major mechanism that could have contributed to clinical diarrhea in TAstV-2 infected poults.

Histological and morphometric studies.

To investigate the histologic changes resulting from TAstV-2 infection, tissues through 1 to 15 days post infection were examined by routine hematoxylin and eosin staining and light microscopy. Histological changes in the infected group were minimal (Fig. 1) and consisted of occasional mild degeneration of enterocytes, loss of the terminal web, infrequent cellularity of the lamina propria, and crypt hyperplasia. Morphometric assessment on different parameters viz. villous height, villous width, crypt hyperplasia, and number of goblet cells revealed no differences between control and TAstV-2 infected jejunum (Table 2). Thus the clinical observation of diarrhea in TAstV-2 infected poults was independent of remarkable histological changes in the intestine. No lesions were seen in any of the control tissues.

Paracellular permeability: Mucosal-to-serosal [^{3}H] mannitol flux.

As paracellular transport forms an important component of epithelial resistance (TER), we conducted mucosal-to-serosal fluxes (J_{ms}) of [^{3}H] mannitol across jejunum of control and TAstV-2 infected poults. As shown in Figure 2, at 4 days post infection, the [^{3}H] mannitol flux did not differ significantly in between control and TAstV-2 infected

jejunum (0.61 ± 0.06 mols/cm^2/hr and 0.53 ± 0.04 mols/cm^2/hr in control and TAstV-2 infected group, respectively). These results indicated that the paracellular transport was not affected after TAstV-2 infection.

Ultrastuctural examination.

Despite the lack of histological abnormalities, we next considered the possibility of ultrastructural changes that might help explain changes in ion transport and diarrheal disease. Therefore we performed transmission electron microscopy on jejunal tissues obtained from control and TAstV-2 infected poults at 4 days post infection. Changes in the form of dense aggregations were observed within terminal web region in the TAstV-2 infected jejunum (Figure 3). Such changes were prominent in epithelial cells at the tips of villi and less frequently in epithelial cells towards intestinal crypts. Such lesions were completely absent in jejunum from control uninfected birds.

Immunofluorescence for F-actin.

To explain further the ultra structural changes seen in the terminal web region of TAstV-2 infected jejunum, we carried out immunofluorescence for F-actin on control and infected jejunum sections. As evidenced in Figure 4, sharp, continuous F-actin fluorescence was present on the apical border of control enterocytes along with thin intracellular stress fibers. In contrast, the TAstV-2 infected jejunum revealed thick and coarse F-actin fluorescence along the apical border of enterocytes. Furthermore, the intracellular stress fibers in infected jejunum were sparse as compared to control jejunum.

These findings indicated F-actin rearrangement in the intestinal epithelium after infection with TAstV-2.

Expression of NHE.

As our electrophysiological and isotopic flux studies revealed impaired electro neutral absorption of Na^+ across TAstV-2 infected jejunum, we sought to study the underlying mechanism. To this end we studied expression of sodium hydrogen exchanger (NHE) isoforms that mediate the major proportion of electroneutral Na^+ transport across mammalian and avian small intestine. NHE2 and NHE3 are the principal intestinal brush border NHEs contributing to electroneutral Na^+ absorption in avian small intestine.[26] Western blot analysis of jejunum mucosal scrapping at 4 days post infection revealed that following TAstV-2 infection NHE3 protein expression was unchanged while expression of NHE2 was increased (Figure 5, *panel A and D*). As NHE3 recycles between the endosomal compartment and the apical plasma membrane and this trafficking is one of the important mechanisms regulating NHE3 function.[27], we separated detergent soluble and insoluble fractions representing cytosolic and membrane components of enterocytes, respectively. We found that expression of NHE3 is shifted from the detergent insoluble fraction to the detergent soluble fraction of TAstV-2 infected jejunum as compared to the control jejunum (Figure 5, *panel C and D*). Similar study of NHE2 expression revealed no significant change in expression pattern in the detergent soluble and insoluble fractions between control and TAstV-2 infected jejunum (Figure 5, *panel E and F*).

Discussion:

The present study was performed to elucidate mechanisms of diarrhea in astrovirus infection using an established model of TAstv-2 infection in young turkey poults. We studied electrophysiology and ion transport in TAstV-2 infected small intestine on Ussing chambers and found that despite the clinical observation of diarrhea, no secretory response is present in TAstV-2 infected jejunum. Though we did not come across citations indicating normal electro physiologic values in turkey small intestine, our findings in control small intestine were similar to those described earlier in chicken where net absorption of Na^+ and minimal secretion of Cl^- takes place in small intestine.[28,29] The major finding in this study was impaired electroneutral Na^+ absorption in TAstV-2 infected poults that could contribute to the development of diarrhea. Failure of Na^+ absorption has been described as a cause for diarrhea in infectious disease,[30] inflammatory bowel disease,[31]and experimental models.[32] As opposed to secretory diarrhea due to Cl^- efflux, impaired Na^+ absorption leads to a reduced gradient for water absorption due to retention of Na^+ in the lumen, causing malabsorptive diarrhea. As net Na^+ and Cl^- did not account completely for the *Isc* in this study (Table 1), the residual ion flux (not shown) could represent defects in other ion transport systems. For example, jejunum was shown to be a major site for K^+ absorption in fowls in an earlier study.[33]

Another characteristics of astrovirus infection as revealed in this and previous studies, is the absence of remarkable histologic changes in the affected intestine. In the present study the histologic changes in intestine were minimal through 1 to 15 days post

infection covering the course of diarrhea. Such lack of overt histopathological changes except for mild crypt hyperplasia or blunting of villi is reported in other astrovirus studies.[11,15,34] To study paracellular permeability, we performed mucosal-to-serosal [^{3}H] mannitol flux and ultra structural examination. In TAstV-2 infected jejunum the paracellular mannitol flux was not different from controls; neither the tight junctions nor paracellular spaces were found dilated in electron microscopic examination. Although there was a trend toward reduced transepithelial resistance (TER) in TAstV-2 infected jejunum, the difference from controls was not significant. In a recent study, human astrovirus is reported to increase epithelial barrier permeability in Caco-2 cells.[35] This difference could be attributable to an *in vitro* cell culture model as against *in vivo* animal model where local and distant cellular responses vary. The barrier permeability measurements in the above mentioned study were from 0 to 48 hours post infection whereas we studied the barrier permeability at 4 days post infection (to match the symptoms of diarrhea). Furthermore, the role of autocrine and paracrine cytokines is also important for intestinal homeostasis. For example, increased activity of TGF-ß, which preserves the epithelial barrier function and dampens the cAMP-mediated Cl^- secretory response,[36] is reported to occur within 1 day post infection and remained elevated for 12 days post TAstV-2 infection in turkey poults.[11]

Transmission electron microscopic examination of TAstV-2 infected jejunum revealed dense aggregations in the terminal web region of enterocytes, suggesting actin rearrangement. The terminal web is a specialized component of the actin cytoskeleton; a

fine meshwork just beneath the cell surface where core microfilaments of microvillus are inserted.[37] The thicker dense aggregating immunofluorescence for apical F-actin further supported the actin rearrangement in astrovirus infected intestine.

To further explain the impaired electroneutral Na^+ transport, we studied protein expression of sodium hydrogen exchangers NHE2 and 3 in control and TAstV-2 infected jejunum. NHE activity largely mediates Na^+ absorption in the jejunum, and deletion of NHE3 greatly reduces net Na^+ absorption leading to diarrhea.[38] In most species e.g. rat, rabbit, and dog NHE3 is a major contributor toward NaCl absorption rather than NHE2.[39-41] In avian intestine however both NHE2 and NHE3 contribute equally toward Na^+/H^+ exchange activity, and importantly, these mechanisms respond to dietary manipulations. For instance, chicken ileum responds to a low sodium diet with increased Na^+/H^+ exchange.[26] In the present study we found that although total expression of NHE3 was unchanged, its expression was increased in the Triton X-100 soluble fraction and decreased in the TritonX-100 insoluble fraction of TAstV-2 infected intestine. In contrast, the total expression of NHE2 was increased in TAstV-2 infected jejunum. Though it is not clear, this increased expression of NHE2 in TAstV-2 infected jejunum could be a compensatory response for loss of NHE3 activity within the apical membrane or it could be a secondary response to maintain intracellular pH or to offset the alkaline luminal conditions created by Na malabsorption, as suggested by Gawenis *et al*.[38] In contrast to NHE3, NHE2 has not been studied in details with regard to the trafficking between plasma membrane and intracellular locations. Unlike NHE3, no clear shift was

found for NHE2 expression in membrane fractions implying that NHE3 was specifically regulated in the intestinal epithelium after TAstV-2 infection.

The complexity of cytoskeletal-plasma membrane interactions is being recognized as important for stabilization, function and trafficking of transport proteins residing within the plasma membrane.[42] NHE3 is associated with the actin cytoskeleton either through direct binding with ezrin or through indirect binding of the PSD95/dlg/zonular occludens-1 (PDZ) domain to ezrin binding proteins and this association of NHE3 with ezrin is important for basal trafficking, including basal exocytosis, delivery from the synthetic pathway and movement of NHE3 in the brush border.[43] Redistribution of NHE3 by the cytoskeleton is reported to occur in by a number of mechanisms, including receptor-mediated inhibition of NHE3 that is prevented by actin stabilization,[42] or activation via exocytic insertion of NHE3 in response to epidermal growth factor.[44] We have shown here that in TAstV-2 infected jejunum, NHE3 is redistributed from the detergent insoluble membrane fraction to the detergent soluble cytosol fraction. Redistribution of NHE3 is described in transfected AP-1 cells following interference with actin polymerization where NHE3 was redistributed to sub cellular locations of actin aggregations. This process was attributed to likely interaction with the cytoskeleton through NHE regulatory factor (NHERF) and the ezrin binding site.[45] As another example, *C. difficile* Toxin B caused translocation of apical NHE3 to sub apical endomembrane compartment in LLC-PK cells.[46] Inactivation of Rho-family GTPases by *C. difficile* Toxin B was suggested to affect interaction of NHE3 with the cytoskeleton

through impaired bridging activity of ezrin. Though dynamic rearrangements of the actin cytoskeleton induced by viral proteins like rotaviral VP4 and NSP4 proteins in intestinal cell lines have been demonstrated recently,[47-49] their impact on ion transport is yet to be established. Based on the current study, we conclude that Na^+ transport is impaired as a result of redistribution of NHE3 associated in turn with rearrangement of F-actin, and this mechanism contributes to development of diarrhea in turkey astrovirus (TAstV-2) infection. We believe that these findings in an *in vivo* animal model add to our current understanding of the pathophysiology of viral agents responsible for diarrheal disease, and in particular, mechanisms of astrovirus-induced diarrhea.

Table 1: Unidirectional Na^+ and Cl^- fluxes across jejunum of control and TAstV-2 infected poults at 4 days post infection

Group	J^{Na}_{ms}	J^{Na}_{sm}	J^{Na}_{net}	J^{Cl}_{ms}	J^{Cl}_{sm}	JCl_{net}	*Isc*	G
Control	**3.98 ± 0.24**	**3.15 ± 0.55**	**0.82 ± 0.52**	**2.88 ± 0.29**	**3.07 ± 0.76**	**-0.19 ± 0.51**	**9.52 ± 0.90**	**9.50 ± 0.95**
Infected	**2.31 ± 0.54**	**3.53 ± 0.36**	**-1.22 ± 0.53**	**2.74 ± 0.56**	**1.50 ± 0.22**	**1.23 ± 0.60**	**6.00 ± 2.00**	**13.75 ± 2.90**
	p<0.05	**NS**	***p<0.05***	**NS**	**NS**	**NS**	**NS**	**NS**

Values are means ± SE. n ≥ 4. Na^+ and Cl^- fluxes (J) and short-circuit current (I_{sc}) are given in $\mu eq \cdot cm^{-2} \cdot h^{-1}$, and tissue conductance (G_t) is given in mS/cm^2. Fluxes commenced after 30 min of equilibrium period on Ussing chamber. Data are shown for fluxes performed during 30-60 min. J_{ms}, mucosal-to-serosal flux; J_{sm}, serosol-to-mucosal flux; J_{net}, net flux. * $P < 0.05$ infected vs. control tissues. NS, non significant (by paired *t*-test).

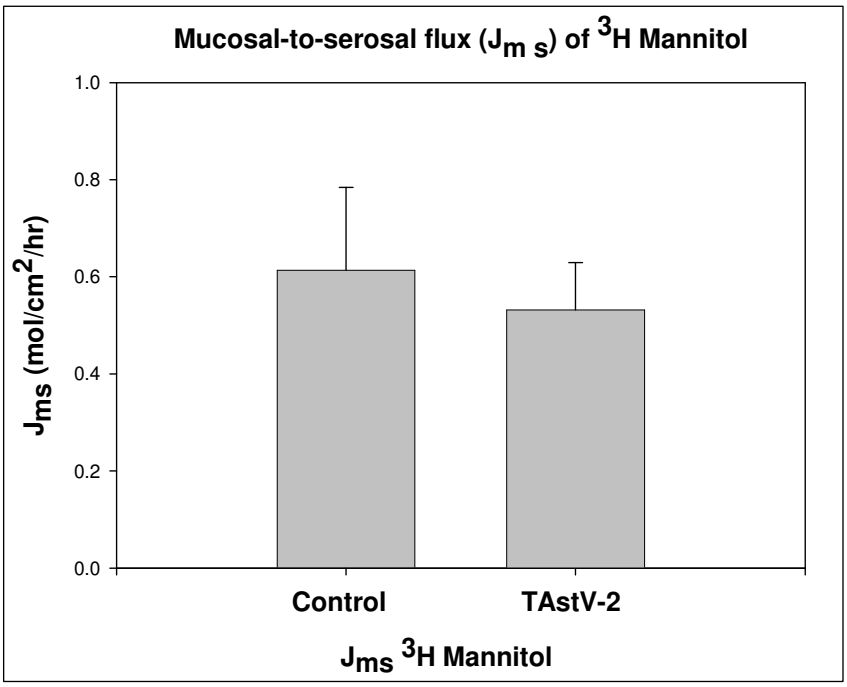

Figure 1. Mucosal-to-serosal fluxes (J_{ms}) of [^{3}H] mannitol across jejunum of control and TAstV-2 infected poults. A single 30-min flux period was initiated after a 30-min equilibration period after mounting tissues on Ussing chamber. There was no significant difference in mannitol permeability between control and TAstV-2 infected jejunum. Bars represent means ± SE; $n = 6$.

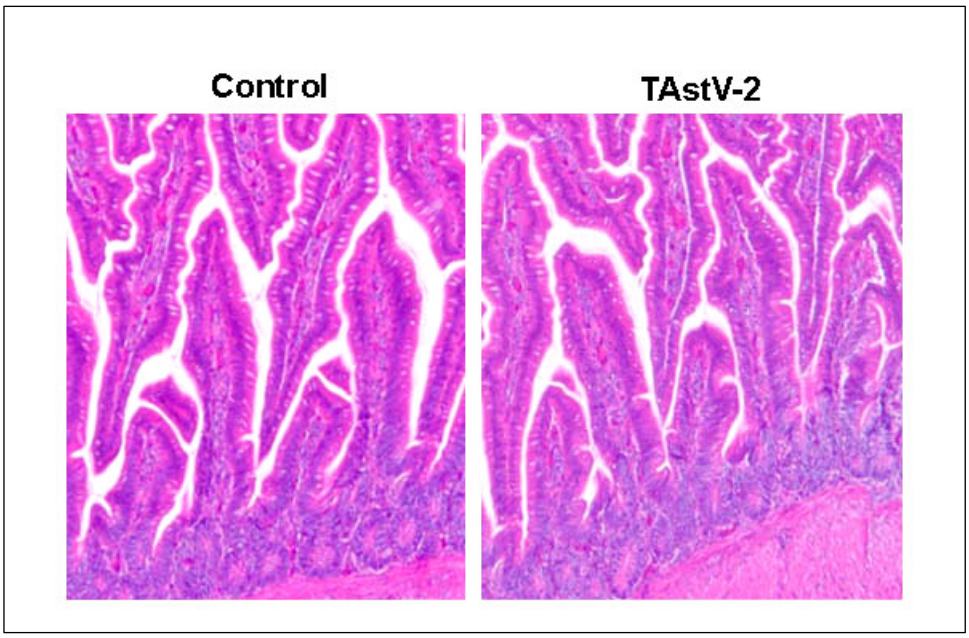

Figure 2. Histology of control and TAstV-2 infected jejunum at 4 days post infection. There were no discernible differences between two groups. H & E X100.

Table 2. Histomorphometry of control and TAstV-2 infected jejunum

DPI	Treatment	Villous Height	Crypt Depth	Villous Width	Villus Surface Area	Villous Height/ Crypt Depth Ratio	Number of Goblet Cells per villi
1 DPI	Control	209.99 ± 8.77	45.30 ± 0.84	52.30 ± 1.85	47495.11 ± 3184.03	4.64 ± 0.24	4.67 ± 0.67
	TAstV-2	205.32 ± 10.79	44.32 ± 1.21	53.82 ± 2.46	47953.79 ± 3781.01	4.64 ± 0.32	6.67 ± 0.88
5 DPI	Control	206.30 ± 23.40	52.03 ± 2.28	58.72 ± 0.78	52870.74 ± 5766.38	3.98 ± 0.49	5.33 ± 1.45
	TAstV-2	191.71 ± 12.82	59.76 ± 3.70	58.90 ± 1.87	49627.67 ± 3650.36	3.24 ± 0.33	6.67 ± 0.33
10 DPI	Control	228.07 ± 6.24	51.74 ± 1.54	50.55 ± 4.60	49613.20 ± 5771.20	4.41 ± 0.04	12.67 ± 0.33
	TAstV-2	207.85 ± 19.26	52.36 ± 1.02	50.82 ± 4.67	45929.58 ± 7549.41	3.99 ± 0.44	7.67 ± 1.20
15 DPI	Control	247.72 ± 14.54	47.62 ± 3.02	55.22 ± 0.97	58694.73 ± 4272.45	5.27 ± 0.57	8.33 ± 0.88
	TAstV-2	248.10 ± 10.31	51.12 ± 2.80	53.24 ± 3.71	56748.55 ± 6134.15	4.87 ± 0.19	7.67 ± 1.20

A minimum of 3 well-oriented villi in jejunum from four subjects from each group at each time point were evaluated. Data represents means ± SE. All values are in microns. There were no differences in the morphometrical values in between control and TAstV-2 infected group.

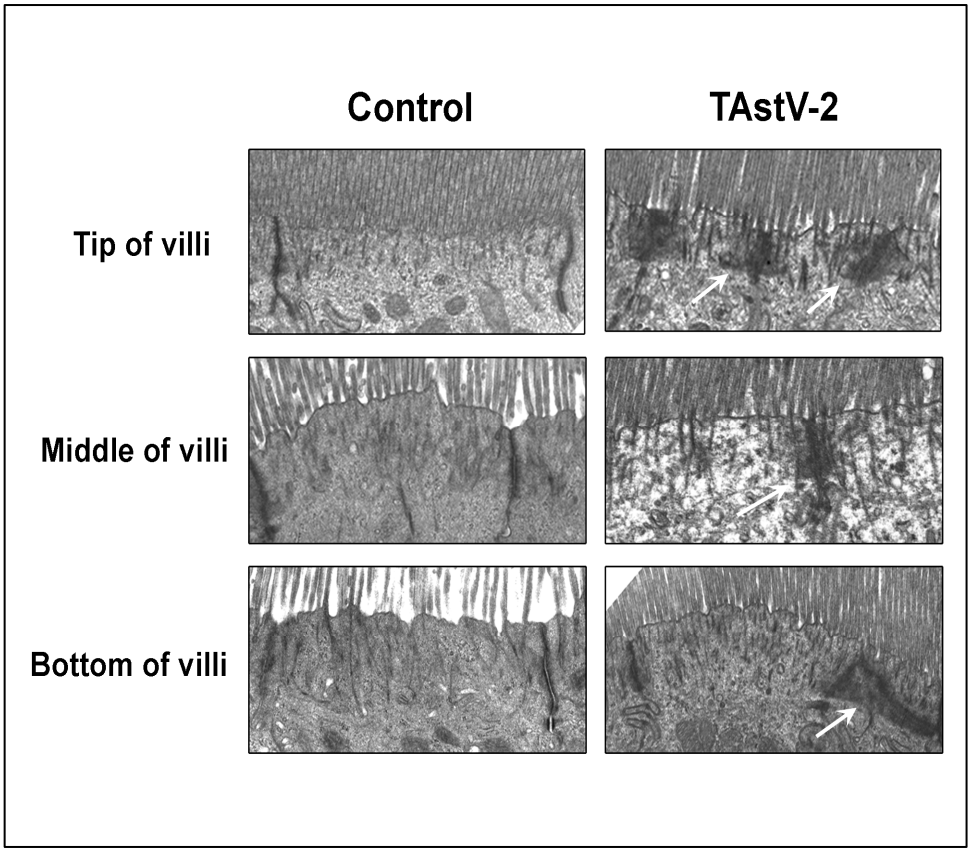

Figure 3. Transmission electronic microscopic examination of control and TAstV-2 infected jejunum at 4 days post infection. The apical terminal web region of TAstV-2 infected jejunum showed electron dense aggregations (arrows). These changes were prominent in enterocytes at the tip of villi. X 28,000.

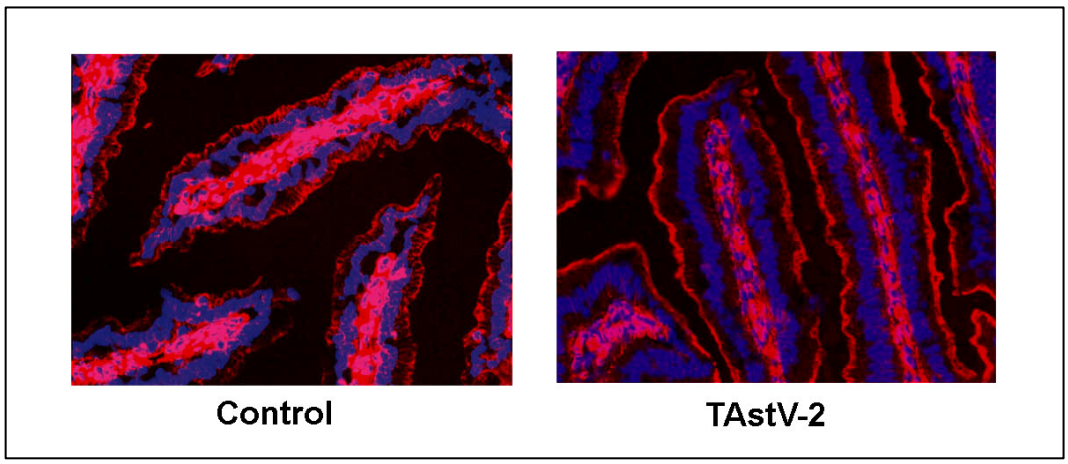

Figure 4. Immunohistochemistry for apical F-actin. The apical F-actin fluorescence (red) was dense and coarse in the TAstV-2 infected jejunum (nuclei are blue). X100

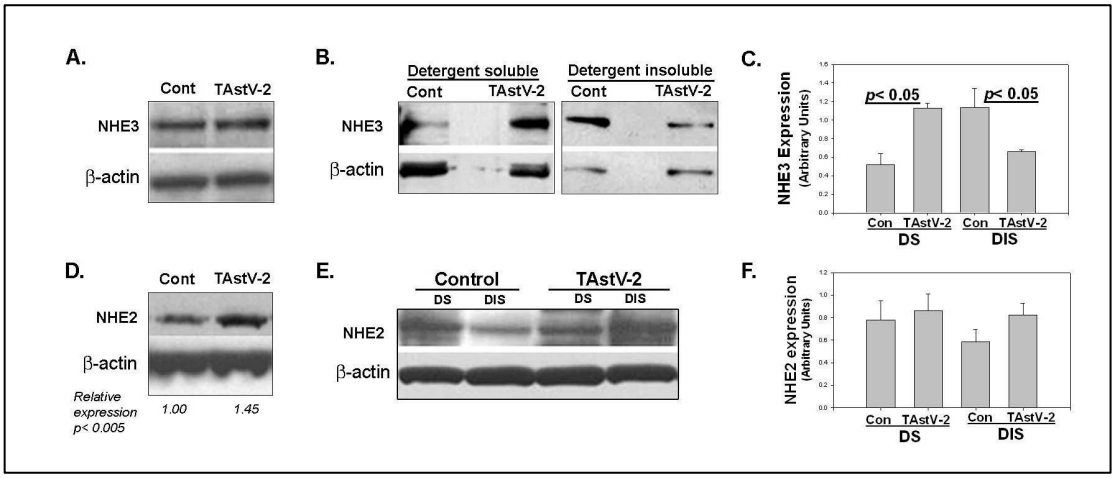

Figure 5. Western analysis for sodium hydrogen exchangers (NHEs) in control and TAstV-2 infected jejunum. TAstV-2 infection did not cause change in total expression of NHE3 in whole jejunal mucosal lysates (A) but led to significant shift of NHE3 expression from the detergent insoluble (DIS) membrane fraction to the detergent soluble (DS) fraction (B). The total expression of NHE2 in jejunal lysates increased after TAstV-2 infection (D). Unlike NHE3, TAstV-2 infection did not cause a clear shift for the expression of NHE2 in detergent soluble or insoluble membrane fractions (E). The densitometric data for NHE3 and NHE2 expression in membrane fractions is presented in panel C and F, respectively. All blots are representative of 3 or more experiments.

References

1. Wilhelmi I, Roman E, Sanchez-Fauquier A. Viruses causing gastroenteritis. Clin.Microbiol.Infect. 2003;9:247-262.

2. Kapikian AZ, ed. Viral infection of gastrointestinal tract. Marcel Dekker, 1996.

3. Christensen ML, ed. Manual of clinical microbiology. Washington: ASM Press, 1999.

4. Shastri S, Doane AM, Gonzales J, Upadhyayula U, Bass DM. Prevalence of astroviruses in a children's hospital. J.Clin.Microbiol. 1998;36:2571-2574.

5. Grohmann GS, Glass RI, Pereira HG, Monroe SS, Hightower AW, Weber R, Bryan RT. Enteric viruses and diarrhea in HIV-infected patients. Enteric Opportunistic Infections Working Group. N.Engl.J.Med. 1993;329:14-20.

6. Glass RI, Noel J, Mitchell D, Herrmann JE, Blacklow NR, Pickering LK, Dennehy P, Ruiz-Palacios G, de Guerrero ML, Monroe SS. The changing epidemiology of astrovirus-associated gastroenteritis: a review. Arch.Virol.Suppl. 1996;12:287-300.

7. Mitchell E, O'Mahony M, McKeith I, Sprott MS, Codd AA, Wright AG. An outbreak of viral gastroenteritis in a psychiatric hospital. J.Hosp.Infect. 1989;14:1-8.

8. Mitchell DK, Matson DO, Jiang X, Berke T, Monroe SS, Carter MJ, Willcocks MM, Pickering LK. Molecular epidemiology of childhood astrovirus infection in child care centers. J.Infect.Dis. 1999;180:514-517.

9. Mead PS, Slutsker L, Dietz V, McCaig LF, Bresee JS, Shapiro C, Griffin PM, Tauxe RV. Food-related illness and death in the United States. Emerg.Infect.Dis. 1999;5:607-625.

10. Guix S, Bosch A, Pinto RM. Human astrovirus diagnosis and typing: current and future prospects. Lett.Appl.Microbiol. 2005;41:103-105.

11. Koci MD, Moser LA, Kelley LA, Larsen D, Brown CC, Schultz-Cherry S. Astrovirus induces diarrhea in the absence of inflammation and cell death. J.Virol. 2003;77:11798-11808.

12. Baxendale W, Mebatsion T. The isolation and characterisation of astroviruses from chickens. Avian Pathol. 2004;33:364-370.

13. Reynolds DL, Saif YM. Astrovirus: a cause of an enteric disease in turkey poults. Avian Dis. 1986;30:728-735.

14. Reynolds DL, Saif YM, Theil KW. Enteric viral infections of turkey poults: incidence of infection. Avian Dis. 1987;31:272-276.

15. Thouvenelle ML, Haynes JS, Reynolds DL. Astrovirus infection in hatchling turkeys: histologic, morphometric, and ultrastructural findings. Avian Dis. 1995;39:328-336.

16. Thouvenelle ML, Haynes JS, Sell JL, Reynolds DL. Astrovirus infection in hatchling turkeys: alterations in intestinal maltase activity. Avian Dis. 1995;39:343-348.

17. Lorrot M, Vasseur M. How do the rotavirus NSP4 and bacterial enterotoxins lead differently to diarrhea? Virol.J. 2007;4:31.

18. Moser LA, Schultz-Cherry S. Pathogenesis of astrovirus infection. Viral Immunol. 2005;18:4-10.

19. Koci MD, Kelley LA, Larsen D, Schultz-Cherry S. Astrovirus-induced synthesis of nitric oxide contributes to virus control during infection. J.Virol. 2004;78:1564-1574.

20. Koci MD. Immunity and resistance to astrovirus infection. Viral Immunol. 2005;18:11-16.

21. Whitsel AI, Johnson CB, Forehand CJ. An in ovo chicken model to study the systemic and localized teratogenic effects of valproic acid. Teratology 2002;66:153-163.

22. Argenzio RA, Liacos JA. Endogenous prostanoids control ion transport across neonatal porcine ileum in vitro. Am.J.Vet.Res. 1990;51:747-751.

23. Little D, Dean RA, Young KM, McKane SA, Martin LD, Jones SL, Blikslager AT. PI3K signaling is required for prostaglandin-induced mucosal recovery in ischemia-injured porcine ileum. Am.J.Physiol.Gastrointest.Liver Physiol. 2003;284:G46-56.

24. Argenzio RA, Lecce J, Powell DW. Prostanoids inhibit intestinal NaCl absorption in experimental porcine cryptosporidiosis. Gastroenterology 1993;104:440-447.

25. Dykstra MJ. A manual of applied techniques for biological electron microscopy. Plenum Press, New York, 1993.

26. Donowitz M, De La Horra C, Calonge ML, Wood IS, Dyer J, Gribble SM, De Medina FS, Tse CM, Shirazi-Beechey SP, Ilundain AA. In birds, NHE2 is major brush-border Na+/H+ exchanger in colon and is increased by a low-NaCl diet. Am.J.Physiol. 1998;274:R1659-69.

27. Zachos NC, Tse M, Donowitz M. Molecular physiology of intestinal Na+/H+ exchange. Annu.Rev.Physiol. 2005;67:411-443.

28. Grubb BR, Driscoll SM, Bentley PJ. Electrical PD, short-circuit current and fluxes of Na and Cl across avian intestine. J.Comp.Physiol.[B]. 1987;157:181-186.

29. Grubb BR. Ion transport across the chick ileum: a good model for transport studies. Comp.Biochem.Physiol.A 1991;100:753-757.

30. Shepherd RW, Gall DG, Butler DG, Hamilton JR. Determinants of diarrhea in viral enteritis. The role of ion transport and epithelial changes in the ileum in transmissible gastroenteritis in piglets. Gastroenterology 1979;76:20-24.

31. Hawker PC, McKay JS, Turnberg LA. Electrolyte transport across colonic mucosa from patients with inflammatory bowel disease. Gastroenterology 1980;79:508-511.

32. Clayburgh DR, Musch MW, Leitges M, Fu YX, Turner JR. Coordinated epithelial NHE3 inhibition and barrier dysfunction are required for TNF-mediated diarrhea in vivo. J.Clin.Invest. 2006;116:2682-2694.

33. Grubb BR, Bentley PJ. Avian colonic ion transport: effects of corticosterone and dexamethasone. J.Comp.Physiol.[B]. 1989;159:131-138.

34. Sebire NJ, Malone M, Shah N, Anderson G, Gaspar HB, Cubitt WD. Pathology of astrovirus associated diarrhoea in a paediatric bone marrow transplant recipient. J.Clin.Pathol. 2004;57:1001-1003.

35. Moser LA, Carter M, Schultz-Cherry S. Astrovirus increases epithelial barrier permeability independently of viral replication. J.Virol. 2007;81:11937-11945.

36. Howe K, Gauldie J, McKay DM. TGF-beta effects on epithelial ion transport and barrier: reduced Cl- secretion blocked by a p38 MAPK inhibitor. Am.J.Physiol.Cell.Physiol. 2002;283:C1667-74.

37. Young B, Heath J W. Wheater's Functional Histology. . Churchill Livingstone, Elsevier Ltd, 2000.

38. Gawenis LR, Stien X, Shull GE, Schultheis PJ, Woo AL, Walker NM, Clarke LL. Intestinal NaCl transport in NHE2 and NHE3 knockout mice. Am.J.Physiol.Gastrointest.Liver Physiol. 2002;282:G776-84.

39. Collins JF, Honda T, Knobel S, Bulus NM, Conary J, DuBois R, Ghishan FK. Molecular cloning, sequencing, tissue distribution, and functional expression of a Na+/H+ exchanger (NHE-2). Proc.Natl.Acad.Sci.U.S.A. 1993;90:3938-3942.

40. Wormmeester L, Sanchez de Medina F, Kokke F, Tse CM, Khurana S, Bowser J, Cohen ME, Donowitz M. Quantitative contribution of NHE2 and NHE3 to rabbit ileal brush-border Na+/H+ exchange. Am.J.Physiol. 1998;274:C1261-72.

41. Maher MM, Gontarek JD, Bess RS, Donowitz M, Yeo CJ. The Na+/H+ exchange isoform NHE3 regulates basal canine ileal Na+ absorption in vivo. Gastroenterology 1997;112:174-183.

42. Khurana S. Role of actin cytoskeleton in regulation of ion transport: examples from epithelial cells. J.Membr.Biol. 2000;178:73-87.

43. Cha B, Tse M, Yun C, Kovbasnjuk O, Mohan S, Hubbard A, Arpin M, Donowitz M. The NHE3 juxtamembrane cytoplasmic domain directly binds ezrin: dual role in NHE3 trafficking and mobility in the brush border. Mol.Biol.Cell 2006;17:2661-2673.

44. Khurana S, Nath SK, Levine SA, Bowser JM, Tse CM, Cohen ME, Donowitz M. Brush border phosphatidylinositol 3-kinase mediates epidermal growth factor stimulation of intestinal NaCl absorption and Na+/H+ exchange. J.Biol.Chem. 1996;271:9919-9927.

45. Kurashima K, D'Souza S, Szaszi K, Ramjeesingh R, Orlowski J, Grinstein S. The apical Na(+)/H(+) exchanger isoform NHE3 is regulated by the actin cytoskeleton. J.Biol.Chem. 1999;274:29843-29849.

46. Hayashi H, Szaszi K, Coady-Osberg N, Furuya W, Bretscher AP, Orlowski J, Grinstein S. Inhibition and redistribution of NHE3, the apical Na+/H+ exchanger, by Clostridium difficile toxin B. J.Gen.Physiol. 2004;123:491-504.

47. Brunet JP, Cotte-Laffitte J, Linxe C, Quero AM, Geniteau-Legendre M, Servin A. Rotavirus infection induces an increase in intracellular calcium concentration in human intestinal epithelial cells: role in microvillar actin alteration. J.Virol. 2000;74:2323-2332.

48. Gardet A, Breton M, Fontanges P, Trugnan G, Chwetzoff S. Rotavirus spike protein VP4 binds to and remodels actin bundles of the epithelial brush border into actin bodies. J.Virol. 2006;80:3947-3956.

49. Berkova Z, Crawford SE, Blutt SE, Morris AP, Estes MK. Expression of rotavirus NSP4 alters the actin network organization through the actin remodeling protein cofilin. J.Virol. 2007;81:3545-3553.

DISSERTATION SUMMARY

The research work described in this thesis demonstrates an important role of the ion transport proteins ClC-2 and NHE2 in the intestinal barrier recovery process. The Chloride channel ClC-2 and sodium hydrogen exchanger NHE2 are members of large ClC and NHE families respectively, and their physiological function are not yet fully known. The present *in vivo* studies in genetically modified mice showed that both ClC-2 and NHE2 null mice have impaired intestinal epithelial barrier recovery after the ischemic injury. The role of ion transport proteins in the epithelial barrier recovery which is largely dependent up on sealing of the paracellular space by assembly of intercellular tight junctions in the intestinal epithelial lining is being explored recently. Though the mechanistic links between above mentioned plasma membrane transport proteins with the apical tight junctions is not fully established in this thesis work, the present findings will form a basis to further explore the cellular mechanisms involved in the recovery of barrier function in the intestinal epithelium that is critical for avoiding breach of host environment by microbial pathogens and their toxic products in the intestinal lumen.

The ClC-2 knockout mice were found to have impaired barrier recovery due to failure of rapid reassembly of tight junctions after ischemic injury. The comparative study between wild type and ClC-2 deficient mice suggests that ClC-2 might act as a scaffold protein to facilitate assembly of tight junction by recruiting core protein occludin to the tight junction. In wild type mice we found evidence for close association between occludin and ClC-2 during post-ischemic barrier recovery. The ClC-2 is localized at apical tight

junction and thus may be involved in a specific signaling pathway leading to the closure of tight junctions.

While impaired post-ischemic barrier recovery in NHE2 deficient mice was also found to be mediated via reassembly of tight junction, the mechanism is probably more intriguing. The assembly of tight junction is influenced by actin cytoskeleton, and NHE proteins have been shown to interact with actin cytoskeleton under the influence of protein kinases. In current study we were able to demonstrate an association of NHE2 with cytoskeleton associated protein, Ezrin Binding Protein (EBP50). Further work will clarify and explore this link between NHE2 and the tight junction.

The work related to ClC-2 and NHE2 is based upon and supports the premises that tight junctions are not static structures but are dynamically regulated by membrane transport proteins. The present work is a part of attempts to generate a comprehensive approach towards improved intestinal barrier function. Though knockout model used in these studies carry adaptation issue due to lack of a particular protein since birth, it has an advantage of being an *in vivo* approach. In order to delineate further signaling pathways involved in recovery of barrier function, a balanced approach of *in vivo*, cell culture, and molecular techniques will be needed.

The work described in a chapter 5 underscores importance of ion transport in a clinical condition. In the experiments aimed at studying pathophysiology of astrovirus induced

diarrhea, we found that Turkey Astrovirus (TAstV-2) led to sodium malabsorption associated with redistribution of sodium hydrogen exchanger NHE3. The interaction of microbial pathogens with the host intestine involves complex cellular processes that attract significant research interest. The findings in this study will help increase our understanding about astrovirus-induced diarrhea in particular and the pathophysiology of intestine in general.